

The influence of chain connectivity on thermodynamic and structural properties of lattice polymers : integral equation and partition function theories

Citation for published version (APA):

Wang, S. (1997). *The influence of chain connectivity on thermodynamic and structural properties of lattice polymers : integral equation and partition function theories*. [Phd Thesis 1 (Research TU/e / Graduation TU/e), Chemical Engineering and Chemistry]. Technische Universiteit Eindhoven. <https://doi.org/10.6100/IR498950>

DOI:

[10.6100/IR498950](https://doi.org/10.6100/IR498950)

Document status and date:

Published: 01/01/1997

Document Version:

Publisher's PDF, also known as Version of Record (includes final page, issue and volume numbers)

Please check the document version of this publication:

- A submitted manuscript is the version of the article upon submission and before peer-review. There can be important differences between the submitted version and the official published version of record. People interested in the research are advised to contact the author for the final version of the publication, or visit the DOI to the publisher's website.
- The final author version and the galley proof are versions of the publication after peer review.
- The final published version features the final layout of the paper including the volume, issue and page numbers.

[Link to publication](#)

General rights

Copyright and moral rights for the publications made accessible in the public portal are retained by the authors and/or other copyright owners and it is a condition of accessing publications that users recognise and abide by the legal requirements associated with these rights.

- Users may download and print one copy of any publication from the public portal for the purpose of private study or research.
- You may not further distribute the material or use it for any profit-making activity or commercial gain
- You may freely distribute the URL identifying the publication in the public portal.

If the publication is distributed under the terms of Article 25fa of the Dutch Copyright Act, indicated by the "Taverne" license above, please follow below link for the End User Agreement:

www.tue.nl/taverne

Take down policy

If you believe that this document breaches copyright please contact us at:

openaccess@tue.nl

providing details and we will investigate your claim.

The Influence of Chain Connectivity on Thermodynamic and Structural Properties of Lattice Polymers

Integral Equation and Partition Function Theories

Suxin Wang

The Influence of Chain Connectivity on Thermodynamic and Structural Properties of Lattice Polymers

Integral Equation and Partition Function Theories

Wang, Suxin

The influence of chain connectivity on thermodynamic and structural properties of lattice polymers : integral equation and partition function theories / by Suxin Wang. - Eindhoven : Technische Universiteit Eindhoven, 1997.

Proefschrift. -

ISBN 90-386-0808-X

NUGI 812

Trefw.: statistische thermodynamica / polymeerstructuur

Subject headings: statistical thermodynamics / excluded volume / polymer chains

Druk: Universiteitsdrukkerij TUE

Het in dit proefschrift beschreven onderzoek werd uitgevoerd onder auspiciën van de Stichting Scheikundig Onderzoek in Nederland (SON) met financiële steun van de Nederlandse Organisatie voor Wetenschappelijk Onderzoek (NWO)

The Influence of Chain Connectivity on Thermodynamic and Structural Properties of Lattice Polymers

Integral Equation and Partition Function Theories

PROEFSCHRIFT

ter verkrijging van de graad van doctor aan de
Technische Universiteit Eindhoven, op gezag van de
Rector Magnificus, prof.dr. M. Rem, voor een
commissie aangewezen door het College voor
Promoties in het openbaar te verdedigen
op donderdag 30 oktober 1997 om 16.00 uur

door

Suxin Wang

geboren te Hebei, China

Dit proefschrift is goedgekeurd door de promotoren:

prof.dr. P.J. Lemstra

en

prof.dr. M.A.J. Michels

Contents

1	Introduction	1
1.1	General introduction	1
1.2	Scope of the thesis	4
1.3	Outline of the thesis	5
2	Statistical thermodynamics and theories of chain liquids	10
2.1	Introduction	10
2.2	Statistical thermodynamics: Partition functions and thermodynamics	10
2.3	Computer simulations: Monte Carlo technique	15
2.4	Molecular model: The lattice model	16
2.5	Partition function theories	17
2.5.1	The Flory-Huggins theory	17
2.5.2	The Huggins theory	18
2.5.3	The non-random mixing Theory	19
2.5.4	The conformational theory of Szleifer	21
2.5.5	The theory of Weinhold, Kumar and Szleifer	23
2.5.6	The lattice cluster theory	24
2.6	Statistical thermodynamics: Integral equation theory	26
2.6.1	Distribution functions	26
2.6.2	Ornstein-Zernike equation	28
2.6.3	RISM: The reference interaction site model	29
2.6.4	PRISM: The polymer-RISM	30
2.7	Concluding remarks	30
3	The Excluded volume problem in the integral equation theory	33
3.1	Introduction	33
3.2	Theory	37

3.2.1	The molecular model	37
3.2.2	Lattice PRISM theory	37
3.2.3	Intra-molecular correlation of the freely jointed chain model	39
3.2.4	Intra-molecular correlation of excluded volume theory	40
3.2.5	Thermodynamic properties	42
3.3	Monte Carlo simulation	45
3.3.1	NpT -simulation	45
3.3.2	Liquid-vapor coexistence curve	45
3.4	Results and discussions	46
3.5	Conclusions	57
4	A theory for compressible binary lattice polymers: Influence of chain conformational properties	63
4.1	Introduction	63
4.2	Theory	67
4.2.1	Partition functions, insertion probabilities and thermodynamics	67
4.2.2	Theoretical expressions for the insertion probabilities of athermal chains	72
4.2.3	Theory of interacting chains	78
4.3	Monte Carlo simulations	83
4.4	Results and discussion	84
4.4.1	Pure components	84
4.4.2	Mixtures	90
4.5	Conclusions	99
5	Thermodynamic properties of compressible lattice polymers: A comparison of MC simulation data and theories. Pure components	104
5.1	Introduction	104
5.2	Model and theories	106
5.2.1	The lattice model for a compressible pure component	106
5.2.2	The Flory-Huggins theory	106
5.2.3	The Huggins theory	107
5.2.4	The NRM theory	107
5.2.5	The ω -theory	109
5.2.6	The conformational theory of Szleifer	110
5.2.7	The theory of Weinhold, Kumar and Szleifer	112

5.2.8	The lattice cluster theory	113
5.3	Thermodynamic properties	116
5.4	Results and discussions	117
5.4.1	Equation of state behavior	117
5.4.2	The liquid-vapor coexistence	123
5.5	Conclusions	128
6	Thermodynamic properties of compressible lattice polymers: A comparison of MC simulation data and theories. Polymer blends	132
6.1	Introduction	132
6.2	Model and theories	133
6.2.1	The lattice model for a compressible polymer blend	133
6.2.2	The Flory-Huggins theory	133
6.2.3	The NRM theory	134
6.2.4	The ω -theory	136
6.2.5	The lattice cluster theory	137
6.3	Thermodynamic properties	137
6.4	Results and discussions	138
6.4.1	Homogeneous mixtures.	139
6.4.2	Liquid-liquid coexistence	142
6.5	Conclusions	143
7	Outlook: Possible extensions and applications	147
7.1	PRISM applications	147
7.2	ω -theory	148
A	The t_{ij}'s calculated from cluster expansion	151
B	The parameters for the Freed theory	156
	Summary	158
	Samenvatting	162
	Notation	166
	Acknowledgments	171
	Curriculum Vitae	172

Chapter 1

Introduction

1.1 General introduction

All through the history of polymer science and technology the thermodynamic behavior of polymer fluids has attracted a great deal of attention. Over the last half century the field has evolved enormously. Initial studies dealt with 'simple' solutions of linear polymers marked by relatively simple phase behavior.¹⁻⁹ Nowadays polymer materials are available having complex molecular architectures and, quite often, a concurring complex thermodynamic behavior. An outstanding example is the micro-phase ordering in (random) block copolymer melts dictated by the block copolymer structure.^{10,11} Other examples of complex thermodynamic behavior are provided by, e.g. solutions and mixtures containing well defined dendrimers, comb-, star- and branched polymers.¹²⁻¹⁷ Evidence is available that these systems are characterized by a substantially richer phase behavior than the 'simple' systems. A quite recent example is offered by the complex miscibility conditions of mixtures of linear and regularly short chain branched polyolefins^{18,19} which have become available with the development of metallocene catalysts.²⁰ These more recent studies indicate that the detailed molecular architecture is quite important for the actual phase behavior. As it turns out, also the quantitative details of the phase behavior of the more 'simple' systems of linear polymers referred to in the beginning of the paragraph, are quite subtle and determined by the molecular architecture, i.e., the chain connectivity of the simple linear molecules. Therefore, to arrive at an accurate prediction of the properties of polymer materials, it is worthwhile to establish the effects of chain connectivity on the phase behavior of linear chain fluids before attempting to attack systems involving more complex molecular architectures. In a next step, an accurate de-

scription of the complex materials could be attempted. This, however, will not be the subject of the present thesis.

The relation between the thermodynamic properties and the details of the molecular architecture and interactions is provided by the specialty of statistical mechanics.²¹ The general laws of statistical mechanics can be exploited in several ways. One approach is to derive theories, based on these laws, employing a model for the molecular architecture and interactions.^{21,22} Theories are inevitably approximate as in the process of translating the general statistical mechanics laws to actual theoretical relations, depending on a limited number of state variables, it is necessary to make some approximations. Another approach which has witnessed much progress recently is large scale Monte Carlo and molecular dynamics computer simulations.^{23,24} These studies provide many insights regarding the physics of model (polymer) fluids, and also essentially exact benchmarks against which approximate theories can be tested.

A first milestone in the theoretical understanding of the thermodynamic behavior of polymer materials can be pointed out in the work of Flory,¹⁻⁵ Huggins^{6,7} and Staverman.^{8,9} These authors independently provided a rationalization of the phase behavior of solutions of linear polymer molecules employing a fully occupied lattice to model the fluid. Their theory rationalized the striking asymmetry with respect to composition of the UCST¹ liquid-liquid miscibility gap in such solutions.¹ Flory-Huggins (FH)-like theories also provided insight in, e.g., the molecular mechanisms responsible for the occurrence of LCST² miscibility gaps in compressible mixtures or solutions. It turned out that the LCST can be attributed to differences in compressibility of the constituents²⁵⁻²⁸ or to the presence of directional-specific interactions.²⁹

Notwithstanding the successes of the simple FH theory, it also has shortcomings. Most imperfections of the FH theory can be related to the use of the lattice model and to the complete lack of reference to the polymer architecture. The problems, related to the lattice model, are not unique to polymers but also appear in atomic and small molecule fluids. Nowadays, to study the structure and the thermodynamic behavior of these 'simple' fluids distribution function theories are widely employed.^{21,22} For a monatomic fluid, distribution functions describe the microscopic features of a fluid on the level of (intermolecular) correlations among a set of particles.^{21,22,30} It turns out that knowledge about the correlations between a pair of particles suffices to predict relevant thermody-

¹UCST: Upper critical solution temperature.

²LCST: Lower critical solution temperature.

dynamic properties.^{21,22,30} Furthermore, these pair correlations can be measured experimentally in scattering experiments.^{31,32}

From the distribution function theories of simple fluids it is understood that the restrictions of the lattice model are particularly problematic if local packing effects are important.³³ Distribution function theories are particularly successful in predicting these microscopic structural features. Unfortunately, the thermodynamic behavior of the fluid predicted from the theoretical correlation functions is plagued with inconsistencies.^{21,34-40} For instance, the equation of state of the fluid can be calculated from the correlation functions in different ways, but, each calculation route yields a different result.^{21,34-40} Of course, if the predicted correlation functions would be exact, the different routes should give the same results.

The distribution function theories have recently also been generalized to macromolecular materials. A successful application is the polymer reference interaction site model (PRISM) initiated by Curro and Schweizer⁴¹⁻⁴⁵ and based on the RISM theory for small molecule fluids of Chandler and collaborators.^{34,35,46-51} In the RISM theory the microscopic structure of the fluid is not only determined by intermolecular correlations but also by intra-molecular correlations. For small (rigid) molecules the intra-molecular correlations are prescribed by the molecular structure and merely put constraints on the possible intermolecular correlations. However, for chain like (flexible) molecules the situation is more complex. The intra-molecular correlations are not only determined by the structure of the single chain but are also perturbed by the environment provided by the surrounding molecules. Thus, intra-molecular and intermolecular correlations exert a mutual influence and should be determined self-consistently.^{49,50,52-56} Only very recently, such a self-consistent scheme has been suggested and its accuracy remains to be established.^{49,50,52-56}

Thus, in principle, the PRISM concept provides the possibility to involve the detailed molecular architecture in the theoretical discussion. Initial applications were restricted to linear chains of which the intra-molecular structure was hypothesized to be ideal³, and hence, independent of the environment.⁴⁴ Having in mind the ideality hypothesis of Flory,⁵⁷ it was argued that this should be a reasonable approximation for a pure homo-polymer. However, the Flory hypothesis can only be valid at length scales comparable to the radius of gyration of the chain molecule. Thus, at the size of a monomer unit, which is important for the local packing, the ideal chain structure is not really appropriate. It turns out that

³Typical for the ideal chain is that the average squared end-to-end distance $\langle r^2 \rangle$ is proportional to the number of point segments s , according to $\langle r^2 \rangle \sim (s-1)^1$.

this may even lead to unphysical behavior both in the intermolecular correlations as well as in the thermodynamic properties.^{58,59} Furthermore, the Flory ideality hypothesis is certainly not universally applicable, e.g. at low densities and in mixtures it is known to fail. As another drawback of the distribution function theories, it was observed that the thermodynamic inconsistencies may become extremely large and it is not always clear which path to the thermodynamics should be preferred.⁶⁰

Hence, although distribution function theories in general and PRISM theory in particular provide an interesting approach to the theory of polymer fluids, there is certainly scope left for alternative developments. Such an alternative approach, due to Freed and coworkers,⁶¹⁻⁶⁴ concentrated on the effect of chain connectivity and molecular structure but keeping the lattice model as it is very convenient for theoretical digressions. Freed et al. proposed a formally exact solution of the lattice model in a cluster expansion, which is quite similar to the Mayer expansion for off-lattice fluids.⁶¹ In the lattice cluster (LC) theory it is possible to mimic chemical details of the molecular structure and to study the influence of these details on the thermodynamic properties.^{18,19} However, the truncation of the expansion makes that the full chain connectivity is not captured and that the expansion is only applicable for small values of the expansion variables.

Beside the PRISM and LC studies, numerous theoretical developments exist, operating more in an *ad hoc* fashion by making some plausible (physical) assumption to push ahead the theoretical discussion. Although such theories are less general than e.g. the PRISM theory and the LC theory they may have the potential to provide insight in the relation between microscopic details and macroscopic properties. They may even yield more accurate predictions for the specific systems considered. Some theories of this type relevant for our purposes are the theories of Szleifer⁶⁵ and Weinhold, Kumar and Szleifer,⁶⁶ which will be discussed in the following chapter.

1.2 Scope of the thesis

In very general terms we aim at understanding the influence of the intra-molecular architecture of macromolecules on the microscopic structure of the fluid and the thermodynamic behavior. Clearly, this objective is too broad and we will limit our contribution to the study of linear, flexible molecules. However, despite this restricted objective, the theoretical development should be sufficiently flexible and facilitate applications to more complicated molecular architectures.

1.3 Outline of the thesis

In **chapter 2** the general principles of classical statistical mechanics are introduced and the connection to thermodynamic properties is explained. From these principles a series of theories will be deduced which will serve as reference points in the development to come in the main body of the thesis.

In **chapter 3** a new intra-molecular correlation function is derived, employing an integral equation approach. In the intra-molecular correlation function the long range correlations due to the chain connectivity are accounted for. The new intra-molecular correlation function is used to predict the intermolecular correlations employing the PRISM theory. The predicted inter- and intra-molecular pair correlations as well as the thermodynamic results are presented and compared to Monte Carlo simulation results.

In **chapter 4** the derivation of a new lattice theory, coined ω -theory, incorporating the long range consequences of chain connectivity is presented. The influence of the chain connectivity on the thermodynamic properties of pure components and binary mixtures is determined self-consistently. A preliminary comparison of the theory to Monte Carlo simulation results is presented.

In **chapter 5** the new lattice theory and its predictions for compressible pure components are compared to those from a selection of lattice theories available in literature. In particular the equation of state and the vapor-liquid coexistence are studied as a function of chain length. The theoretical results are again confronted with Monte Carlo simulation results.

In **chapter 6** the analysis of the different theories, initiated in the previous chapter, is extended to binary polymer mixtures. Special attention is given to the equation of state and the liquid-liquid coexistence of such mixtures. Again a comparison to available MC simulation data is presented.

Finally in **chapter 7**, the main results of this thesis are emphasized and potential applications and extensions of the ω -theory are sketched.

References

- [1] Flory, P. J., *Principles of Polymer Chemistry*. Cornell University Press, Ithaca, 1953.
- [2] Flory, P. J., *J. Chem. Phys.* 9, 660, 1941.
- [3] Flory, P. J., *J. Chem. Phys.* 10, 51, 1942.
- [4] Flory, P. J., *Proc. R. Soc. London, A* 234, 60, 1956.
- [5] Flory, P. J., *Proc. Natl. Acad. Sci. U. S. A.* 79, 4510, 1941.
- [6] Huggins, M. L., *Ann. N.Y. Acad. Sci* 43, 1, 1942.
- [7] Huggins, M. L., *J. Chem. Phys.* 9, 440, 1941.
- [8] Staverman, A. J., van Santen, J. H., *Rec. Trav. Chim. Pays-Bas* 60, 76, 1941.
- [9] Staverman, A. J., *Rec. Trav. Chim. Pays-Bas* 60, 640, 1941.
- [10] Fredrickson, G. H., Milner, S. T., Leibler, L., *Macromolecules* 25, 6341, 1992.
- [11] Patel, N. M., Dwight, D. W., Hedrick, J. L., Webster, D. C., McGrath, J. E., *Macromolecules* 21, 2689, 1988.
- [12] Mishra, M., *Macromolecule Design: Concept and Practice*. Polymer Frontiers International Inc., NY, New York, 1993.
- [13] Halperin, A., Tirrel, M., Lodge, T. P., *Adv. Polym. Sci.* 100, 31, 1990.
- [14] Tsukahara, Y., Tsutsumi, K., Yamashita, Y., Shimada, S., *Macromolecules* 23, 5201, 1990.
- [15] Gitsow, I., Ivanova, P. T., Frechet, J. M. J., *Macromol. Rapid Commun.* 15, 387, 1994.

- [16] Beachaouch, S., Coutin, B., Sekiguchi, H., *Macromol. Rapid Commun.* 15, 125, 1994.
- [17] Antonietti, M., Nestl, T., *Macromol. Rapid Commun.* 15, 111, 1994.
- [18] Freed, K. F., Dudowicz, J., *Macromolecules* 29, 625, 1996.
- [19] Dudowicz, J., Freed, K. F., *Macromolecules* 24, 5112, 1991.
- [20] van Aert, H., *PhD - thesis*. Eindhoven University of Technology, The Netherlands, 1997.
- [21] McQuarrie, D. A., *Statistical Mechanics*. Harper and Row Publishers, New York, 1976.
- [22] Hansen, J. P., McDonald, I. R., *Simple theory of liquids*. Academic Press, London, UK, second edn., 1986.
- [23] Allen, M. P., Tildesley, D. J., *Computer Simulation of Liquids*. Clarendon, Oxford, 1987.
- [24] Frenkel, D., Smit, B., *Understanding Molecular Simulation from Algorithm to Applications*. Academic Press, Inc., San Diego, 1996.
- [25] Lacombe, R. H., Sanchez, I. C., *J. Phys. Chem.* 80, 2568, 1976.
- [26] Sanchez, I. C., Lacombe, R. H., *J. Phys. Chem.* 80, 2352, 1976.
- [27] Kleintjens, L. A., Koningsveld, R., *Colloid Polym. Sci.* 258, 711, 1980.
- [28] Nies, E., Cifra, P., *Macromolecules* 27, 6033, 1994.
- [29] ten Brinke, G., Karasz, F. E., *Macromolecules* 17, 815, 1984.
- [30] Kalikmanov, V. I., *Statistical Thermodynamics of Liquids*. Lecture course at the Eindhoven University of Technology, The Netherlands, 1995.
- [31] Wignall, G. D., *Encyclopedia of Polym. Sci. and Eng.*, vol. 10. John Wiley and Sons, New York, 2nd edn., 1987.
- [32] Baltá-Calleja, F. J., Vonk, C. G., in A. D. Jenkins (ed.), *Polymer Science Library*, vol. 8. Elsevier, Amsterdam, 1989.
- [33] Schweizer, K. S., Curro, J. G., *Advances in Polymer Science* 116, 321, 1994.

- [34] Lowden, L. J., Chandler, D., *J. Chem. Phys.* 59, 6587, 1973.
- [35] Lowden, L. J., Chandler, D., *J. Chem. Phys.* 62, 4246, 1975.
- [36] Freasier, B. C., *Chem. Phys. Lett.* 35, 280, 1975.
- [37] Jolly, D., Freasier, B. C., Bearman, R. J., *Chem. Phys. Lett.* 46, 75, 1977.
- [38] Freasier, B. C., Jolly, D., Bearman, R. J., *Mol. Phys.* 31, 255, 1976.
- [39] Tildesley, D. J., Street, W. B., *Mol. Phys.* 41, 85, 1980.
- [40] Aviram, I., Tildesley, D. J., *Mol. Phys.* 34, 881, 1977.
- [41] Schweizer, K. S., Curro, J. G., *Phys. Rev. Lett.* 58, 246, 1987.
- [42] Curro, J. G., Schweizer, K. S., *Macromolecules* 20, 1928, 1987.
- [43] Curro, J. G., Schweizer, K. S., *J. Chem. Phys.* 87, 1842, 1987.
- [44] Schweizer, K. S., Curro, J. G., *Macromolecules* 21, 3070, 1988.
- [45] Schweizer, K. S., Curro, J. G., *Macromolecules* 21, 3082, 1988.
- [46] Chandler, D., in E. W. Montroll, J. L. Lebowitz (eds.), *Studies in Statistical Mechanics VIII*, p. 275. North - Holland, Amsterdam, 1982.
- [47] Chandler, D., Andersen, H. C., *J. Chem. Phys.* 57, 1930, 1972.
- [48] Chandler, D., *J. Chem. Phys.* 59, 2742, 1973.
- [49] Hsu, C. S., Pratt, L. R., Chandler, D., *J. Chem. Phys.* 68, 4213, 1978.
- [50] Pratt, L. R., Hsu, C. S., Chandler, D., *J. Chem. Phys.* 68, 4213, 1978.
- [51] Lowden, L. J., Chandler, D., *J. Chem. Phys.* 61, 5228, 1974.
- [52] Grayce, C. J., Schweizer, K. S., *J. Chem. Phys.* 100, 6846, 1994.
- [53] Grayce, C. J., Yethiraj, A., Schweizer, K. S., *J. Chem. Phys.* 100, 6857, 1994.
- [54] Schweizer, K. S., Honnell, K. G., Curro, J. G., *J. Chem. Phys.* 96, 3211, 1992.

- [55] Melenkevitz, J., Schweizer, K. S., Curro, J. G., *Macromolecules* 26, 6190, 1993.
- [56] Melenkevitz, J., Curro, J. G., Schweizer, K. S., *J. Chem. Phys.* 99, 5571, 1993.
- [57] Flory hypothesized that in a polymer melt the intra-molecular excluded volume interactions, which tend to expand a polymer chain, are nominally cancelled by the inter-molecular excluded volume interactions, because a chain molecule is unable to differentiate neighbouring segments belonging to itself or to other molecules. The net results of these two opposite forces is that the average intra-molecular structure of a chain is ideal. Computer simulations and neutron scattering experiments on polymer melts corroborate the Flory ideality hypothesis.
- [58] Baxter, R. J., *J. Chem. Phys.* 49, 2770, 1968.
- [59] Lomba, E., in E. Kiran, J. M. H. L. Sengers (eds.), *Supercritical Fluids*. Kluwer Academic Publishers, The Netherlands, 1928-1931.
- [60] Janssen, R. H. C., Nies, E., Cifra, P., *Langmuir* 13, 2784, 1997.
- [61] Freed, K. F., *J. Phys. A* 18, 871, 1985.
- [62] Bawendi, M. G., Freed, K. F., Mohanty, U., *J. Chem. Phys.* 84, 7036, 1986.
- [63] Freed, K. F., Bawendi, M. G., *J. Phys. Chem.* 93, 2194, 1989.
- [64] Dudowicz, J., Freed, K. F., Madden, W. G., *Macromolecules* 23, 4830, 1990.
- [65] Szleifer, I., *J. Chem. Phys.* 92, 6940, 1990.
- [66] Weinhold, J. D., Kumar, S. K., Szleifer, I., *Europhysics Letters* 35, 695, 1996.

Chapter 2

Statistical thermodynamics and theories of chain liquids

2.1 Introduction

The relation between the thermodynamical and microscopic representation of molecular system is provided by the specialty of statistical mechanics. A selection of statistical mechanics results, necessary for the developments to come, are summarized. These general statistical mechanical tools are invoked to derive a number of (lattice) theories for polymer systems, that will serve as reference points for the new theoretical results derived in this thesis.

2.2 Statistical thermodynamics: Partition functions and thermodynamics

A sample of a real fluid contains in the order of 10^{23} particles. It is impossible and also not desirable to describe its behavior in all molecular details. For systems containing such large number of particles, we are rather interested in, e.g., the equilibrium thermodynamic properties which only depend on a limited number of state variables. Statistical mechanics provides the relationships between the details of the microscopic interactions of particles and the macroscopic behavior. Consider an isolated system of N structureless particles in a volume V and at temperature T . The total energy, or Hamiltonian, \mathcal{H}_N , of the system reads¹

$$\mathcal{H}_N = \sum_{i=1}^N \frac{\mathbf{p}_i^2}{2m} + U_N(\mathbf{r}^N) + U_{N,ext}(\mathbf{r}^N) \quad (2.1)$$

where, \mathbf{p}_i is the momentum of particle i , m is the mass of a particle, and $\mathbf{r}^N = (\mathbf{r}_1, \dots, \mathbf{r}_N)$ are the positions of the particles. The first term is the kinetic energy contribution to the total energy, $U_N(\mathbf{r}^N)$ is the total interaction potential energy and $U_{N,ext}$ is the contribution of an external field

$$U_{N,ext}(\mathbf{r}^N) = \sum_{i=1}^N u_{ext}(\mathbf{r}_i) \quad (2.2)$$

One of the basic results of statistical mechanics relates the probability $dW_N(\mathbf{r}^N, \mathbf{p}^N)$ to find N particles in the vicinity of the positions $\mathbf{r}_1, \dots, \mathbf{r}_N$ and having momenta in the vicinity of values $\mathbf{p}_1, \dots, \mathbf{p}_N$ to the Hamiltonian \mathcal{H}_N according to²

$$dW_N(\mathbf{r}^N, \mathbf{p}^N) = \frac{1}{Z_N} e^{-\beta \mathcal{H}_N} d\Gamma_N \quad (2.3)$$

where $e^{-\beta \mathcal{H}_N}$ is the Boltzmann factor with $\beta = 1/k_B T$, k_B is the Boltzmann constant and $d\Gamma_N$ is an element of the phase space volume

$$d\Gamma_N = \frac{d\mathbf{r}^N d\mathbf{p}^N}{(2\pi\hbar)^{3N}} \quad (2.4)$$

with $\hbar = h/2\pi$, and h the constant of Planck. The factor $(2\pi\hbar)^{3N}$ accounts for the Heisenberg's uncertainty principle.² The normalizing factor Z_N in eq 2.3 is called the canonical partition function given by¹

$$Z_N = \frac{1}{N!} \int \dots \int e^{-\beta \mathcal{H}_N(\mathbf{r}^N, \mathbf{p}^N)} d\Gamma_N \quad (2.5)$$

$1/N!$ accounts for the indistinguishability of the N particles.

In view of the independence of $U_N(\mathbf{r}^N)$ and $U_{N,ext}(\mathbf{r}^N)$ on \mathbf{p}^N , we can integrate Z_N over momenta. Moreover, this integration can be performed independently for all particles. The final result reads

$$Z_N = \frac{1}{N! \Lambda^{3N}} Q_N \quad (2.6)$$

where $\Lambda = (2\pi\beta\hbar^2/m)$ is the de Broglie thermal wavelength with m the mass of a particle and Q_N is the configurational partition function given by

$$Q_N = \int \dots \int e^{-\beta(U_N(\mathbf{r}^N) + U_{N,ext}(\mathbf{r}^N))} d\mathbf{r}^N \quad (2.7)$$

The configurational probability can be also found by integrating eq 2.3 over all momenta and is given by¹

$$dW_N(\mathbf{r}^N) = D_N(\mathbf{r}^N) d\mathbf{r}_1 \dots d\mathbf{r}_N \quad (2.8)$$

where

$$D_N(\mathbf{r}^N) = \frac{1}{Q_N} \exp[-\beta(U_N(\mathbf{r}^N) + U_{N,ext}(\mathbf{r}^N))] \quad (2.9)$$

is the probability density function in configurational space with the normalization $\int D_N(\mathbf{r}^N) d\mathbf{r}^N = 1$. The configurational probability $D_N(\mathbf{r}^N)$ can be used to calculate the average of any function of the coordinates, $X(\mathbf{r}^N)$, according to

$$\langle X(\mathbf{r}^N) \rangle = \int X(\mathbf{r}^N) D_N(\mathbf{r}^N) d\mathbf{r}^N \quad (2.10)$$

The Helmholtz free energy A of the system is related to the partition function as³

$$A = -k_B T \ln Z_N \quad (2.11)$$

which gives upon combination with eq 2.6

$$A = k_B T \ln(N! \Lambda^{3N}) - k_B T \ln Q_N \quad (2.12)$$

The first term in this equation is the kinetic contribution to the free energy and the second term gives the configurational contribution to the free energy.

As soon as the Helmholtz free energy is available, other thermodynamic functions are easily obtained via exact thermodynamic relations⁴

$$dA = -SdT - pdV + \mu dN \quad (2.13)$$

Thus,

$$S = -\left(\frac{\partial A}{\partial T}\right)_{V,N} = k_B T \left(\frac{\partial \ln Z_N}{\partial T}\right)_{V,N} + k \ln Z_N \quad (2.14a)$$

$$p = -\left(\frac{\partial A}{\partial V}\right)_{T,N} = k_B T \left(\frac{\partial \ln Z_N}{\partial V}\right)_{T,N} \quad (2.14b)$$

$$U_N = -T^2 \left(\frac{\partial A/T}{\partial T}\right)_{V,N} = k_B T^2 \left(\frac{\partial \ln Z_N}{\partial T}\right)_{V,N} \quad (2.14c)$$

$$\mu = \left(\frac{\partial A}{\partial N}\right)_{T,V} \quad (2.14d)$$

Furthermore, the thermodynamic relation such as eqs 2.12, 2.13 and 2.14 can be used to discuss heterogeneous phase equilibria. For instance, a pure component may exhibit liquid-vapor coexistence. In the pV -plane of a pure component depicted in figure 2.1, a stable, a metastable and an unstable region can be defined. In the stable region the fluid remains in one phase, whereas in the unstable

and metastable regions, a fluid will ultimately phase separate into two phases. These three regions are separated by the binodal and spinodal curves. The liquid-vapor binodal curve defines the coexistence between a liquid and a vapor phase and delineates the stable and meta-stable regions. Coexisting liquid and vapor phases obey the thermodynamic equilibria criteria

$$\mu_l = \mu_v \tag{2.15a}$$

$$p_l = p_v \tag{2.15b}$$

$$T_l = T_v \tag{2.15c}$$

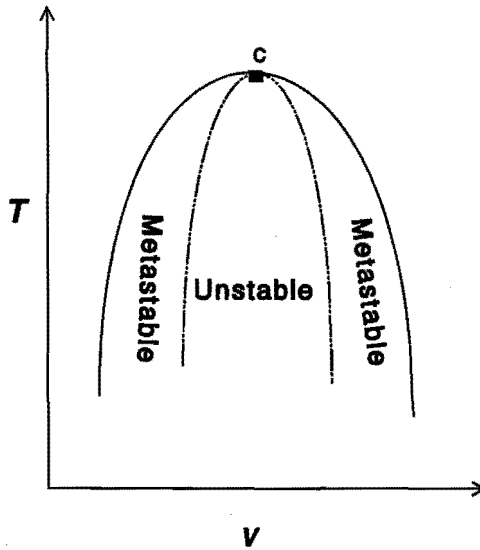


Figure 2.1: Phase diagram of a pure substance, showing liquid-vapor coexistence region. Binodal (—) and spinodal (---) curves, critical state (■).

At the spinodal curve, separating the meta-stable and unstable regions, the compressibility diverges, i.e. $\kappa_T \rightarrow \infty$, which corresponds to the following condition

$$\left. \frac{\partial^2 A}{\partial V^2} \right|_{N,T} = \left. \frac{-\partial p}{\partial V} \right|_{N,T} = \frac{1}{V\kappa_T} = 0 \tag{2.16}$$

Binodal and spinodal curves share a common tangent in the critical state obeying the conditions $\partial^2 A/\partial V^2|_{N,T} = 0$ and $\partial^3 A/\partial V^3|_{N,T} = 0$.

In addition to the vapor-liquid coexistence mixtures may also show heterogeneous liquid-liquid equilibria. Consider a binary mixture of components 1 and 2. Generally in the $pT\phi_2$ -space, with ϕ_2 the concentration of component 2, of a binary system a two-phase region or miscibility gap may exist bounded by the binodal condition

$$\mu'_1 = \mu''_1 \quad (2.17a)$$

$$\mu'_2 = \mu''_2 \quad (2.17b)$$

$$p' = p'' \quad (2.17c)$$

$$T' = T'' \quad (2.17d)$$

with the primes indicating the coexisting phases.

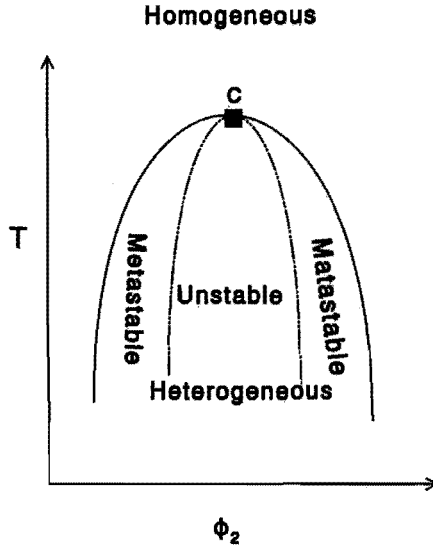


Figure 2.2: Phase diagram of a binary mixture, showing the liquid-liquid miscibility gap. Binodal (—) and spinodal (---) curves, critical state (■).

Again, the miscibility gap is subdivided by the spinodal in two metastable and one unstable regions. Binodal and spinodal make contact at the critical state, which for a strictly binary system is situated at the top of both curves. The spinodal and critical conditions obey the following conditions

$$\begin{aligned} \text{spinodal: } & \partial^2 G / \partial \phi_2^2 |_{T,p} = 0 \\ \text{critical: } & \partial^2 G / \partial \phi_2^2 |_{T,p} = 0 \quad \text{and} \quad \partial^3 G / \partial \phi_2^3 |_{T,p} = 0 \end{aligned} \quad (2.18)$$

with G the Gibbs free energy or free enthalpy.

2.3 Computer simulations: Monte Carlo technique

The average of configurational functions, such as $X(\mathbf{r}^N)$ defined in eq 2.10, can be obtained directly from computer simulation studies. For actual calculation, $\langle X \rangle$ may be estimated by approximating the integrals of eq 2.10 with sums over a finite number, \mathcal{N} , of configurations in the sample

$$\langle X \rangle \simeq \frac{\sum_l X(l) \exp[-\beta U_N(l)]}{\sum_l \exp[-\beta U_N(l)]} \quad (2.19)$$

where the sums run from $l = 1$ to $l = \mathcal{N}$, $U_N(l)$ is the total potential of configuration l . In order to eliminate the bias and balance the contribution of configurations, an appropriate weight is attached to each configuration. If $W(l)$ is the probability of choosing a configuration l , eq 2.19 will be

$$\langle X \rangle \simeq \frac{\sum_l X(l) \exp[-\beta U_N(l)]/W(l)}{\sum_l \exp[-\beta U_N(l)]/W(l)} \quad (2.20)$$

If the Boltzmann distribution is selected for $W(l)$, i.e.

$$W(l) = \exp[-\beta U_N(l)] \quad (2.21)$$

eq 2.20 reduces to

$$\langle X \rangle \simeq \frac{1}{\mathcal{N}} \sum_{l=1}^{\mathcal{N}} X(l) \quad (2.22)$$

In the well known Monte Carlo simulation technique the configurations are sampled by successive random displacements of N molecules in a box of volume V . The moves are accepted or rejected according to the Metropolis acceptance rules.⁵ Let $\Delta U_N = U_N(n) - U_N(l)$ denotes the change of total potential energy when the system changes from configuration l to n . A trial move is accepted unconditionally if ΔU_N is negative, but it is accepted only with a possibility $\exp(-\beta \Delta U_N)$ if ΔU_N is positive. It can be shown that the Metropolis acceptance rules lead to the correct Boltzmann distribution.

Computer simulations provide direct access to the thermodynamic properties based on the microscopic details embodied in the interactions of the system. Due to their empirical status, simulations are also referred as computer *experiments* and can be used, e.g. to test approximate theories.

2.4 Molecular model: The lattice model

To put the general statistical mechanical relationships to use, a model for the molecular interactions must be chosen. In the following applications it will be assumed that the total potential energy $U_N(\mathbf{r}^N)$ is pairwise decomposable

$$U_N(\mathbf{r}^N) = \sum_{i < j}^N u(\mathbf{r}_i, \mathbf{r}_j) \quad (2.23)$$

with $u(\mathbf{r}_i, \mathbf{r}_j)$ the interaction potential between segments i and j .

Furthermore, we will also adopt the lattice model. Despite the drawbacks connected to the lattice model, it is still quite popular in the theoretical studies of polymers. More precisely we will assume that the molecules can be placed on a cubic lattice (lattice coordination number $z = 6$) of N_L lattice sites in total of which N_h sites are vacant. Each molecule occupies s consecutive lattice sites. Hence the total volume V is given by

$$V = N_L v^* = (sN + N_h)v^* \quad (2.24)$$

with v^* the lattice site volume.

Furthermore, the interactions between non-covalently bonded segments are defined by nearest neighbor interaction energy, $-\epsilon$ ($\epsilon \geq 0$). Hence, the total interaction potential given by eq 2.23 can be written as

$$U_N(\Psi) = -n(\Psi)\epsilon \quad (2.25)$$

with $n(\Psi)$ the number of nearest neighbor contact pairs in the lattice configuration Ψ , which is described by all positions of all segments on the lattice. On the lattice the configurational integral, eq 2.7, reduces to a configurational sum over the set $\{\Psi\}$ of all allowed lattice configurations

$$Q_N = \sum_{\{\Psi\}} \exp(-\beta U_N(\Psi)) \quad (2.26)$$

There are several practical advantages to the lattice model. First, the actual calculation on the lattice is significantly easier than the calculation of the off-lattice model.⁶ Second, simulations are much easier and less time consuming on-lattice than off-lattice.⁶⁻¹⁰ It is well known and explained in paragraph 2.3 that molecular simulations provide essentially exact information for the investigated model.¹¹ Hence, the more efficient lattice simulations can provide more information and make a more extensive comparison amenable.

2.5 Partition function theories

2.5.1 The Flory-Huggins theory

The Flory-Huggins (FH) mean field theory has been formulated more than half a century ago. The starting point of these authors was a mixture of N_h solvents and N chain molecules each occupying 1 and s connective sites respectively on the lattice. The volume of the system does not change upon mixing, i.e. $V = N_h v^* + sNv^* = N_L v^*$. Assuming that the interaction potential energy U_N does not depend on the particular configuration Ψ of the system, eq 2.26 can be factored as follows

$$Q_N = \exp(-\beta U_N) \sum_{\Psi} 1 = \exp(-\beta U_N) \Omega \quad (2.27)$$

where Ω is the total number of allowed lattice configurations. Combining eqs 2.27, 2.12 and 2.14a and concentrating on the configurational aspects, the entropy of the system is given by

$$S = k_B \ln \Omega \quad (2.28)$$

Flory assumed that each segment can be placed independently on the lattice, therefore, the total number of configurations Ω is given by the product of independent segmental contributions¹²

$$\Omega(N, T, V) = \frac{(N_h + sN)!}{N_h! N!} \left(\frac{z-1}{N_L}\right)^{N(s-1)} \quad (2.29)$$

By introducing Stirling's approximation for the factorials, $n! = (n/e)^n$, and some algebraic manipulation the entropy, S , is given by

$$S = -k_B \{ N_h \ln [N_h / (N_h + sN)] + N \ln [sN / (N_h + sN)] - N \ln s - N(s-1) \ln [(z-1)/e] \} \quad (2.30)$$

The composition dependent contribution to S , the first two terms on the rhs, are known as the FH(S) combinatorial entropy. The other contributions are due to the conformational entropy of the molecules. The entropy of mixing ΔS can be calculated according to

$$\Delta S = S - S_p - S_h = -k_B [N_h \ln \phi_h + N \ln \phi] \quad (2.31)$$

with S_h and S_p the entropies of solvent and s -mer in the pure state; $\phi = sN/N_L$ and $\phi_h = 1 - \phi$ the volume fractions of polymer and solvent respectively.

The excess interaction energy ΔU is given by¹²

$$\frac{\beta\Delta U}{N_L} = \frac{\beta(U - U_h - U_p)}{N_L} = \left(\frac{N_h}{N_h + N_s}\right)\left(\frac{N_s}{N_h + N_s}\right)z\beta(\epsilon_{hp} - \frac{\epsilon_{hh} + \epsilon_{pp}}{2}) = \phi_h\phi_s\chi \quad (2.32)$$

where $\chi = z\beta[-2\epsilon_{hp} + (\epsilon_{hh} + \epsilon_{pp})]/2$ is the Flory-Huggins parameter, U_p and U_h are the internal energies of pure s -mers and pure solvent respectively. Combining eqs 2.31 and 2.32 the corresponding expression for the excess Helmholtz free energy of the binary mixture *per lattice site* is

$$\frac{\beta\Delta A}{N_L} = \frac{\beta(A - A_h - A_p)}{N_L} = \phi_h \ln \phi_h + \frac{\phi_s}{s} \ln \phi_s + \chi\phi_h\phi_s \quad (2.33)$$

Eq 2.33 is the celebrated Flory-Huggins (Staverman) expression and was independently derived by Flory, Huggins and Staverman. However, it is the Flory derivation that leads to the simple result, eq 2.33. Huggins and also Staverman derived extra refinements to this basic result. In particular, the Huggins expression is discussed in the subsequent paragraph. Eq 2.33 can be recast to describe the excess Helmholtz free energy of a compressible pure component. In this case, the lattice sites occupied by solvent molecules are assumed to be vacant. Making the following associations: $\epsilon_{hh} = \epsilon_{hp} = 0$, $\epsilon_{pp} = \epsilon$, $\phi = y$ and $\phi_h = 1 - y$; with y occupied site fraction, the excess free energy expression *per segment* reads¹³

$$\frac{\beta\Delta A}{N_s} = \frac{1-y}{y} \ln(1-y) + \frac{1}{s} \ln y - \frac{z}{2}\beta\epsilon(1-y) \quad (2.34)$$

The corresponding expression for the Helmholtz free energy of the pure component is given by¹³

$$\frac{\beta A}{N_s} = \frac{1-y}{y} \ln(1-y) + \frac{1}{s} \ln y - \frac{z}{2}\beta\epsilon y \quad (2.35)$$

2.5.2 The Huggins theory

In the Flory-Huggins theory the influence of chain connectivity on the configurational properties is completely ignored and segments in a chain can be inserted independently. Huggins formulated a correction for chain connectivity, including the effect of nearest neighbor covalent bonds, resulting in an additional entropic contribution. If the nearest neighbor connectivity is also taken into consideration for the internal energy an additional composition or density dependence is found. The Huggins Helmholtz free energy for a single pure component is given by

$$\frac{\beta A}{N_s} = \frac{1-y}{y} \ln(1-y) + \frac{1}{s} \ln y - \frac{1-\alpha y}{\gamma y} \ln(1-\alpha y) + \frac{(1-\alpha)}{\gamma} \beta\epsilon y \quad (2.36)$$

where $\gamma = 2/z$; $\alpha = \gamma(1 - 1/s)$ is the average fraction of covalent contacts of a segment in an s -mer; $q = (1 - \alpha)y/(1 - \alpha y)$ is the inter-segmental contact fraction of a chain, which is a measure for the number of non-covalent contacts the s -mers can make.

The Flory-Huggins theory is recovered by assuming an infinite coordination number, i.e. $z \rightarrow \infty$, thus, $\alpha = 0$ and the inter-segmental contact fraction reduces to the occupied site fraction, i.e. $q = y$. The Flory-Huggins and Huggins theories successfully and qualitatively explain a number of features of the thermodynamic properties of polymers. However, in these simple mean field theories random mixing is assumed. The random mixing theory is a good approximation for weakly interacting polymers, but it is certainly not for stronger interactions.

2.5.3 The non-random mixing Theory

a. Mixture of monomers A/B Guggenheim came to meet the dissatisfaction with the random mixing approximation by developing his quasi-chemical (non-random mixing) theory.¹⁴ At first, consider a binary mixture of monomers of type A and B . Although for a mixture of two monomers the total number of configurational states on the lattice is given by eq 2.29 ($s = 1$), the distinct configurational states Ψ need further specification according to the number of C_{AA} , C_{BB} and C_{AB} contact pairs. Let us denote, for a mixture of monomers, the number of AB pairs in a particular configuration by zx . Then the number of AA pairs equals $\frac{1}{2}z(N_A - x)$ and the number of BB pairs is $\frac{1}{2}z(N_B - x)$. Guggenheim assumed the different type of contact pairs to be independent and proposed the following expression for the number of configurations with a given number of AB pairs zx , $\Omega(N_A, N_B, x)$ ¹⁴

$$\Omega(N_A, N_B, x) = h(N_A, N_B) \frac{\{\frac{1}{2}z(N_A + N_B)\}!}{\{\frac{1}{2}z(N_A - x)\}! \{\frac{1}{2}zx\}! \{\frac{1}{2}zx\}! \{\frac{1}{2}z(N_B - x)\}!} \quad (2.37)$$

where $h(N_A, N_B)$ is a normalizing factor and $\frac{1}{2}z(N_A + N_B)$ is the total number of contact pairs.

The summation of eq 2.37 over all values of x must equal the total number of configurations, given by eq 2.29 ($s = 1$)

$$\sum_x \Omega(N_A, N_B, x) = \frac{(N_A + N_B)!}{N_A! N_B!} \quad (2.38)$$

As an approximation the sum on the left hand side of eq 2.38 can be replaced by its maximum term which can be found by differentiating eq 2.37 with respect to

x and setting the result equal to zero. The most likely value of x , obtained in the case of random mixing and denoted by x^* , obeys the condition

$$x^{*2} = (N_A - x^*)(N_B - x^*) \quad (2.39)$$

Combining eqs 2.37 and 2.38 with the maximum condition, the normalizing factor, $h(N_A, N_B)$, can be obtained

$$h(N_A, N_B) = \frac{(N_A + N_B)! \{\frac{1}{2}z(N_A - x^*)\}! \{\frac{1}{2}zx^*\}! \{\frac{1}{2}zx^*\}! \{\frac{1}{2}z(N_B - x^*)\}!}{N_A!N_B! \{\frac{1}{2}z(N_A + N_B)\}!} \quad (2.40)$$

Substituting eqs 2.40 into 2.37 we then have

$$\Omega(N_A, N_B, x) = \frac{(N_A + N_B)! \{\frac{1}{2}z(N_A - x)\}! \{\frac{1}{2}zx\}! \{\frac{1}{2}zx\}! \{\frac{1}{2}z(N_B - x)\}!}{N_A!N_B! \{\frac{1}{2}z(N_A - x)\}! \{\frac{1}{2}zx\}! \{\frac{1}{2}zx\}! \{\frac{1}{2}z(N_B - x)\}!} \quad (2.41)$$

For the interacting monomer mixture, the internal energy of a particular configuration with a given number of contact pairs is given by

$$U_N = -\beta z/2(N_A\epsilon_{AA} + N_B\epsilon_{BB} - x\Delta W) \quad (2.42)$$

where $\Delta W = \epsilon_{AA} + \epsilon_{BB} - 2\epsilon_{AB}$.

Note that only the last term depends on the configuration of the molecules on the lattice as prescribed by the parameter x . The configurational partition function is given by

$$Q_N = \sum_x \Omega(N_A, N_B, x) \exp\{-\beta z/2(N_A\epsilon_{AA} + N_B\epsilon_{BB} - x\Delta W)\} \quad (2.43)$$

Again we may approximate the sum by its maximum term. If we denote the value of x in the maximum term by \bar{x} , we have

$$Q_N = \Omega(N_A, N_B, \bar{x}) \exp\{-\beta z/2(N_A\epsilon_{AA} + N_B\epsilon_{BB} - \bar{x}\Delta W)\} \quad (2.44)$$

where \bar{x} , determined by $\partial \ln Q_N / \partial \bar{x} = 0$, obeys the so-called quasi-chemical condition

$$\bar{x}^2 = (N_A - \bar{x})(N_B - \bar{x})e^{-\Delta W/k_B T} \quad (2.45)$$

Alternatively, for athermal mixture ($\Delta W = 0$) we recover the random mixing result¹⁴

$$\bar{x}^2 = (N_A - \bar{x})(N_B - \bar{x}), \text{ i.e. } \bar{x} = x^* \text{ for } \Delta W = 0 \quad (2.46)$$

b. Pure component s -mers A similar procedure can be applied to a compressible pure polymer. Here we will only summarize the main results. Let us define some useful variables pertinent to the subsequent discussion: the non-bonded contacts of an s -mer $zq_c = s(z-2) + 2 = sz(1-\alpha)$; the total number of segmental contact pairs $q_t = zq_c N/2$; the number of segment-vacancy contact pairs $q_t x$, with x a microscopic parameter defining the fraction of segment-vacancy contact pairs in relation to the total number of segmental contact pairs q_t . The number of segment-segment contacts is $q_t(q-x)$ and the number of hole-hole contacts is $q_t(1-q-x)$. Following Guggenheim, the number of configuration $\Omega(N, T, V, \bar{x})$ is approximated by¹⁴

$$\Omega(N, T, V, x) = N_H \frac{[q_t(q-x^*)]! [(q_t x^*)!]^2 [q_t(1-q-x^*)]!}{[q_t(q-x)]! [(q_t x)]^2 [q_t(1-q-x)]!} \quad (2.47)$$

where $x^* = q(1-q)$ is the value of x for random mixing, and N_H is a normalization factor that assures that eq 2.47 reduces to the combinatorial entropy of Huggins, eq 2.36, for the random mixing case. The partition function is given by an equation similar to eq 2.43 and can again be approximated by the maximum term of the sum

$$\begin{aligned} Q_N(N, T, V) &= \sum_x \Omega(N, T, V, x) \exp[-\beta\epsilon(N, T, V, x)] \\ &\cong \Omega(N, T, V, \bar{x}) \exp[-\beta\epsilon(N, T, V, \bar{x})] \end{aligned} \quad (2.48)$$

The microscopic parameter \bar{x} can be computed from the maximum condition

$$\bar{x}^2 = e^{\epsilon/k_B T} (1-q-\bar{x})(q-\bar{x}) \quad (2.49)$$

2.5.4 The conformational theory of Szleifer

Another interesting approach is due to Szleifer et al.^{15,16} The configurational energy of a polymer solution is given by an expression similar to eq 2.25

$$U_N(\Psi) = n_{hh}(\Psi)\epsilon_{hh} + n_{pp}(\Psi)\epsilon_{pp} + n_{hp}(\Psi)\epsilon_{hp} \quad (2.50)$$

where $n_{pp}(\Psi)$, $n_{hh}(\Psi)$ and $n_{hp}(\Psi)$ are the number of polymer-polymer, solvent-solvent and polymer-solvent contacts in the lattice configuration Ψ and ϵ_{ij} are the corresponding interaction energies. The number of contacts can be written in terms of the total number of polymer or solvent molecules and the number of polymer-solvent contacts.

$$2n_{hh}(\Psi) = zN_h - n_{ph}(\Psi) \quad (2.51a)$$

$$2n_{pp}(\Psi) = [s(z-2) + 2]N - n_{ph}(\Psi) \quad (2.51b)$$

The configuration Ψ is specified by the conformations of the N chains, denoted by $(\nu_1, \nu_2, \dots, \nu_N)$, and the positions of the molecules \mathbf{r}^N , i.e. $\Psi \equiv \{\nu_1, \nu_2, \dots, \nu_N, \mathbf{r}^N\}$. Substituting eqs 2.51 in eq 2.25 we have

$$U_N(\Psi) = \frac{z}{2} N_h \epsilon_{hh} + \frac{1}{2} [s(z-2) + 2] N \epsilon_{pp} + [\epsilon_{hp} - \frac{1}{2}(\epsilon_{pp} + \epsilon_{hh})] n_{hp}(\Psi) \quad (2.52)$$

In this equation only the last term depends on the configuration Ψ of the molecules, the first two terms merely add a constant to the internal energy, therefore, the partition function can be written as

$$Q_N = C \sum_{\{\Psi\}} \exp[-\beta \frac{\Delta W}{2} n_{hp}(\Psi)] \quad (2.53)$$

where C is a constant that has no influence on thermodynamic mixing properties. As an approximation, the partition function is factorized in two independent contributions accounting for the conformational and translational degrees of freedom. More precisely, from the partition function the contribution $\Omega(\mathbf{r}^N)$, representing the different ways the molecules can be placed on the lattice taking account of their connectivity but not of their different conformations, is factored. This configurational contribution is multiplied by N sums over all possible conformations of a single chain (all chains are assumed to be independent). Thus, the total partition function Q_N is approximated by

$$Q_N \cong \Omega(\mathbf{r}^N) \left(\sum_{\nu} \exp[-\beta \frac{\Delta W}{2} n_{hp}(\nu)] \right)^N \quad (2.54)$$

where the sum is now only over all possible conformations ν of a single molecule, irrespective of the position.

Szleifer invoked for $\Omega(\mathbf{r}^N)$ the FH(S) combinatorial entropy (see eq 2.29). To evaluate the sums in eq 2.54 the number of contacts that a polymer molecule in conformation ν has with solvent molecules, $n_{hp}(\nu)$, must be known. Szleifer suggested the following approximation¹⁵

$$n_{hp}(\nu) = (1 - \phi) n_e(\nu) \quad (2.55)$$

where $(1 - \phi)$ is the solvent volume fraction, and $n_e(\nu)$ is the total number of neighbors the chain in conformation ν has with other polymer molecules or with solvent molecules. Combining eqs 2.54 and 2.55 with the combinatorial entropy of Flory-Huggins theory, we have

$$\frac{\beta A}{N_L} = (1 - \phi) \ln(1 - \phi) + \frac{\phi}{s} - \frac{\phi}{s} \ln q_f(\phi, T) \quad (2.56)$$

where q_f is the effective *internal partition function* given by

$$q_f(\phi, T) = \sum_{\nu} \exp\left[-\beta \frac{\Delta W}{2} n_e(\nu)(1 - \phi)\right] \quad (2.57)$$

The total number of neighbors of a single chain in conformation ν can be obtained from a single chain Monte-Carlo simulation.

Similarly, as we discussed for the Flory-Huggins theory, eq 2.56 can be applied to describe a compressible pure polymer system. The excess Helmholtz free energy per segment for a compressible pure s -mer is

$$\frac{\beta \Delta A}{sN} = \frac{1-y}{y} \ln(1-y) + \frac{1}{s} \ln y - \frac{1}{s} \ln q_f(y, T) \quad (2.58)$$

with $q_f(y, T) = \sum_{\nu} \exp[-\beta \frac{\epsilon}{2} n_e(\nu)(1-y)]$.

In this theory the correction of chain conformation properties is limited in the energetic part of the free energy expression. For athermal conditions ($\epsilon = 0$ or $\Delta W = 0$) the Szleifer theory reduces to the simple FH theory combinatorial entropy.

2.5.5 The theory of Weinhold, Kumar and Szleifer

More recently, the influence of the conformational properties of polymers on the combinatorial entropy was considered also for athermal ($\epsilon = 0$) chains.¹⁶ In this theory the total entropy was split in configurational and conformational contributions. The configurational entropy S_{pack} was assumed to be given by a Huggins-Guggenheim-type combinatorial expression¹⁶

$$\frac{S_{pack}}{k_B N s} = -\frac{1-y}{y} \ln(1-y) - \frac{1}{s} \ln y + \frac{1-\omega'y}{\gamma y} \ln(1-\omega'y) \quad (2.59)$$

with $\omega' = 1 - \langle n_e(\nu) \rangle / zs$, $\langle n_e(\nu) \rangle$ the average total number of neighbors the chain in conformation ν has with other polymer molecules or with solvent molecules.

This entropy expression is very similar to that of the Huggins theory given in eq 2.36, provided the intra-molecular contact fraction ω' is defined.

The conformational entropy S_{conf} is

$$\frac{S_{conf}}{k_B} = -N \sum_{\nu} P(\nu) \ln P(\nu) \quad (2.60)$$

where $P(\nu)$ denotes the probability of the chains being in conformation ν . The total entropy of the system, $S = S_{pack} + S_{conf}$, is now maximized subject to the constraint that

$$\sum_{\nu} P(\nu) = 1 \quad (2.61)$$

to produce the final result for the probability of the chain being in conformation ν ,

$$P(\nu) = \frac{P_0(\nu)}{q_{sc}} \exp[\chi_{pack} n_e(\nu)] \quad (2.62)$$

where q_{sc} is a normalization factor, $P_0(\nu)$ is the probability of a single athermal chain in conformation ν and χ_{pack} is the ‘interaction parameter’ which originates exclusively from entropic packing considerations and is given by

$$\chi_{pack} = \frac{1}{2} + \frac{1}{2\omega'y} \ln(1 - \omega'y) \quad (2.63)$$

Again $P_0(\nu)$ can be obtained from a MC simulation of the isolated chain.

2.5.6 The lattice cluster theory

a. Athermal chains Freed and coworkers followed a quite different path to evaluate the lattice configurational partition function Q_N , given by eq 2.26.¹⁷⁻²⁰ The condition that lattice sites i and j are nearest neighbors can be presented by a Kronecker delta function, $\delta(\mathbf{r}_i, \mathbf{r}_j + \mathbf{a}_\sigma)$, with \mathbf{r}_i denoting the position of the i th lattice site with respect to the origin of coordinates and \mathbf{a}_σ , $\sigma = 1, \dots, z$, designating the vectors from a given lattice site to the z nearest neighbor lattice sites. The $\delta(i, j + \sigma) = \delta(\mathbf{r}_i, \mathbf{r}_j + \mathbf{a}_\sigma)$ function can be used to represent the bonding constraints for a set of N linear polymers with $s - 1$ bonds each. For example, the first bond on the first chain enters into the counting scheme with the factor of $\sum_{\sigma_1} \delta(i_1^1, i_2^1 + \sigma_1^1)$, where the superscript labels the chain number, the subscript labels the sequential monomer numbering along the chain. The bond in question may be in z different possible orientations. The next bond has the weight factor of $\sum_{\sigma_2} \delta(i_2^1, i_3^1 + \sigma_2^1)$ with the additional excluded volume constraint that sites $i_3^1 \neq i_1^1$, etc. Continuing this process for all bonds and all chains the partition function may be derived. Summarizing, the partition function for an athermal monodisperse linear polymer of chain length s may be written in terms of delta

functions, prohibiting bonded monomers from occupying the same lattice site

$$Q_N = \frac{1}{2^N} \sum_{i_1^1 \neq i_2^1 \neq \dots \neq i_1^s, \neq i_1^2 \neq i_2^2 \neq \dots \neq i_2^s, \neq i_1^N \neq i_2^N \neq \dots \neq i_N^s} \prod_{m=1}^N \left\{ \prod_{l=1}^{s-1} \sum_{\sigma_l^m} \delta(i_l^m, i_{l+1}^m + \sigma_l^m) \right\} \quad (2.64)$$

where the factor $1/2$ stems from the symmetry number of each chain. The Kronecker δ -function can be replaced by its lattice Fourier transform

$$\delta(i, j + \sigma) = N_L^{-1} \sum_{\mathbf{q}} \exp[i\mathbf{q} \cdot (\mathbf{r}_i - \mathbf{r}_j - \mathbf{a}_\sigma)] \quad (2.65)$$

where the sum involving \mathbf{q} runs over the first Brillouin zone.²¹ The sum over all z possible orientations, $\sum_{\sigma} \delta(i, j + \sigma)$, can be rewritten as

$$\sum_{\sigma} \delta(i, j + \sigma) = \frac{z}{N_L} \left\{ 1 + \frac{1}{z} \sum_{\mathbf{q} \neq 0} f(\mathbf{q}) \exp[i\mathbf{q} \cdot (\mathbf{r}_i - \mathbf{r}_j)] \right\} \quad (2.66)$$

with $f(\mathbf{q}) = \sum_{\sigma=1}^z \exp(-i\mathbf{q} \cdot \mathbf{a}_\sigma)$. The unity term at the rhs is the $\mathbf{q} = 0$ contribution.

Employing eq 2.65 for each Kronecker δ the partition function, Q_N , for N athermal chains is given by

$$Q_N = \frac{1}{2^N} \sum_{i_1^1 \neq \dots \neq i_N^s} \prod_{m=1}^N \prod_{l=1}^{s-1} \left[\frac{z}{N_L} (1 + X_{l,m}) \right] \quad (2.67a)$$

$$X_{l,m} = \frac{1}{z} \sum_{\mathbf{q}_l^m \neq 0} f(\mathbf{q}_l^m) \exp[i\mathbf{q}_l^m \cdot (\mathbf{r}_{i_l^m} - \mathbf{r}_{i_{l+1}^m})] \quad (2.67b)$$

with $X_{l,m}$ accounting for the corrections arising from the correlations in monomer positions. The leading contribution in eq 2.67a, i.e the unity terms for each l and m , yields the Flory-Huggins mean field approximation. Thus corrections to the Flory-Huggins mean field theory from correlations in monomer positions are given by $X_{l,m}$.

b. Interacting chains The total interaction energy may be written as

$$U_N = \sum_{i \in S_k, j \in S_k} \beta \epsilon^{ij} = \sum_{i \in S_k, j \in S_k} \beta \epsilon \quad (2.68)$$

where $\epsilon^{ij} = \epsilon$ is the interaction potential between nearest neighbor segments i and j , S_k is the set of lattice sites occupied by segments. The total interaction

energy may be expanded as

$$\begin{aligned}
 \exp(\beta \sum_{i \in S_k, j \in S_k} \epsilon^{ij}) &= \prod_{i \in S_k, j \in S_k} [1 + \sum_{\sigma=1}^z \delta(i, j + \sigma) f^{ij}] \\
 &= 1 + \sum_{\sigma=1}^z \sum_{i > j} \delta(i, j + \sigma) f^{ij} + \sum_{\sigma, \sigma'=1}^z \sum_{i > j \neq i' > j'} \delta(i, j + \sigma) \delta(i', j' + \sigma') f^{ij} f^{i'j'} + \dots
 \end{aligned} \tag{2.69}$$

where f^{ij} is the Mayer f function

$$f^{ij} = \exp(\beta \epsilon^{ij}) - 1 = \exp(\beta \epsilon) - 1 = f \tag{2.70}$$

The total partition function for interacting polymers can be obtained by multiplying the right-hand side of eq 2.64 by the right-hand side of eq 2.69, viz.

$$Q_N = \frac{1}{2^N} \sum_{i_1^1 \neq i_2^1 \neq \dots \neq i_N^1} \prod_{m=1}^N \prod_{l=1}^{s-1} \sum_{\sigma_l^m} \delta(i_l^m, i_{l+1}^m + \sigma_l^m) \exp\left(\sum_{i \in S_k, j \in S_k} \beta \epsilon^{ij}\right) \tag{2.71}$$

The sum over i and j in eq 2.71 runs over all pairs of lattice sites that are occupied by polymers. Therefore the summation indices in the exponent portion of eq 2.71 are connected to the overall ones that also appear in the “configuration contribution” arising from eq 2.64.

Making use of eqs 2.67a and 2.69 the partition function can be cast into an expansion in z^{-1} and $\beta\epsilon$. Currently the LC expansion has been presented for the first-order energy contribution through order z^{-2} corrections, for the second-order energy contribution through order z^{-1} corrections, and for the leading third- and fourth-order energies. The lattice cluster theory has been presented for compressible polymer mixtures and solutions involving structural details such as polymers with short chain branching, block copolymers and structured monomers.^{22,23}

2.6 Statistical thermodynamics: Integral equation theory

2.6.1 Distribution functions

Another successful theoretical route to the thermodynamic properties and the microscopic structure of fluids is provided by integral equation theory. Eq 2.8 has defined the probability to find particle 1 in volume element dr_1 , particle 2

in $d\mathbf{r}_2 \dots$ and particle N in $d\mathbf{r}_N$. We can also define the s -particle distribution functions $\rho^s(\mathbf{r}^s)$ as¹

$$\rho^s(\mathbf{r}^s) = \frac{N!}{(N-s)!} \int D_N(\mathbf{r}^N) d\mathbf{r}_{s+1} \dots d\mathbf{r}_N \quad (2.72)$$

with normalization

$$\int \rho^{(s)}(\mathbf{r}^s) d\mathbf{r}^s = \frac{N!}{(N-s)!} \quad (2.73)$$

The s -particle distribution function $\rho^s(\mathbf{r}^s)$ represents the probability that any particle in volume element $d\mathbf{r}_1, \dots$, and any particle is in $d\mathbf{r}_s$. As a special case, the 1-particle distribution function is $\int \rho^{(1)}(\mathbf{r}) d\mathbf{r} = N$, irrespective of the position of all other particles. For a homogeneous system $\rho^{(1)}(\mathbf{r})$ is constant throughout the system and equal to the overall number densities ρ , i.e. $\rho^{(1)}(r) = \rho = N/V$.

Now let's define s -particle correlation functions as

$$g^{(s)}(\mathbf{r}_1 \dots \mathbf{r}_s) = \frac{\rho^{(s)}(\mathbf{r}_1 \dots \mathbf{r}_s)}{\rho^s} \quad (2.74)$$

Combining this equation with eqs 2.9 and 2.72, the s -particle correlation functions is given by^{1,4}

$$g^{(s)}(\mathbf{r}_1 \dots \mathbf{r}_s) = \frac{N!}{(N-s)! \rho^s Q_N} \int \dots \int \exp(-\beta U_N(\mathbf{r}^N)) d\mathbf{r}_{s+1} \dots d\mathbf{r}_N \quad (2.75)$$

Among the s -particle correlation functions, $g^{(2)}(\mathbf{r}_1, \mathbf{r}_2) = g(\mathbf{r}_1, \mathbf{r}_2)$ plays an important role. Physically, $\rho g(\mathbf{r}_1, \mathbf{r}_2)$ gives the number of particles in volume element $(\mathbf{r}_2, \mathbf{r}_2 + d\mathbf{r}_2)$ while there is a molecule in $(\mathbf{r}_1, \mathbf{r}_1 + d\mathbf{r}_1)$. In an isotropic liquid of spherically symmetric molecules, $g(\mathbf{r}_1, \mathbf{r}_2)$ depends only upon the relative distance between molecules 1 and 2, i.e. upon r_{12} . we usually denote r_{12} simply by r . Clearly, $g \rightarrow 0$ as $r \rightarrow 0$ since molecules become effectively 'hard' as $r \rightarrow 0$ and $g \rightarrow 1$ as $r \rightarrow \infty$ since the influence of the central particle diminishes as r becomes large.

The pair distribution function is of central importance in the theory of fluid for two reasons. First, if the potential energy of the N -body system is pair-wise additive, all the thermodynamic functions of the system can be written in terms of $g(r)$. The following relations exist

$$\frac{U_N}{Nk_B T} = \frac{3}{2} + \frac{\rho}{2k_B T} \int_0^\infty u(r) g(r, \rho, T) 4\pi r^2 dr \quad (2.76a)$$

$$\frac{p}{k_B T} = \rho - \frac{\rho^2}{6k_B T} \int_0^\infty r \frac{\partial u(r)}{\partial r} g(r) 4\pi r^2 dr \quad (2.76b)$$

$$\frac{\mu}{k_B T} = \ln \rho \Lambda^3 + \frac{\rho}{k_B T} \int_0^1 \int_0^\infty u(r) g(r, \xi) 4\pi r^2 d\xi dr \quad (2.76c)$$

where U_N is the total energy of the system, p is the pressure, μ , the chemical potential and ξ is a coupling parameter. The coupling parameter, varying from 0 to 1, is chosen in order to “couple” one molecule, say molecule 1, to the studied system. Thus, a theory for the pair correlation function yields an alternative way to the thermodynamics of the system. Second, the static structure factor $S(k)$, involving the Fourier transform of $\rho g(r)$, can be directly measured in X-ray or neutron scattering experiments.²⁴

$$S(k) = 1 + \rho \int dr e^{ik \cdot r} (g(r) - 1) \quad (2.77)$$

2.6.2 Ornstein-Zernike equation

In this study, the Ornstein-Zernike (OZ) equation is applied to facilitate the calculation of the 2-particle correlation function $g(r)$. In the OZ equation the total correlation function, $h(r_{12}) = g(r_{12}) - 1$, between particles 1 and 2 is decoupled into a direct and an indirect part. The direct part is given by a function, $c(r_{12})$, the direct correlation function. The indirect part is the influence propagated directly from molecule 1 to a molecule 3, which in turn exerts its influence on 2. This effect is weighted by the density and averaged over all positions of molecule 3,

$$\begin{aligned} h(\mathbf{r}_1, \mathbf{r}_2) = & c(\mathbf{r}_1, \mathbf{r}_2) + \rho \int \rho(\mathbf{r}_3) c(\mathbf{r}_1, \mathbf{r}_3) c(\mathbf{r}_3, \mathbf{r}_2) d\mathbf{r}_3 \\ & + \int \rho(\mathbf{r}_3) \rho(\mathbf{r}_4) c(\mathbf{r}_1, \mathbf{r}_3) c(\mathbf{r}_3, \mathbf{r}_4) c(\mathbf{r}_4, \mathbf{r}_2) d\mathbf{r}_3 d\mathbf{r}_4 + \dots \end{aligned} \quad (2.78)$$

In eq 2.78 the integrals over the repeated coordinates $d\mathbf{r}_i$ can be collected, resulting the OZ integral equation

$$h(r_{12}) = c(r_{12}) + \rho \int c(r_{13}) h(r_{23}) d\mathbf{r}_3 \quad (2.79)$$

Eq 2.79 is merely a convenient reformulation of the total pair correlation function in terms of the direct correlation function, which is shown to be of a much shorter spatial range.^{1,4} In order to solve the OZ equation an additional relation between $h(r_{12})$ and $c(r_{12})$ is required. So far only approximate, so-called closure relations, are available. Two well known closure relations are the Percus-Yevick (PY) and the mean-spherical approximation (MSA) closures. The PY approximation is^{25,26}

$$c(r) = g(r)(1 - e^{\beta u(r)}) \quad (2.80)$$

and the MSA approximation is given by²⁷

$$c(r) = -\beta u(r) \quad (2.81)$$

The OZ equation has been analytically solved for hard spheres within the approximate PY closure²⁵ by Wertheim²⁸ and Thiele.²⁹ The OZ equation offers a satisfactory prediction for the corresponding simulation results.³⁰ The MSA approximation has been applied to the Lennard-Jones fluids³¹ and a model of liquid potassium.³² In each case, satisfactory results have been obtained.

2.6.3 RISM: The reference interaction site model

The OZ integral equation was generalized by Chandler and co-workers to molecular fluids by employing a reference interaction site model (RISM) with a given intra-molecular structure.³³ In the RISM theory, a molecule is viewed as consisting of a collection of spherically symmetric interacting sites or chemical subunits connected by covalent bonds. The total interaction potential is taken as the sum over all pairs of interaction sites.

In analogy with the OZ equation of a simple fluid, the total correlation function $h_{ij}(\mathbf{r}_1, \mathbf{r}_2)$ between the pair of segments i and j is considered to propagate in a sequential manner by direct correlations, $c_{ij}(r_1, r_2)$, between segments belonging to different molecules and by intra-molecular correlations among segments, $\omega_{ij}^{intr}(r_1, r_2)$, belonging to the same molecule. The OZ equations for the reference interaction site model can be represented by an $s \times s$ matrix equation^{7-10, 33, 34}

$$\mathbf{H}(\mathbf{r}_1, \mathbf{r}_2) = \int \int (\Omega^{intr}(\mathbf{r}_1, \mathbf{r}_3) \mathbf{C}(\mathbf{r}_3, \mathbf{r}_4) (\Omega^{intr}(\mathbf{r}_4, \mathbf{r}_2) + \rho \mathbf{H}(\mathbf{r}_4, \mathbf{r}_2))) d\mathbf{r}_3 d\mathbf{r}_4 \quad (2.82)$$

where ρ is the number density, $\mathbf{H}(\mathbf{r}_1, \mathbf{r}_2)$, $\mathbf{C}(\mathbf{r}_1, \mathbf{r}_2)$ and $\Omega^{intr}(\mathbf{r}_1, \mathbf{r}_2)$ are $s \times s$ matrices with elements $h_{ij}(\mathbf{r}_1, \mathbf{r}_2)$, $c_{ij}(\mathbf{r}_1, \mathbf{r}_2)$ and $\omega_{ij}^{intr}(\mathbf{r}_1, \mathbf{r}_2)$ respectively. For instance, the $s \times s$ matrix $\mathbf{H}(\mathbf{r}_1, \mathbf{r}_2)$ is given by

$$\mathbf{H}(\mathbf{r}_1, \mathbf{r}_2) = \begin{pmatrix} h_{11} & \dots & h_{1s} \\ \vdots & \ddots & \vdots \\ h_{s1} & \dots & h_{ss} \end{pmatrix} (\mathbf{r}_1, \mathbf{r}_2) \quad (2.83)$$

where $(\mathbf{r}_1, \mathbf{r}_2)$ on the rhs denotes that all elements h_{ij} depend on $(\mathbf{r}_1, \mathbf{r}_2)$. The direct and intra-molecular correlations are given by similar matrices $\mathbf{C}(\mathbf{r}_1, \mathbf{r}_2)$ and $\Omega^{intr}(\mathbf{r}_1, \mathbf{r}_2)$.

2.6.4 PRISM: The polymer-RISM

In principle, the RISM theory can be applied to long chain molecules. However, for s -mers the generalized OZ $s \times s$ matrix equation, is virtually impossible to handle. Recently, Curro and Schweizer simplified the OZ matrix eq 2.82 considerably. For long chains the different correlation functions $h_{ij}(\mathbf{r}_1, \mathbf{r}_2)$, $c_{ij}(\mathbf{r}_1, \mathbf{r}_2)$ will be almost identical for all segments, except maybe for correlations involving segments located at the ends of the chains. Assuming that all correlation functions $h_{ij}(\mathbf{r}_1, \mathbf{r}_2)$ and $c_{ij}(\mathbf{r}_1, \mathbf{r}_2)$ are independent of the site indices i, j the full $s \times s$ OZ matrix equation can be reduced to a single algebraic equation

$$h(r) = \int \int \omega^{intr}(|\mathbf{r} - \mathbf{r}'|) c(|\mathbf{r}' - \mathbf{r}''|) [\omega^{intr}(r'') + \rho_s h(r'')] d\mathbf{r}' d\mathbf{r}'' \quad (2.84)$$

with ρ_s the segmental density and ω^{intr} the average intra-molecular correlation function given by

$$\omega^{intr}(r) = \frac{1}{s} \sum_{i=1}^s \sum_{j=1}^s \omega_{ij}^{intr}(r) \quad (2.85)$$

In the polymer-RISM theory, the chain conformational properties are accounted for by the average intra-molecular correlation function. In most applications of the PRISM theory it is assumed that the intra-molecular correlations are independent on the inter-molecular correlations and are sufficiently accurately described by ideal chain models.⁶⁻¹⁰ With input of such intra-molecular correlation functions, the inter-molecular correlation functions can be obtained provided a closure approximation is invoked. In this study we will use the approximations for simple fluids, i.e. MSA and PY approximations, as shown in eqs 2.80 and 2.81.

So far we have introduced the OZ integral equation for simple fluids and PRISM theory for polymers in continuum space. In this study, the lattice model is adopted. The integral equations in continuum space can be easily transferred onto the lattice model by changing the \int -signs to \sum -signs. Each $\int d\mathbf{r}_1$ should be altered to $v^* \sum_{\mathbf{r}_1}$ with v^* the volume of a lattice site. On the lattice the appropriate density variable is the packing fraction y , which is related to ρ_s by $\rho v^* = y$.

2.7 Concluding remarks

We have now presented a series of useful statistical mechanical relationships and a set of theories for polymer fluids. They serve as a starting point for the development of new theoretical results described in this thesis.

References

- [1] Kalikmanov, V. I., *Statistical Thermodynamics of Liquids*. Lecture course at the Eindhoven University of Technology, The Netherlands, 1995.
- [2] Landau, L. D., Lifshitz, E. M., *Statistical physics*. Pergamon Press-Oxford, 1980.
- [3] Hill, T. L., *An introduction to Statistical thermodynamics*. Addison - Wesley Publishing Company, London, 1960.
- [4] McQuarrie, D. A., *Statistical Mechanics*. Harper and Row Publishers, New York, 1976.
- [5] Metropolis, N., Rosenbluth, A. W., Rosenbluth, M. N., Teller, A. H., Teller, E., *J. Chem. Phys.* *21*, 1087, 1953.
- [6] Janssen, R. H. C., *PhD - thesis*. Eindhoven University of Technology, The Netherlands, 1996.
- [7] Curro, J. G., Schweizer, K. S., *Macromolecules* *20*, 1928, 1987.
- [8] Schweizer, K. S., Curro, J. G., *J. Chem. Phys.* *89*, 3350, 1988.
- [9] Schweizer, K. S., Curro, J. G., *Macromolecules* *21*, 3070, 1988.
- [10] Curro, J. G., Schweizer, K. S., *Macromolecules* *24*, 6736, 1991.
- [11] Frenkel, D., Smit, B., *Understanding Molecular Simulation from Algorithm to Applications*. Academic Press, Inc., San Diego, 1996.
- [12] Flory, P. J., *Principles of Polymer Chemistry*. Cornell University Press, Ithaca, 1953.
- [13] Nies, E., Cifra, P., *Macromolecules* *27*, 6033, 1994.

- [14] Guggenheim, E. A., *Mixtures*. Oxford University Press, London, 1952.
- [15] Szleifer, I., *J. Chem. Phys.* *92*, 6940, 1990.
- [16] Weinhold, J. D., Kumar, S. K., Szleifer, I., *Europhysics Letters* *35*, 695, 1996.
- [17] Freed, K. F., *J. Phys. A* *18*, 871, 1985.
- [18] Bawendi, M. G., Freed, K. F., Mohanty, U., *J. Chem. Phys.* *84*, 7036, 1986.
- [19] Freed, K. F., Bawendi, M. G., *J. Phys. Chem.* *93*, 2194, 1989.
- [20] Dudowicz, J., Freed, K. F., Madden, W. G., *Macromolecules* *23*, 4830, 1990.
- [21] Chaikin, P. M., Lubensky, T. C., *Principle of Condensed Matter Physics*. Cambridge University Press, 1995.
- [22] Dudowicz, J., Freed, K. F., *Macromolecules* *24*, 5112, 1991.
- [23] Freed, K. F., Dudowicz, J., *Macromolecules* *29*, 625, 1996.
- [24] Wignall, G. D., *Encyclopedia of Polym. Sci. and Eng.*, vol. 10. John Wiley and Sons, New York, 2nd edn., 1987.
- [25] Percus, J., Yevick, G., *Phys. Rev.* *110*, 1, 1958.
- [26] Percus, J. K., *Phys. Rev. Lett.* *8*, 462, 1962.
- [27] Lebowitz, J. L., Percus, J. K., *Phys. Rev.* *144*, 251, 1966.
- [28] Wertheim, M. S., *Phys. Rev. Lett.* *10*, 321, 1963.
- [29] Thiele, E., *J. Chem. Phys.* *39*, 474, 1963.
- [30] Hansen, J. P., McDonald, I. R., *Simple theory of liquids*. Academic Press, London, UK, second edn., 1986.
- [31] Madden, W. G., Rice, S. A., *J. Chem. Phys.* *72*, 4208, 1980.
- [32] Murphy, R. D., *Phys. Rev. A* *15*, 1188, 1977.
- [33] Chandler, D., Andersen, H. C., *J. Chem. Phys.* *57*, 1930, 1972.
- [34] Chandler, D., in E. W. Montroll, J. L. Lebowitz (eds.), *Studies in Statistical Mechanics VIII*, p. 275. North - Holland, Amsterdam, 1982.

Chapter 3

The Excluded volume problem in the integral equation theory

3.1 Introduction

The interest in the thermodynamic behavior of polymers runs almost in parallel with the advent of polymer science. Already in the 40's Flory¹ and Huggins² independently formulated the, by now, classic Flory-Huggins (FH) expression for the free enthalpy of mixing and revealed the importance of the chain like structure for the phase behavior of polymer solutions. It was realized from the start that the FH theory was a rather crude approximation for real liquids since it is based on the lattice model.³ For instance, it is known that packing effects typical of the dense fluid state are not captured by the lattice model. However, these packing effects have been incorporated quite early in e.g. cell⁴ and hole theories^{5,6} or, more recently, by combining the FH expression with insights gained from off-lattice theories for mono-atomics or simple molecules.⁷ Nevertheless, the simple lattice model for polymers was further refined and elaborated for e.g. compressible lattice fluids⁸ and systems involving specific interactions.^{9,10}

Nowadays, many different macromolecular architectures have been synthesized and in addition to simple linear homopolymers, well defined branched, comb and star polymers, block-copolymers, etc. are available. These more complex materials require a more detailed description of the thermodynamic behavior in relation to their particular molecular structure. Unfortunately, such details in molecular architecture are not easily incorporated in a FH-like theory. An important advancement in lattice theories is the Lattice Cluster (LC) theory designed by Freed and co-workers.¹¹⁻¹⁵ The LC theory not only provided systematic improvements

to the primitive FH result for linear chains but also makes it feasible to study the influence of more complicated molecular structures on the thermodynamic behavior. The LC theory has been successfully applied to investigate the influence of monomer structure in, e.g., mixtures of polystyrene/polyvinylmethylether¹⁶ and mixtures of linear and short chain branched polymers.¹⁷ Despite the beautiful developments facilitated by the LC theory the major drawback of the lattice model is not alleviated.

Another line of approach, relying on the integral equation theory of mono-atomic and simple molecular fluids, was investigated by Curro, Schweizer and collaborators.¹⁸⁻²¹ Integral equation theories were initially developed for simple mono-atomic fluids to study the microscopic structure of dense fluids employing correlation functions. The thermodynamic properties can be derived from the correlation functions employing exact statistical mechanical relationships.^{22,23} Unfortunately, and this is a major drawback of all integral equation theories, these calculations are plagued with so called thermodynamic inconsistencies which are related to the necessary approximations involved in the calculation of the theoretical correlations.²⁴⁻³⁰

These liquid state theories, employing correlation functions, were extended to simple molecular fluids in the reference interaction site model (RISM) theory by Chandler and co-workers.³¹ The RISM theory makes it feasible to predict the inter-molecular correlations among segments or interaction sites on different molecules from information of the intra-molecular correlations, which are set by the molecular architecture, between segments of the same molecule. For simple (rigid) molecules the intra-molecular correlations are known in advance and the RISM theory is quite successful in describing the subtle packing effects in dense liquids induced by the intra-molecular structure. It should be noted that, in contrast with the integral equation theory for simple mono-atomic, the RISM calculations are not as accurate at low densities.^{24,25,32} It even can be shown that the RISM theory does not yield the correct ideal gas limiting behavior.³³

The application of the RISM theory to flexible chain molecules (Polymer-RISM or PRISM) was initiated by Curro and Schweizer to study the microscopic structure of polymer single components and mixtures.¹⁸⁻²¹ For flexible macromolecules, the intra-molecular structure is not *a priori* known and it must be expected to depend on the inter-molecular correlations which according to the (P)RISM theory are determined by the intra-molecular correlations. Hence, a complicated interdependence between inter- and intra-molecular correlations exists and, in principle, both types of correlations must be calculated self-consistently.³⁴⁻⁴⁰ The first at-

tempts to establish this self-consistency have been published only recently and are still a matter of further investigation.³⁴⁻⁴⁰

In the initial applications of the PRISM theory, a more simple approach was taken by assuming that the intra-molecular structure was *a priori* given.¹⁸⁻²¹ In certain instances this additional approximation turns out to be quite reasonable. In particular in the dense melt it is known from the ideality hypothesis of Flory^{3,41} that the intra-molecular correlations are successfully described by an ideal chain model. Typical for the ideal chain model is that the average squared end-to-end distance $\langle r^2 \rangle$ depends on the chain length s according to $\langle r^2 \rangle \sim (s - 1)^1$. However, at low densities the screening of inter- and intra-molecular interactions becomes less efficient and the intra-molecular correlations evolve to those of a self-avoiding walk.⁴² In this case the average squared end-to-end distance scales with the chain length according to $\langle r^2 \rangle \sim (s - 1)^{1.2}$. Furthermore, deviations from ideal chain statistics must be expected and are known to exist in polymer mixtures.^{43,44}

Nevertheless, the PRISM theory has been quite successful to predict the inter-molecular correlations starting from the intra-molecular correlations. Several intra-molecular correlation functions, derived from different ideal chain models and incorporating varying chemical details such as the Gaussian chain,^{18-21,45} the freely jointed chain^{18-21,45} and the rotational isometric state model,^{18-21,45} have been investigated. Most of these applications involved rather dense fluids and the correlations are mainly governed by segmental packing effects which are equally active in simple molecular and mono-atomic fluids. In these circumstances the additional subtleties related to the chain connectivity are not that easily appreciated and, in order to study these effects, lower densities should be investigated. Unfortunately at lower densities, and irrespective of the ideality assumption necessary for chain like molecules, it is known that the PRISM approach becomes less accurate.^{24,25,32,33}

In order to make a systematic study of these chain connectivity effects possible, previous research in our laboratory applied the (P)RISM theory to the lattice model.²² At first sight this approach might seem counterintuitive or even counterproductive. Integral theories were precisely developed to study the intricacies of the continuum that are not captured by the lattice model. However, a few practical advantages of the lattice model immediately become obvious. First, the actual calculation of lattice correlation functions is significantly easier than the calculation of the off-lattice correlations.²² Second, also molecular simulation techniques, in particular Monte Carlo simulations, are much easier and more ef-

ficient on-lattice than off-lattice.¹⁸⁻²² It is well known that molecular simulations provide essentially exact information for the investigated model.⁴² Hence, the more efficient lattice simulations can provide more information and make a more extensive comparison amenable.

Apart from these practical advantages, more fundamental reasons can be thought of also. As already mentioned in a previous paragraph, the overwhelming off-lattice packing effects, which are very similar for mono-atomic, simple fluids and polymeric fluids, are absent on the lattice. This makes a more detailed study of chain connectivity effects feasible, even at high densities where the PRISM theory is expected to be at its best.

Furthermore, it has already been shown that the effects of theoretical approximations can be studied equally well on the lattice. For instance, the problems found in the Percus-Yevick (PY) theory for the sticky sphere^{46,47} model of Baxter are also found on the lattice.²² Therefore, it may be expected that the effects of chain connectivity, operating on length scales larger than the lattice spacing, will be equally present on the lattice as in off-lattice models.

As mentioned previously, most applications of PRISM theory involved ideal chain structure factors. All these models fail to incorporate the long range correlations resulting from the excluded volume present in chain molecules.¹⁸⁻²¹ As a result these intra-molecular correlation functions include unphysical overlaps of chain segments.¹⁸⁻²¹ It is known that these intra-molecular overlaps especially have a profound influence on the thermodynamic properties of the polymer fluid.¹⁸⁻²¹ This has been shown on several occasions both off-lattice¹⁸⁻²¹ as well as on-lattice.²² To correct for this overlap it was suggested to correct the intra-molecular correlation function *ad hoc* but keeping at the same time the overall ideal chain behavior.¹⁸⁻²²

In the present work we assume, in line with previous work on the PRISM theory, the intra-molecular correlation *a priori* given and investigate a single chain intra-molecular correlation function which accounts for the excluded volume. The present development, invoking a finite difference integral equation for the isolated chain, was previously investigated by Curro, Blatz and Pings for an athermal off-lattice polymer chain.⁴⁸ This new intra-molecular correlation function is then injected in the PRISM theory and the influence on the intermolecular correlations and the thermodynamic properties is examined at both high and low densities. In the second paragraph the lattice PRISM theory and several frequently used intra-molecular correlation functions are discussed. In addition the new excluded volume intra-molecular correlation function is introduced and finally the routes

to the thermodynamic properties discussed in this work are presented. The theoretical results are compared to Monte Carlo simulation results and evaluated in section 4. The simulation algorithms have been extensively presented previously.⁴⁹ Hence, only the most important aspects are summarized in section 3. Finally, in the concluding section the main results are recapitulated and related consequences are summarized.

3.2 Theory

3.2.1 The molecular model

Consider N linear s -mers each of which occupies s consecutive sites on a cubic lattice. The overall fraction of filled lattice sites or the segmental packing fraction, y , is given by

$$y = sN/N_L \quad (3.1)$$

Non-covalently bonded polymer segments i and j are assigned a nearest neighbor interaction potential, $u_{ij}(l, m, n) = u(l, m, n)$

$$u(l, m, n) = \begin{cases} \infty, & l^2 + m^2 + n^2 = 0 \\ \epsilon, & l^2 + m^2 + n^2 = 1 \\ 0, & \text{otherwise} \end{cases} \quad (3.2)$$

The covalent bonds between consecutive segments i and $i + 1$ can be represented by the following pair potential, $w_{ii+1}(l, m, n) = w(l, m, n)$

$$w(l, m, n) \rightarrow +\infty, \quad l^2 + m^2 + n^2 \neq 1 \quad (3.3a)$$

$$w(l, m, n) \rightarrow -\infty, \quad l^2 + m^2 + n^2 = 1 \quad (3.3b)$$

$$\exp(-\beta w) = \delta[(l^2 + m^2 + n^2) - 1] \quad (3.3c)$$

where δ is the dirac delta function and the position of the second segment relative to the first one is given by the lattice indices (l, m, n) ; each index can attain the values $0, \pm 1, \pm 2, \dots$

3.2.2 Lattice PRISM theory

A successful theoretical route to the inter-molecular correlations in simple atomic fluids is given by the Ornstein-Zernike integral equation. The OZ integral equation was generalized by Chandler and co-workers to molecular fluids with a given

intra-molecular structure. Here we only consider homogeneous systems for which all correlation functions are translationally invariant and, hence, are only functions of the relative distance between segments. If the total inter-molecular pair correlation function, $h_{ij}(l, m, n)$, between the pair of segments i and j is considered to propagate in a sequential manner by direct inter-molecular correlations $c_{ij}(l, m, n)$ and intra-molecular correlations $\omega_{ij}^{intr}(l, m, n)$, the Fourier transform of the generalized Ornstein-Zernike matrix equation on a cubic lattice can be written as^{18-21,31,50}

$$\hat{\mathbf{H}}(k_l, k_m, k_n) = \hat{\Omega}(k_l, k_m, k_n) \hat{\mathbf{C}}(k_l, k_m, k_n) [\hat{\Omega}(k_l, k_m, k_n) + \frac{y}{s} \hat{\mathbf{H}}(k_l, k_m, k_n)] \quad (3.4)$$

where the hat denotes Fourier transformation and (k_l, k_m, k_n) are the Fourier variables conjugate to (l, m, n) ; $\hat{\mathbf{H}}(k_l, k_m, k_n)$, $\hat{\mathbf{C}}(k_l, k_m, k_n)$ and $\hat{\Omega}(k_l, k_m, k_n)$ are $s \times s$ matrices with elements $\hat{h}_{ij}(k_l, k_m, k_n)$, $\hat{c}_{ij}(k_l, k_m, k_n)$ and $\hat{\omega}_{ij}^{intr}(k_l, k_m, k_n)$ respectively (the lattice Fourier transform is defined in the A by eq A.12). For instance, the $s \times s$ matrix $\hat{\mathbf{H}}(k_l, k_m, k_n)$ is given by

$$\hat{\mathbf{H}}(k_l, k_m, k_n) = \begin{vmatrix} \hat{h}_{11} & \dots & \hat{h}_{1s} \\ \vdots & \ddots & \vdots \\ \hat{h}_{s1} & \dots & \hat{h}_{ss} \end{vmatrix} (k_l, k_m, k_n) \quad (3.5)$$

The direct and intra-molecular correlations are given by similar matrices $\hat{\mathbf{C}}(k_l, k_m, k_n)$ and $\hat{\Omega}(k_l, k_m, k_n)$.

For linear s -mers this matrix equation, eq 3.4, becomes virtually impossible to handle. Fortunately, as shown by Curro and Schweizer,⁵¹ eq 3.4 can be simplified substantially if one realizes that for sufficiently long chain molecules the matrix elements $\hat{h}_{ij}(k_l, k_m, k_n)$, $\hat{c}_{ij}(k_l, k_m, k_n)$ and $\hat{\omega}_{ij}^{intr}(k_l, k_m, k_n)$ are quite similar for most pairs of segments. The end effects of long linear chains were estimated by Curro and Schweizer⁵¹ using an optimized perturbative scheme. For long linear chains it was shown that the end effects can be neglected to a good approximation. Hence, $\hat{h}_{ij}(k_l, k_m, k_n)$ and $\hat{c}_{ij}(k_l, k_m, k_n)$ are site index independent, i.e. $\hat{h}_{ij}(k_l, k_m, k_n) = \hat{h}(k_l, k_m, k_n)$ and $\hat{c}_{ij}(k_l, k_m, k_n) = \hat{c}(k_l, k_m, k_n)$ and the matrix equation can be reduced to a single algebraic equation for the inter-molecular correlations.

$$\hat{h}(k_l, k_m, k_n) = \hat{\omega}^{intr}(k_l, k_m, k_n) \hat{c}(k_l, k_m, k_n) [\hat{\omega}^{intr}(k_l, k_m, k_n) + y \hat{h}(k_l, k_m, k_n)] \quad (3.6)$$

where the average intra-molecular 2-segment correlation function $\hat{\omega}^{intr}(k_l, k_m, k_n)$

is defined as

$$\hat{\omega}^{intr}(k_l, k_m, k_n) = \frac{1}{s} \sum_{i=1}^s \sum_{j=1}^s \hat{\omega}_{ij}^{intr}(k_l, k_m, k_n) \quad (3.7)$$

In order to solve the equation, eq 3.6, for the inter-molecular segmental correlations given $\hat{\omega}$ we need another relation between $h(l, m, n)$ and $c(l, m, n)$. So far only approximate relations (closures) are available and the closure used here is the MSA approximation given by⁵²

$$h(0, 0, 0) = -1 \quad (3.8a)$$

$$c(l, m, n) = \begin{cases} -\beta\epsilon, & l^2 + m^2 + n^2 = 1 \\ 0, & \text{otherwise} \end{cases} \quad (3.8b)$$

For athermal conditions, the PY and MSA approximations are identical. In both of the closures, the condition on the inter-molecular pair correlation $h(0, 0, 0)$ is exact whereas the conditions for the direct correlations are approximate. It is known from the study of mono-atomic particles that the PY closure is less suited for interacting systems.^{22, 46, 47} Henceforth, for systems involving attractive nearest neighbor interaction energies we only consider the MSA closure.

In addition to the closure relation an expression for the intra-molecular correlations is required. The choices for $\hat{\omega}^{intr}(k_l, k_m, k_n)$ employed in this investigation will be discussed in the next subsections. Combining eqs 3.6 and 3.8 and an expression for the intra-molecular correlations, eq 3.7, the inter-molecular correlations of the lattice fluid can be calculated.

3.2.3 Intra-molecular correlation of the freely jointed chain model

For a chain molecule in its own melt we may resort to the ideality hypothesis put forward by Flory. It is well accepted that due to the screening of inter- and intra-molecular interactions the inter- and intra-molecular correlations of a chain molecule in its own melt are effectively similar to those of an ideal chain. Flory's idea has been proven fundamentally correct by neutron scattering experiments on labeled chains^{53, 54} and by computer simulations.^{55, 56} Invoking the ideality assumption the intra-molecular correlation function can be calculated independently and the results serve as input in the integral equation. Several ideal chain models with varying chemical details have been tested, e.g. the Gaussian chain,¹⁸⁻²¹ the freely jointed chain,¹⁸⁻²¹ the rotational isometric state model,¹⁸⁻²¹

etc. The freely jointed chain has been used in previous studies²² and will serve here as a reference. It must be pointed out that the ideality hypothesis will be particularly useful in the dense state. However, at lower densities the screening between inter- and intra-molecular interaction is no longer complete and the intra-molecular correlations of the chain molecule will tend more to those of a self-avoiding walk.

The intra-molecular correlations of the ideal chain model can be described solely in terms of the 1-bond-jump probability $\tau(l, m, n)$, on the cubic lattice, given by

$$\tau(l, m, n) = \begin{cases} \frac{1}{6}, & l^2 + m^2 + n^2 = 1 \\ 0, & \text{otherwise} \end{cases} \quad (3.9)$$

In the case of the freely jointed chain model the summation in eq 3.7 can be performed explicitly and the intra-molecular correlation function can be shown to be given by²⁰⁻²²

$$\hat{\omega}_{id}^{intr}(k_l, k_m, k_n) = \frac{1 - \hat{\tau}^2 - \frac{2}{s}\hat{\tau} + \frac{2}{s}\hat{\tau}^{s+1}}{(1 - \hat{\tau})^2} \quad (3.10)$$

where $\hat{\tau} = \hat{\tau}(k_l, k_m, k_n) = \psi/3$ and $\psi = [\cos(u) + \cos(v) + \cos(w)]$.

The intra-molecular correlation function given in eq 3.10 can be used as the input to eq 3.6 of the PRISM theory. It is analogous to its continuum version^{18,57} and the derivation is given elsewhere.^{22,58}

In the freely jointed chain model unphysical intra-molecular overlaps are possible. Thus, some thermodynamic properties of athermal and interacting polymers obtained from this kind of ideal chain model are expected to be inadequate or unphysical. In order to investigate the influence of the intra-molecular correlation function on the thermodynamic properties, an alternative single chain molecule model, accounting for the intra-molecular short and long range excluded volumes is investigated.

3.2.4 Intra-molecular correlation of excluded volume theory

For the off-lattice single chain in vacuum the excluded volume was discussed by Curro, Blatz and Pings (CBP) starting from the distribution function for the endpoints.⁴⁸ Employing a diagrammatic analysis, similar to that leading to the

OZ equation of a simple fluid, a $(N - 1)$ th-order integro-differential equation for the end point distribution function was derived. Here we develop this method for the cubic lattice and in addition calculate the intra-molecular correlation function. Just as in conventional liquid state theory of simple fluids this integro-differential equation can only be solved provided an additional closure relation is introduced. Following CBP, the analogue of the PY closure is adopted. A detailed description of the theoretical considerations is given in Appendix A.

Here we summarize the results applicable to an athermal chain with intra-molecular segmental interactions given by eqs 3.2 and 3.3 at $\epsilon = 0$. In particular, the Fourier transform of the intra-molecular 2-segment correlation function $\hat{\omega}_{ij}^{intr}(k_l, k_m, k_n)$ of a chain consisting of s segments are given by

$$\hat{\omega}_{ij}^{intr}(k_l, k_m, k_n) = \frac{\hat{t}_{ij}(k_l, k_m, k_n) - t_{ij}(0, 0, 0)}{\hat{t}_{ij}(0, 0, 0) - t_{ij}(0, 0, 0)} \quad (3.11a)$$

$$t_{ij}(l, m, n) = \left(\frac{1}{2\pi}\right)^3 \int_{-\pi}^{\pi} \int_{-\pi}^{\pi} \int_{-\pi}^{\pi} \hat{t}_{ij}(k_l, k_m, k_n) \cos(lu) \cos(mv) \cos(nw) du dv dw \quad (3.11b)$$

The functions $\hat{t}_{ij}(k_l, k_m, k_n)$ can be obtained from the recurrent formula

$$\hat{t}_{12}(k_l, k_m, k_n) = 2\psi \quad (3.12a)$$

$$\begin{aligned} \hat{t}_{ij}(k_l, k_m, k_n) &= 2\psi [\hat{t}_{ij-1}(k_l, k_m, k_n) - t_{i+1j}(0, 0, 0) - t_{ij-1}(0, 0, 0)] \\ &\quad - \sum_{k=3}^{s-2} t_{1k}(0, 0, 0) [\hat{t}_{ks}(k_l, k_m, k_n) - t_{ks}(0, 0, 0)] \end{aligned} \quad (3.12b)$$

Thus, to calculate the terms $\hat{\omega}_{ij}^{intr}(k_l, k_m, k_n)$, the corresponding $\hat{t}_{ij}(k_l, k_m, k_n)$ are required. These can be calculated in sequence starting from $\hat{t}_{ij}(k_l, k_m, k_n) = \hat{t}_{12}(k_l, k_m, k_n)$. The functions $t_{ij}(l, m, n)$ appearing in eq 3.11a are obtained from $\hat{t}_{ij}(k_l, k_m, k_n)$ by inverse Fourier transformation (eq 3.11b). For short s -mers ($s \leq 6$), the required factors $\hat{t}_{ij}(k_l, k_m, k_n)$ and corresponding segmental intra-molecular correlations $\hat{\omega}_{ij}^{intr}(k_l, k_m, k_n)$ are summarized in Table 3.1. Further explicit summation according to eq 3.7 leads to the average 2-segment intra-molecular correlation function $\hat{\omega}_{excl}^{intr}(k_l, k_m, k_n)$ that can be written as a polynomial in the variable (2ψ) ,

$$\hat{\omega}_{excl}^{intr}(k_l, k_m, k_n) = \sum_{i=0}^{s-1} c_i^s (2\psi)^i \quad (3.13)$$

the coefficients c_i^s for short s -mers ($s \leq 6$) are given in Table 3.2. The intra-

i,j	$\hat{t}_{ij}(k_l, k_m, k_n)$	$\hat{t}_{ij}(0)$	$t_{ij}(0)$	$\hat{\omega}_{ij}^{intr}(k_l, k_m, k_n)$
1,2	2ψ	6	0	$\psi/3$
1,3	$(2\psi)^2$	36	6	$((2\psi)^2 - 6)/30$
1,4	$(2\psi)^3 - 24\psi$	144	0	$((2\psi)^3 - 12(2\psi))/144$
1,5	$(2\psi)^4 - 18(2\psi)^2 + 36$	684	18	$((2\psi)^4 - 18(2\psi)^2 + 18)/666$
1,6	$(2\psi)^5 - 24(2\psi)^3 + 72(2\psi)$	3024	0	$((2\psi)^5 - 24(2\psi)^3 + 72(2\psi))/3024$

Table 3.1: The segmental intra-molecular correlations $\hat{\omega}_{ij}^{intr}(k_l, k_m, k_n)$ and the t_{ij} 's for s -mers, $s \leq 6$.

s	c_0^s	c_1^s	c_2^s	c_3^s	c_4^s	c_5^s
2	1	$\frac{1}{6}$				
3	$\frac{13}{15}$	$\frac{2}{9}$	$\frac{2}{90}$			
4	$\frac{4}{5}$	$\frac{5}{24}$	$\frac{1}{30}$	$\frac{1}{288}$		
5	$\frac{2139}{2775}$	$\frac{1}{5}$	$\frac{243}{8325}$	$\frac{1}{180}$	$\frac{1}{1665}$	
6	$\frac{3753}{4995}$	$\frac{5508}{27216}$	$\frac{396}{14985}$	$\frac{117}{27216}$	$\frac{1}{999}$	$\frac{1}{9072}$

Table 3.2: The coefficients for the average intra-molecular segmental correlation function for s -mers, $s \leq 6$.

molecular correlation function 3.13 can be used as input to the PRISM integral theory. In the derivation of eqs 3.11 and 3.12 an approximate analogous to the Percus-Yevick approximation has been used. In continuum it has been shown that the calculated average end-to-end distance for athermal chains are larger than the exact value. For example, the exact and calculated values of the mean-square end-to-end distances for an off-lattice athermal 4-mers are $\langle r_{14}^2 \rangle = 4.31l_b^2$ and $\langle r_{14}^2 \rangle = 4.5l_b^2$ respectively.⁴⁸ Furthermore, the scaling of the average squared end-to-end distance with chain length depends on the ratio of bond length and segment diameter and can be tuned to the scaling behavior of self-avoiding walk by a proper choice of this ratio.

3.2.5 Thermodynamic properties

Once the correlation functions are known, the thermodynamic properties can be calculated from exact statistical mechanical relations. The isothermal compress-

ibility is defined as

$$\kappa_T = -\frac{1}{V} \left(\frac{\partial V}{\partial p} \right)_{T,N} = \frac{1}{y} \left(\frac{\partial y}{\partial p} \right)_{T,V} \quad (3.14)$$

The isothermal compressibility can be found from the zero wave vector limit of the structure factor $\hat{S}(0, 0, 0)$ ¹⁸⁻²² and can be related to the correlations in the fluid

$$\frac{\kappa_T}{v^*} = \frac{\beta \hat{S}(0)}{y} = \frac{\beta \hat{\omega}^{intr}(0, 0, 0)}{y[1 - \hat{\omega}^{intr}(0, 0, 0)y\hat{c}(0, 0, 0)]} \quad (3.15)$$

Eq 3.15 can be rewritten in terms of the total 2-segment distribution function $G(l, m, n)$ according to

$$\frac{\kappa_T}{v^* \beta} = \sum_{l,m,n} [G(l, m, n) - 1] \quad (3.16)$$

with $yG(l, m, n) = \omega^{intr}(l, m, n) + yg(l, m, n)$ denotes the total density of segments at position (l, m, n) from a chosen particle, $g(l, m, n) = h(l, m, n) + 1$ is the radial distribution function. The equation of state can be obtained from the inverse isothermal compressibility by direct integration

$$\beta p v^* = \int_0^y \left[\frac{1}{\hat{\omega}^{intr}(0, 0, 0)} - y' \hat{c}(0, 0, 0) \right] dy' \quad (3.17)$$

This equation of state is hence a thermal compressibility equation of state. Note that the compressibility equation of state is determined by the total 2-segment distribution function $G(l, m, n)$.

Other possible routes to the equation of state are, e.g. *the energy equation*, *the virial equation* and *the wall equation of state*.^{22-30,59} If the the theoretically calculated correlation functions were exact the equation of state obtained from these different routes would be identical. However, the approximate closures make the results depend on the chosen route. Here we use the compressibility route to the equation of state. It is known that the PRISM equation does not yield the correct limiting low density behavior and this will have its consequence for the integration to be conducted in eq 3.17.⁶⁰ Off-lattice studies pointed out that the compressibility equation of state underestimates the compressibility factor whereas the virial equation of state results in an overestimation.⁶⁰ It was further shown that the wall equation of state produced results which were believed to be nearest to the true behavior.⁶⁰ However, in a lattice study it was shown

that the wall equation of state was by no means in good agreement with MC simulation data and in this case the compressibility equation of state was in better agreement.⁶⁰ Irrespective of which route to select, it is generally accepted that the calculation of thermodynamic properties, such as the equation of state with integral equation theory, meets always with great difficulties.

To calculate the pressure via eq 3.17, the intra- and inter-molecular correlation functions, $\hat{\omega}^{intr}(k_l, k_m, k_n)$ and $\hat{c}(k_l, k_m, k_n)$, must be calculated for each y' . The numerical integration can altogether be prevented in some cases. For atomic fluids, Baxter performed the integration analytically employing the PY closure. Baxter's approach can be extended to the PRISM theory and the compressibility equation of state for chain molecules is⁶¹

$$\begin{aligned} \beta p v^* = & \frac{y}{s} + \frac{y^2}{2} [-2c(0, 0, 0) + 6c(1, 0, 0) \left(\frac{c(1, 0, 0)}{1 - e^{\beta\epsilon}} - 2 \right)] \\ & + \left(\frac{1}{2\pi} \right)^3 \int_{-\pi}^{\pi} \int_{-\pi}^{\pi} \int_{-\pi}^{\pi} (y \hat{\omega}^{intr}(k_l, k_m, k_n) \hat{c}(k_l, k_m, k_n) \\ & + \ln(1 - y \hat{\omega}^{intr}(k_l, k_m, k_n) \hat{c}(k_l, k_m, k_n))) d u d v d w \end{aligned} \quad (3.18)$$

Although, eq 3.18 was initially derived using the PY closure, it is applicable to athermal systems studied in the MSA approximation since then the MSA and PY closures are identical. Hence, numerical integration according to eq 3.17 is only necessary for systems with a non-zero nearest neighbor interaction potential when the MSA closure is used.

In the PV -plane of a 1-component fluid three regions, i.e. a stable, a meta-stable and an unstable region can be defined. In the stable region, a fluid always remains in the one phase and in the unstable region the fluid will always separate into two phases. On the other hand, a meta-stable fluid is stable with respect to small density fluctuations, but large fluctuations, i.e. the formation of critical nuclei, will cause phase separation. These three regions are separated by two lines, i.e. the binodal and spinodal curves. The liquid-gas binodal defines the coexistence between a liquid and a vapor phase and delineates the stable and meta-stable regions. At the spinodal curve, separating the meta-stable and unstable regions, the compressibility diverges, i.e. $\kappa_T \rightarrow \infty$ which corresponds to the following condition

$$\frac{1}{\hat{\omega}^{intr}(0, 0, 0)} - y \hat{c}(0, 0, 0) = 0 \quad (3.19)$$

It is known from the study of mono-atomic particles that the PY-closure is less suited for interacting systems.^{22, 46, 47} Therefore, in this case only the MSA closure is discussed.

3.3 Monte Carlo simulation

3.3.1 NpT -simulation

The NpT -ensemble simulation technique used here to obtain the equation of state data for $s = 20, 30$ and 60 athermal chains has been described elsewhere.⁴⁹ These simulations are operated in the NpT ensemble. The self-avoiding lattice chains are placed on a cubic lattice and each site is occupied at most once. A rectangular section of a cubic lattice with a wall is used here with 50 sites in the l -direction, perpendicular to the wall, and 22 sites in the other two directions. The solid wall is placed at $l = 1$ position and 200 - 500 chains are put in the rectangular section. Periodic boundary conditions are used in the m - and n -direction. A finite pressure is exerted by changing the total volume. The necessary volume fluctuations are created by building/destroying a solid piston scanning site-by-site with respect to the solid wall. The configuration space is sampled by moving the polymer molecules on the lattice with reptation moves. A volume fluctuation move was applied every 200 reptations. Up to 1.2×10^9 reptation moves were used, from which the first $0.4 - 0.6 \times 10^9$ were used only for equilibration of each state. The particle distribution were only obtained from the last 0.1×10^9 moves. Averages of $g_{MC}(l, m, n)$ and $\omega_{MC}^{intr}(l, m, n)$ were collected every 5000 reptations from a middle section of the polymer slab, at least 7 sites away from the solid wall and from the jagged edge of the piston. The $g_{MC}(l, m, n)$ and $\omega_{MC}^{intr}(l, m, n)$ were only obtained for $r^2 = l^2 + m^2 + n^2 \leq 16$. The single chain intra-molecular correlation data are obtained from the same simulation algorithm at very low concentration of chains.

3.3.2 Liquid-vapor coexistence curve

The MC simulation data for the liquid-vapor binodal curve is taken from recent papers of Yan et al.^{62,63} The phase-equilibrium coexistence curve is extracted from a new simulation algorithm, i.e. the configurational-bias-vaporization method, which is designed for studying phase equilibria for lattice polymers. A single simulation cell is used in this method where all polymers are introduced in the lower portion of the cell upon initiation. Vaporization is then carried out by randomly eliminating a chain followed by generating a new chain through the configurational-bias method.⁶⁴ The compositions of coexistence phases are determined directly. The phase-equilibrium coexistence curves for polymer systems with chain length up to 200 can be obtained from this simulation.

3.4 Results and discussions

In figures 3.1, 3.2 and 3.3 theoretical and simulation results for the average intra-molecular correlation function of 16-, 30 and 60-mers are presented as a function of $r^2 = l^2 + m^2 + n^2$, the radial distance between two segments.

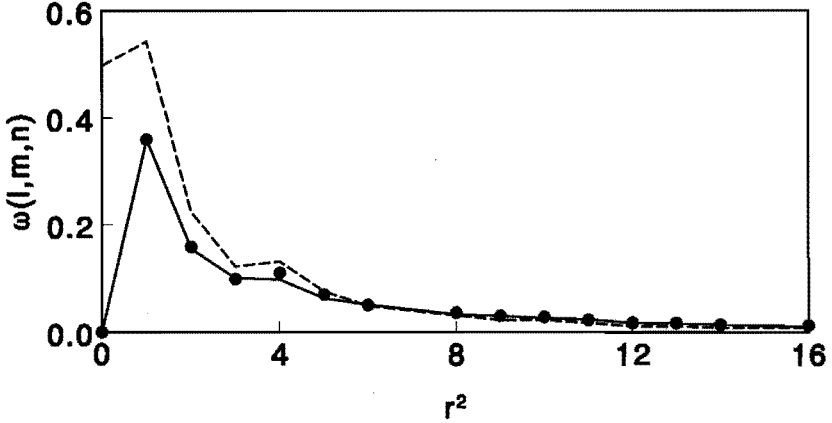


Figure 3.1: Intra-molecular correlation function $\omega^{intr}(r)$ for 16-mers as function of radial distance r^2 between two segments. MC simulations (●); Full lines represent the $\omega^{intr}(r)$ from the excluded volume theory; dashed lines refer to the freely jointed chain model.

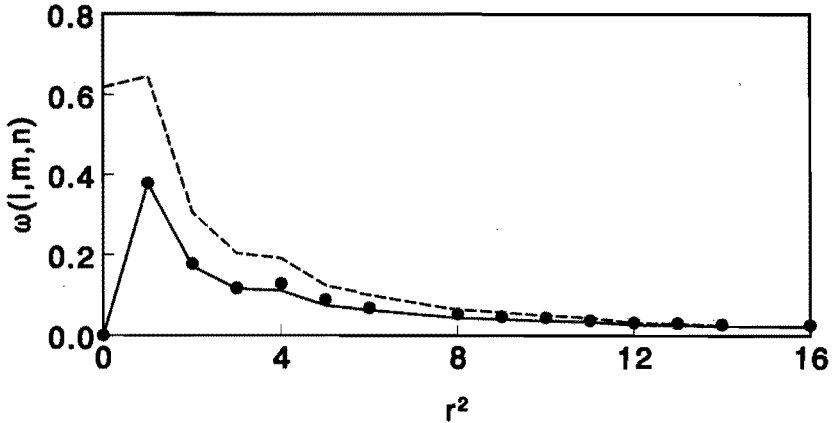


Figure 3.2: Caption as in figure 3.1, but for for 30-mers.

The symbols (●) are MC data and theoretical intra-molecular correlation functions $\omega^{intr}(l, m, n)$ are denoted by lines: the dashed line refers to the freely jointed

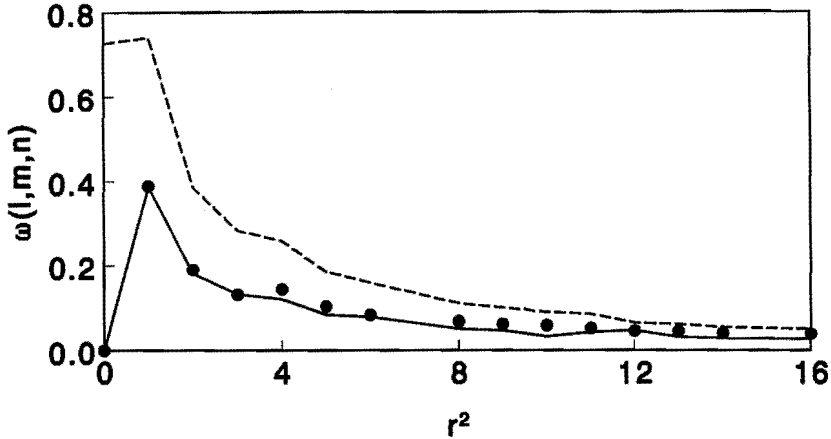


Figure 3.3: *Caption as in figure 3.1, but for 60-mers.*

chain and the solid line depicts the excluded volume chain. To focus on the interesting part of the intra-molecular correlation the trivial self correlation at the $(0, 0, 0)$ position is not depicted, i.e. at the origin $\omega^{intr}(0, 0, 0) - 1$ is shown, whereas for all other positions, $(l, m, n) \neq (0, 0, 0)$, the complete intra-molecular correlation $\omega^{intr}(l, m, n)$ is presented. In agreement with the simulation data the theoretical $\omega^{intr}(l, m, n)$ is only defined at lattice positions and the lines are merely a convenient manner to distinguish the theoretical results from the simulation data. The larger value for the intra-molecular correlation function at $r^2 = 4$ compared to the value at $r^2 = 3$ is typical for the cubic lattice. The shortest possible path between a central segment and a segment located at the position $(1, 1, 1)$ contains three ‘bonds’ whereas the shortest path for a segment located at $(2, 0, 0)$ position is only two ‘bonds’. Consequently, the correlation at the $r^2 = 4$ position is larger than at the $r^2 = 3$ position. The incomplete ‘radial symmetry’ of the lattice also yields slightly different values for, e.g., $\omega^{intr}(2, 2, 1)$ and $\omega^{intr}(3, 0, 0)$, although both positions represent the same radial distance. Hence, the value of $\omega^{intr}(9)$ in figures 3.1, 3.2 and 3.3 is obtained as the average involving the different lattice positions with the same radial distance.

In figure 3.1 it can be observed that at short radial distances, say $r^2 \leq 6$, the ideal chain intra-molecular correlations are larger than those from the excluded volume chain. In the ideal chain, segments can fold back and several segments can occupy the same lattice site making more compact conformations possible. This also leads to a large residual correlation, i.e. $\omega_{id}^{intr}(0, 0, 0) - 1$, is nonzero and leads inevitably to too high correlations at shorter distances. Since the summation of

the intra-molecular correlation function over all distances yields the total number of segments in the chain, the overestimated correlation at small distances must result in an underestimation of the correlations at larger distances. This is indeed observed in figure 3.1. On the other hand, the excluded volume chain offers quite accurate predictions of the MC data. For the 16-mers the theoretical line for the intra-molecular correlation function from the excluded volume chain passes through the MC data for all presented distances except at $r^2 = 4$. Note also that in agreement with the MC results $\omega^{intr}(0, 0, 0) - 1$ is identically zero.

In figures 3.2 and 3.3 a comparison between MC simulation data and theory is presented for longer chain length, i.e. $s = 30$ and $s = 60$. Clearly, the predictions of the freely jointed chain for the intra-molecular correlations deteriorate with increasing chain length (compare figures 3.1, 3.2 and 3.3). The predictions according to the excluded volume chain remain good to fair for these chain lengths although also in this case the agreement between theory and simulation data is found to deteriorate with increasing chain length.

In figure 3.4 the intra-molecular correlation functions of 30-mers for two densities, $y = 0.00225$ and $y = 0.6865$ obtained from NpT MC simulations, are shown. The theoretical results for the ideal and excluded volume single chain correlation functions are also depicted by the dashed and solid lines respectively.

The theoretical correlation functions provide lower and upper bounds for the MC data. As already observed in figures 3.1, 3.2 and 3.3 the single chain intra-molecular correlation function at zero density is quite successfully predicted by the excluded volume theory. Upon increasing the density, the MC intra-molecular correlations for distance $r^2 \geq 1$ gradually shift towards the ideal chain structure factor, indicating that the screening between intra- and inter-molecular interactions indeed leads to more ideal chain behavior. However, the full ideal chain limit is never reached. Especially the correlations at short distances are much smaller in the MC data than in the ideal chain ω^{intr} -function. Although with increasing density the real chains tend to more ideal chain behavior, they always experience the short range excluded volume effects since two segments cannot occupy the same lattice site, i.e. $\omega_{MC}^{intr}(0, 0, 0) - 1 = 0$. From figure 3.4 one might conclude that the excluded volume theory offers a reasonable prediction of the actual intra-molecular correlation also at higher densities. Especially if one is interested in properties involving short distances, the predictions of the excluded volume theory are certainly not worse than those of the ideal chain model.

In figures 3.5, 3.6 and 3.7 the inter-molecular correlations, calculated from the PRISM theory in combination with ω_{id}^{intr} (dashed lines) and ω_{excl}^{intr} (solid lines)

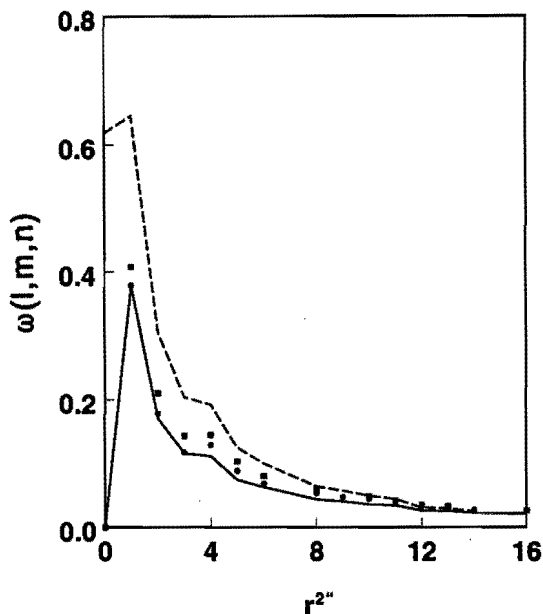


Figure 3.4: Intra-molecular correlation function as a function of distance r^2 for different densities $\gamma = 0.00225$, (\bullet); $\gamma = 0.6865$, (\blacksquare). Full line represents excluded volume theory and dashed line for freely jointed chain.

are compared to MC simulation data for athermal chains ($\epsilon = 0$) at 3 different densities, $\gamma = 0.00455, 0.0788$ and 0.5383 .

Both theory and simulation show the well known correlation hole, inside of which the concentration of monomers from other chains is reduced.⁶⁵ Therefore, at small distances the inter-molecular correlations are very low. The predicted limiting zero-density inter-molecular correlations are extremely poor irrespective of the theoretical intra-molecular correlation function used. Similar, discrepancies at low densities for the inter-molecular correlations have already been found in off-lattice studies for short chain fluids³² and small rigid molecules^{24,25} and are related to the inexact limiting low density behavior of the (P)RISM theory.³³ Apparently, the use of a more accurate intra-molecular correlation function for these low densities only results in a modest improvement. Clearly, the incorrect low density behavior of the PRISM theory is far more important. Upon increasing the density, the simulation data and the theoretical inter-molecular correlations are in better agreement. Surprisingly, at the highest density shown here, the predictions using ω_{id}^{intr} are in excellent agreement at all distances. In line with the Flory ideality hypothesis, the ideal chain intra-molecular correlation function

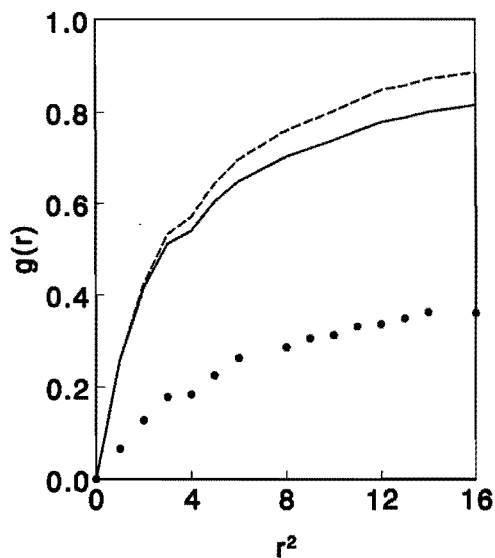


Figure 3.5: Inter-molecular correlation function $g(r)$ as function of distance r^2 at $s = 30$, $\epsilon = 0$ and $y = 0.00455$. MC simulations (\bullet); Full line represents the excluded volume theory and the dashed line depicts the results for freely jointed chains.

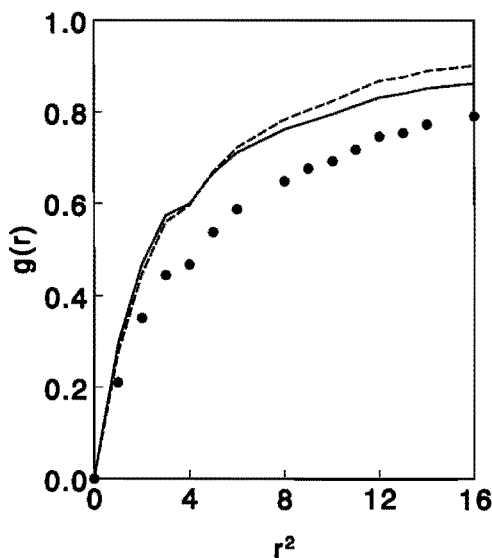


Figure 3.6: Caption as in figure 3.5 but for $y=0.0788$.

captures quite accurately the correlations at large distances. But also at the short distances the predictions employing ω_{id}^{intr} are quite accurate and have the

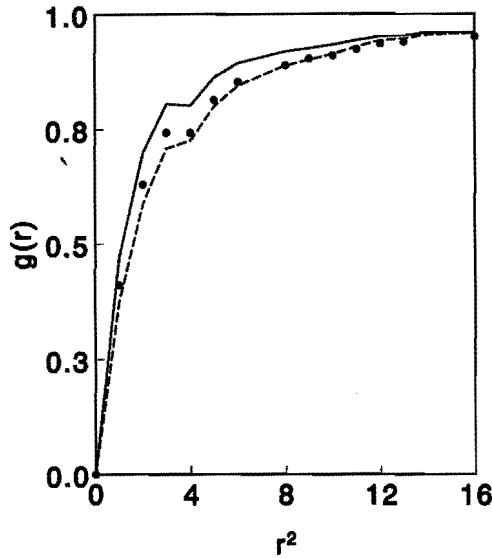


Figure 3.7: Caption as in figure 3.5 but for $y=0.5383$.

correct behavior at $(l, m, n) = 0$ which is a result of the exact closure condition $g(0, 0, 0) = 0$. At high density, the prediction of ω_{excl}^{intr} for the inter-molecular correlations are not as accurate as those of ω_{id}^{intr} . The improvements found for the intra-molecular correlation are not reflected in the inter-molecular correlations.

The compressibility equation of state can now be obtained from the inter- and intra-molecular correlations by numerical integration, presented in eq 3.16, or directly by eq 3.17. The latter equation only requires information about the final density.

In figure 3.8 the compressibility factor $\beta p v^* s / y$ is presented as a function of packing fraction y for athermal chains ($\epsilon = 0$) with chain length $s = 20$ and $s = 30$. The solid circles and squares denote the MC simulation data for 20-mers and 30-mers respectively. The dashed lines in figure 3.8 is the result obtained from the lattice-PRISM theory in combination with ω_{id}^{intr} and solid lines are obtained from ω_{excl}^{intr} . The freely jointed chain model result surely underestimates the compressibility factor $\beta p v^* s / y$ at all packing fraction. Moreover, at full packing, $y = 1$, the compressibility factor does not tend to infinity as it must be expected on physical grounds. From eq 3.16, we can appreciate that both the inter- and intra-molecular correlations are important quantities for the EoS. At full packing of the lattice ($y = 1$) the total density of segments, given by $yG(l, m, n)$, equals unity for all distances. Hence, the compressibility is equal to zero and the com-

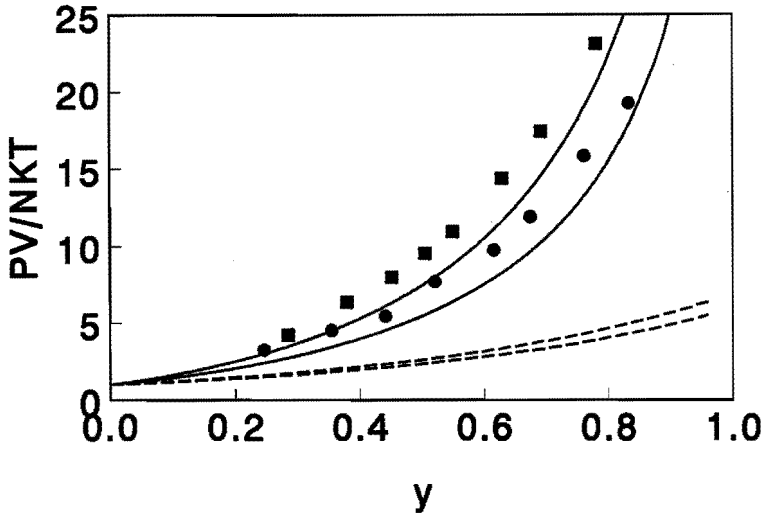


Figure 3.8: Compressibility factor as function of packing fraction at $\epsilon = 0$. MC simulations $s=20$ (\bullet) and $s=30$ (\blacksquare); Full lines represent the excluded volume theory and the dashed lines depict the results for freely jointed chains.

compressibility factor tends to infinity at $y = 1$. However, the ideal chain model, allowing for non-physical intra-molecular overlap of segments, leads to a too high value of $\omega(l, m, n)$ at short distances. Consequently, the total density of particles (intra- and inter-molecular) is larger than unity even at full packing and the compressibility becomes non-zero. This then results in a too small compressibility factor upon integration according to eq 3.17 or 3.18. On the other hand, the excluded volume theory, although approximate, accounts for these intra-molecular excluded volume interactions and provides the correct limiting behavior at $y = 1$ for $G(l, m, n)$. This clearly results in a significantly improved agreement between theory and simulation and the correct limiting behavior for the compressibility factor at full packing is obtained.

In figures 3.9, 3.10 and 3.11 the inter-molecular correlations for interacting 30-mers ($\beta\epsilon = -0.2$) are presented. In these calculations the PRISM equation combined with ω_{id}^{intr} (dashed lines) or ω_{excl}^{intr} (solid lines) is solved using the MSA closure.

It should be noted that the calculations for the interacting chains carry a certain inconsistency. The influence of the nearest neighbor interactions, contained in the closure relations, is only incorporated in the inter-molecular correlations. For the intra-molecular correlation function, the segmental interactions are as-

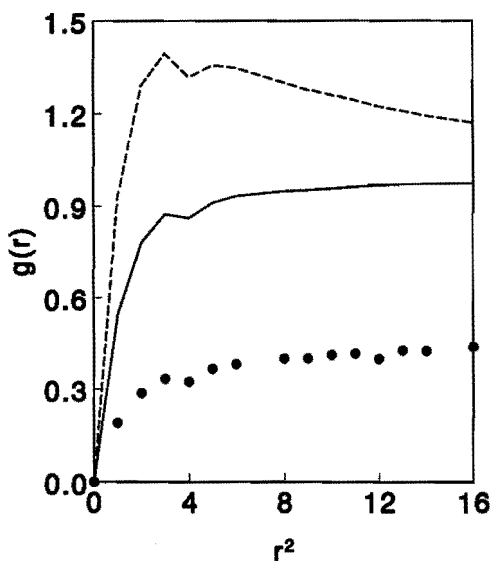


Figure 3.9: Inter-molecular correlation function $g(r)$ as function of distance r^2 at $s = 30$, $\epsilon = -0.2$ and $y = 0.0043$. MC simulations (\bullet); Full line represents the excluded volume theory and the dashed line depicts the results for freely jointed chains.

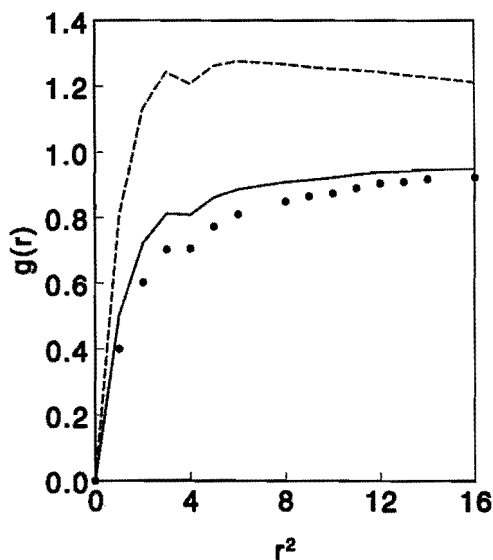


Figure 3.10: Caption as in figure 3.9, but for $y = 0.294$.

sumed to be athermal. This inconsistency is not typical of the present discussion but is a consequence of the *a priori* treatment of intra-molecular interactions

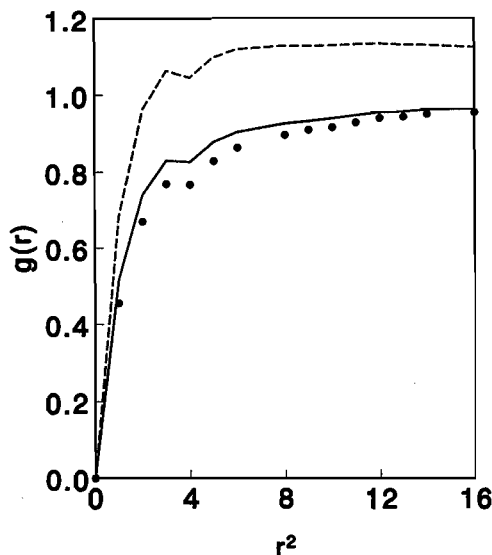


Figure 3.11: *Caption as in figure 3.9, but for $y = 0.5681$.*

independently of the inter-molecular correlations. A self-consistent calculation of inter- and intra-molecular correlations should provide an adequate remedy for this inconsistency. Despite this inconsistency, the theoretical variation with densities are quite similar to those observed for athermal chains and at low densities the PRISM predictions are particularly poor. However, also significant differences for these interacting systems are noticeable. At low and intermediate densities (figure 3.9 and 3.10) the intermolecular correlations derived from the ideal chain model first reach a maximum at rather short distances before decreasing to the larger distance limiting behavior $g(r \rightarrow \infty) = 1$. Thus instead of a correlation hole a correlation maximum is predicted in qualitative disagreement with the MC simulation data. A correlation maximum although less pronounced is still present at the highest investigated density (figure 3.11). The excluded volume intra-molecular correlation function ω_{excl}^{intr} correctly predicts the existence of the correlation hole also in these interacting systems and the predictions using ω_{excl}^{intr} are closer to the MC data at all densities. One can also observe that at high densities (compare 11 and 7) the inter-molecular correlations for interacting and athermal systems are very similar. This is also correctly predicted by the PRISM/ ω_{excl}^{intr} theory.

The equation of state for the interacting chains is depicted in figure 3.12. The packing fraction is shown as a function of pressure for 3 values of the reduced

interaction energy $\beta\epsilon = 0, -0.45, -0.5$.

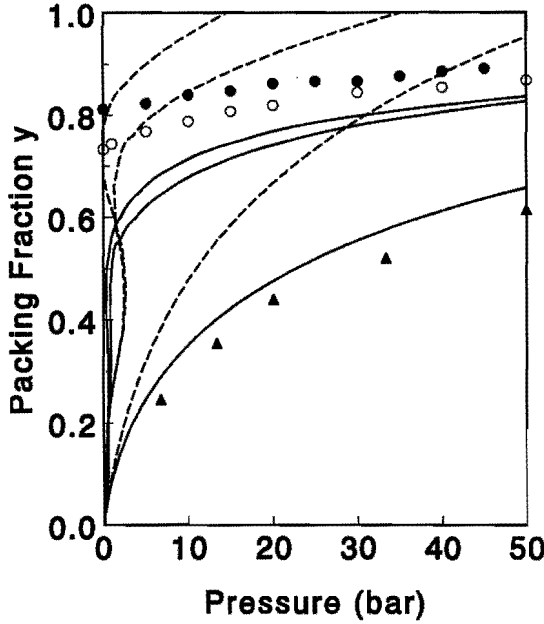


Figure 3.12: Density as a function of pressure for 30-mers and different interactions $\epsilon = 0(\blacktriangle)$, $-0.45(\circ)$, $-0.5(\bullet)$. Full lines represent the ω_{excl}^{intr} with MSA, dashed lines the ω_{id}^{intr} with MSA.

Both in theory and simulation the density increases with pressure and reduced interaction energy. For the nonzero interaction parameters investigated here the theoretical prediction based on ω_{id}^{intr} (---) results in unphysical packing fractions larger than unity. Just as in the case of the athermal chains, the unphysically large densities are related to the intra-molecular segmental overlap still present in the ideal chain model. In addition, however, the inter-molecular correlations, presented in figure 3.11, result in an extra densification of the system. The theoretical prediction based on ω_{excl}^{intr} (—) leads to a correct physical behavior although the predicted densities are too low for all investigated pressures and non-zero interactions. For ω_{excl}^{intr} model the observed change in density with interaction energy is somewhat too small in comparison to the MC simulation data, whereas for ω_{id}^{intr} it is too large.

Finally it can be observed that both the PRISM/ ω_{excl}^{intr} and PRISM/ ω_{id}^{intr} theoretical isotherms possess a van der Waals loop for sufficiently large attractive energies or low temperatures at low pressures. This is indicative of the vapour-liquid coexistence in this temperature and pressure region.

The MC simulation data do not show this van der Waals loop. However, it is also not possible to locate the V-L coexistence gap with the NpT MC simulation algorithm employed in this study.⁴⁹ The coexistence gap can be investigated employing other simulation algorithms as demonstrated by Yan et al.^{62,63}

The V-L binodal of a 16-mers obtained by Yan et al. is depicted in figure 3.13. Together with the MC binodal data the liquid-vapor spinodal curves calculated according to the PRISM theory in combination with ω_{id}^{intr}

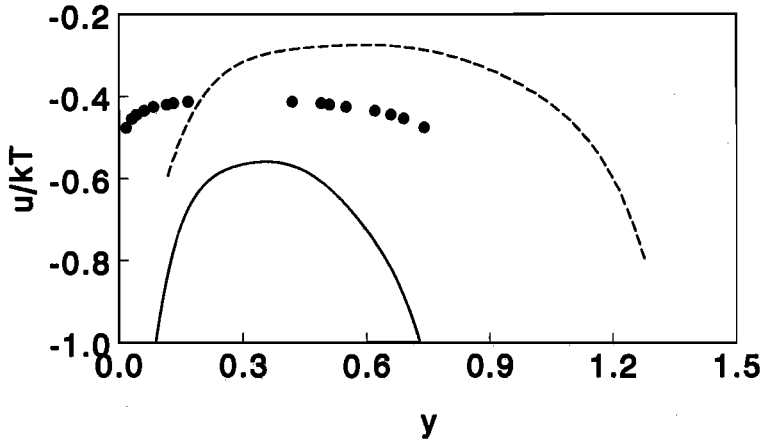


Figure 3.13: *Liquid-vapor spinodal curves for 16-mers. Full lines represent the excluded volume theory; dashed lines the freely jointed chain model, (•) MC simulation for binodal curve.*

The finite size employed in the simulation makes it impossible to investigate the binodal curve down to lower temperature. Nevertheless, it may be anticipated that the binodal curve tend to $y = 0$ and $y = 1$ at $0K$. Spinodals and binodal are plotted as reduced interaction potential $\beta\epsilon$ versus packing fraction. The spinodal curve obtained from ω_{id}^{intr} is located at too high temperature and extends to packing fractions larger than unity. Again, the unphysical intra-molecular overlaps of the ideal chain molecules lead to densities larger than one. The combination ω_{excl}^{intr} /PRISM produces an at least qualitatively correct spinodal curve. The maximum of the spinodal curve is known to be the critical state for a mono-disperse lattice fluid. The estimated critical density $y_c \cong 0.34$ compares favorably to the critical density $y_c \cong 0.295$ estimated from the MC simulations. However, the total spinodal curve is shifted towards too low temperatures.

3.5 Conclusions

An intra-molecular correlation function ω_{excl}^{intr} that accounts for the segmental overlaps related to the excluded volume of the flexible chain molecule has been derived employing diagrammatic techniques similar to those leading to the (P)RISM theory for the inter-molecular correlations. Using this excluded volume intra-molecular correlation function in the lattice-PRISM theory the inter-molecular correlations for athermal and interacting chains have been calculated and the thermodynamic properties of the dense chain fluid have been studied. The theoretical results of the combinations lattice-PRISM/ ω_{excl}^{intr} and lattice-PRISM/ ω_{id}^{intr} have been compared to MC simulation data for the lattice model.

The intra-molecular excluded volume theory compares favorably to the MC data for the single chain. On the other hand, the freely jointed chain model overestimates the single chain intra-molecular correlation function at short distances and the quality of the predictions deteriorates with increasing chain length. Upon increasing the density, the MC intra-molecular correlation function ω_{MC}^{intr} moves towards the freely jointed chain results but, even at the highest investigated densities, they are actually never reached. In fact, visual inspection of all results indicates that the new intra-molecular correlation function ω_{excl}^{intr} in eq 3.13 yields a better prediction, especially at smaller distances, even at the highest investigated density.

Employing the intra-molecular correlation functions ω_{excl}^{intr} and ω_{id}^{intr} the inter-molecular correlations for athermal and interacting chains at several densities have been calculated according to the lattice-PRISM theory. Intimately related to the inexact limiting behavior at low density of the PRISM theory the predicted zero and low density inter-molecular correlations are particularly poor. For athermal chains, the freely jointed chain model produces quite excellent predictions of the inter-molecular correlation functions at higher density which is likely due to some effective cancellation of errors in theories used to produce the inter- and intra-molecular correlations. For interacting chains the excluded volume theory produces better predictions for the inter-molecular correlation functions for all investigated densities.

The compressibility factor of the athermal lattice fluid is underestimated by the freely jointed chain model and qualitatively incorrect and unphysical results are obtained due to the total neglect of intra-molecular excluded volume. On the other hand, the combination lattice-PRISM/ ω_{excl}^{intr} provides, at least, a qualitatively correct description of the equation of state properties compared to the

MC data. From off-lattice studies it has been found that the compressibility route to the equation of state is not the most accurate. For instance, Yethiraj et al. found some indications that the wall equation of state was closer to experimental data than, e.g., the compressibility and free energy 'charging' routes.⁶⁰ However, irrespective of the relative success of the wall equation of state, the results are far from quantitative. Furthermore, previous lattice investigations have shown that the the wall equation of state is not really preferable above e.g. the compressibility equation of state.⁶⁶

The liquid-vapor spinodal curve calculated for the freely jointed chain model is located at lower temperatures compared to the vapor-liquid coexistence curve obtained from MC simulations. Moreover, the spinodal curve extends to packing fractions larger than unity. The excluded volume theory offers a qualitatively correct spinodal curve. The maximum of the spinodal curve is known to be the critical state for a mono-disperse lattice fluid. The estimated critical density $y_c = 0.34$ compares favorably to the critical density $y_c = 0.295$ estimated from the MC simulation results. However, the spinodal curve is shifted towards too high temperatures.

The single chain intra-molecular correlation function ω_{excl}^{intr} can also be used in a study of polymer mixtures. In this case also the liquid-liquid miscibility behavior becomes of interest. This will be the subject of a future research.

References

- [1] Flory, P. J., *J. Chem. Phys.* 10, 51, 1942.
- [2] Huggins, M. L., *Ann. N.Y. Acad. Sci* 43, 1, 1942.
- [3] Flory, P. J., *Principles of Polymer Chemistry*. Cornell University Press, Ithaca, 1953.
- [4] Prigogine, I., Bellemans, A., Mathot, V., *The Molecular Theory of Solutions*. North-Holland Publishing Co, Amsterdam, 1957.
- [5] Simha, R., Somcynsky, T., *Macromolecules* 2, 341, 1969.
- [6] Nies, E., Stroeks, A., *Macromolecules* 23, 4092, 1990.
- [7] Dickman, R., Hall, C. K., *J. Chem. Phys.* 89, 3168, 1988.
- [8] Sanchez, I. C., Lacombe, R. H., *J. Phys. Chem.* 80, 2352, 1976.
- [9] ten Brinke, G., Karasz, F. E., *Macromolecules* 17, 815, 1984.
- [10] Sanchez, I. C., Balazes, A. C., *Macromolecules* 22, 2325, 1989.
- [11] Freed, K. F., *J. Phys. A* 18, 871, 1985.
- [12] Bawendi, M. G., Freed, K. F., Mohanty, U., *J. Chem. Phys.* 84, 7036, 1986.
- [13] Bawendi, M. G., Freed, K. F., *J. Chem. Phys.* 88, 2741, 1988.
- [14] Pesci, A. I., Freed, K. F., *J. Chem. Phys.* 90, 2003, 1989.
- [15] Nemirovsky, A. M., Bawendi, M. G., Freed, K. F., *J. Chem. Phys.* 87, 7272, 1987.
- [16] Freed, K. F., Dudowicz, J., *J. Chem. Phys.* 97, 2105, 1992.

- [17] Dudowicz, J., Freed, K. F., *Macromolecules* 24, 5112, 1991.
- [18] Curro, J. G., Schweizer, K. S., *Macromolecules* 20, 1928, 1987.
- [19] Schweizer, K. S., Curro, J. G., *J. Chem. Phys.* 89, 3350, 1988.
- [20] Schweizer, K. S., Curro, J. G., *Macromolecules* 21, 3070, 1988.
- [21] Curro, J. G., Schweizer, K. S., *Macromolecules* 24, 6736, 1991.
- [22] Janssen, R. H. C., *PhD - thesis*. Eindhoven University of Technology, The Netherlands, 1996.
- [23] McQuarrie, D. A., *Statistical Mechanics*. Harper and Row Publishers, New York, 1976.
- [24] Lowden, L. J., Chandler, D., *J. Chem. Phys.* 59, 6587, 1973.
- [25] Lowden, L. J., Chandler, D., *J. Chem. Phys.* 62, 4246, 1975.
- [26] Freasier, B. C., *Chem. Phys. Lett.* 35, 280, 1975.
- [27] Jolly, D., Freasier, B. C., Bearman, R. J., *Chem. Phys. Lett.* 46, 75, 1977.
- [28] Freasier, B. C., Jolly, D., Bearman, R. J., *Mol. Phys.* 31, 255, 1976.
- [29] Tildesley, D. J., Street, W. B., *Mol. Phys.* 41, 85, 1980.
- [30] Aviram, I., Tildesley, D. J., *Mol. Phys.* 34, 881, 1977.
- [31] Chandler, D., Andersen, H. C., *J. Chem. Phys.* 57, 1930, 1972.
- [32] Yethiraj, A., Hall, C. K., Honnell, K. G., *J. Chem. Phys.* 93, 4453, 1990.
- [33] Chandler, D., *J. Chem. Phys.* 59, 2742, 1973.
- [34] Hsu, C. S., Pratt, L. R., Chandler, D., *J. Chem. Phys.* 68, 4213, 1978.
- [35] Pratt, L. R., Hsu, C. S., Chandler, D., *J. Chem. Phys.* 68, 4213, 1978.
- [36] Grayce, C. J., Schweizer, K. S., *J. Chem. Phys.* 100, 6846, 1994.
- [37] Grayce, C. J., Yethiraj, A., Schweizer, K. S., *J. Chem. Phys.* 100, 6857, 1994.

- [38] Schweizer, K. S., Honnell, K. G., Curro, J. G., *J. Chem. Phys.* 96, 3211, 1992.
- [39] Melenkevitz, J., Schweizer, K. S., Curro, J. G., *Macromolecules* 26, 6190, 1993.
- [40] Melenkevitz, J., Curro, J. G., Schweizer, K. S., *J. Chem. Phys.* 99, 5571, 1993.
- [41] Flory, P. J., *Statistical Mechanics of Chain Molecules*. Hanser Publishers, New York, 1989.
- [42] Frenkel, D., Smit, B., *Understanding Molecular Simulation from Algorithm to Applications*. Academic Press, Inc., San Diego, 1996.
- [43] Cifra, P., Karasz, F. E., Macknight, W. J., *Macromolecules* 25, 4895, 1992.
- [44] Cifra, P., Karasz, F. E., Macknight, W. J., *Macromolecules* 25, 192, 1992.
- [45] The Gaussian chain consists of segments connected by bonds having a Gaussian distribution of bond length. In the freely jointed chain the segments are connected by constant bond lengths. The rotational isometric state model introduces some additional chemical details by allowing for rotational potentials.
- [46] Baxter, R. J., *J. Chem. Phys.* 49, 2770, 1968.
- [47] Lomba, E., in E. Kiran, J. M. H. L. Sengers (eds.), *Supercritical Fluids*. Kluwer Academic Publishers, The Netherlands, 1928-1931.
- [48] Curro, J. G., Blatz, P. J., Pings, C. J., *J. Chem. Phys.* 50, 2199, 1969.
- [49] Nies, E., Cifra, P., *Macromolecules* 27, 6033, 1994.
- [50] Chandler, D., in E. W. Montroll, J. L. Lebowitz (eds.), *Studies in Statistical Mechanics VIII*, p. 275. North - Holland, Amsterdam, 1982.
- [51] Curro, J. G., Schweizer, K. S., *J. Chem. Phys.* 87, 1842, 1987.
- [52] Lebowitz, J. L., Percus, J. K., *Phys. Rev.* 144, 251, 1966.
- [53] Ballard, D. G., Schelten, J., Wignall, G. D., *Eur. Polym. J.* 9, 965, 1973.

- [54] Cotton, J. P., Decker, D., Benoit, H., Farnoux, B., Huggins, J., Jannik, G., Ober, R., Picot, C., des Cloizeaux, J., *Macromolecules* 7, 863, 1974.
- [55] Vacetello, M., Avitabile, G., Corradini, P., Tuzi, A., *J. Chem. Phys.* 73, 543, 1980.
- [56] Weber, T. A., Helfand, E., *J. Chem. Phys.* 71, 4760, 1979.
- [57] Koyama, R., *J. Phys. Soc. Jpn.* 34, 1092, 1973.
- [58] Chandrasekhar, S., *Rev. Mod. Phys.* 15, 1, 1943.
- [59] Prigogine, I., Defay, R., *Chemical Thermodynamics*. Longmans Green and Co., London, 1954.
- [60] Yethiraj, A., Curro, J. G., Schweizer, K. S., McCoy, J. D., *J. Chem. Phys.* 98, 1635, 1993.
- [61] Janssen, R. H. C., Nies, E., Cifra, P., *Macromolecules*, submitted 1997.
- [62] Yan, Q., Liu, H., Hu, Y., *Macromolecules* 29, 4066, 1996.
- [63] Yan, Q., Jian, J., Liu, H., Hu, Y., *J. Chem. Ind. Eng. (China)* 46, 517, 1995.
- [64] Allen, M. P., Tildesley, D. J., *Computer Simulation of Liquids*. Clarendon, Oxford, 1987.
- [65] de Gennes, G., *Scaling Concepts in Polymer Physics*. Cornell University Press Ltd., London, 1979.
- [66] Janssen, R. H. C., Nies, E., Cifra, P., *Langmuir* 13, 2784, 1997.

Chapter 4

A theory for compressible binary lattice polymers: Influence of chain conformational properties

4.1 Introduction

The interest in the lattice model in polymer science can be retraced to Flory and Huggins more than half a century ago. Their independent works resulted in the celebrated theoretical Flory Huggins (FH) expression for the free enthalpy of mixing of a polymer solution.¹⁻⁴ At the same time Flory pointed to the inadequacies of the lattice model for the real off-lattice fluid state, thereby relativizing the importance of refinements to the primitive FH result which carry details of the model.² Although the limits of the lattice model for understanding the liquid state have over the years been unravelled in more detail, it has persistently attracted attention. Especially the advent of molecular simulation techniques, becoming feasible with modern computer facilities, renewed the interest in the lattice model. In the framework of statistical mechanics and properly accounting for finite size effects simulations essentially provide the exact properties of a model.^{5,6} Thus by comparing theory and simulations it is possible to study the approximations invoked in theoretical investigations. From these comparative studies it is now clear that the different refinements of the primitive FH theory indeed lead to improved predictions of the thermodynamic properties of the lattice model.⁷⁻¹²

One of the first systematic studies of the lattice model by Monte Carlo (MC) computer simulations was pursued by Sariban and Binder who investigated sym-

metric binary polymer mixtures on a cubic lattice with a constant fraction of vacancies.⁹⁻¹² A variety of properties was investigated in these simulations. Of interest to the present contribution we report the study of liquid-liquid coexistence as a function of chain length, temperature and vacancy fraction. In addition to this sheer thermodynamic data also the average number of the different types of contacts in the mixture was collected in the simulations. The simulation results were compared to the FH and Guggenheim expressions for the lattice model.^{2,4,13}

The FH free enthalpy density equals the sum of the internal energy, given by a van Laar-Hildebrand expression, and the combinatorial entropy derived for the athermal systems. Thus, the influence of the interactions on the entropy is completely ignored and a random mixing of all segments is assumed. In addition the chain connectivity is fully ignored and the FH expression is given in terms of the occupied site or volume fraction. It should be mentioned that Huggins already predicted an entropy correction to the FH result, including the influence of the nearest neighbor covalent bonds of each segment. The Huggins correction is most naturally formulated employing the external contact fraction, so excluding the covalent bonds making up the linear chains from participating in inter-segmental contacts.

A next important theoretical advancement was established by Guggenheim. Employing his quasi-chemical approximation, Guggenheim incorporated the influence of the segmental interactions on the free enthalpy, thus removing the random mixing assumption adopted by Flory and Huggins. Sariban and Binder clearly showed that the Guggenheim expression is substantially better than the simple FH theory. At the same time they exposed the main shortcomings of the investigated theories. For the relatively short chain lengths studied in the simulations the real (simulated) coexistence curves clearly have a non-parabolic shape due to a non-classical critical scaling behavior.⁹ In contrast, the theoretical coexistence curves have a parabolic shape associated with their mean-field character.¹³ A second deficiency of the FH and Guggenheim theories was found for the different types of segmental contacts. In the simulation a significant number of intra-molecular or self-contacts was found; such contacts are completely ignored in the theories. Further detailed studies of the equation of state and miscibility behavior of compressible symmetric binary mixtures in combination with the segmental contacts demonstrated the influence of the intra-molecular contacts on the thermodynamic results and it was anticipated that a theory incorporating the intra-molecular contacts might further improve the agreement with MC simulation.¹⁴

An important theoretical advancement for the lattice model is provided by the Lattice Cluster (LC) Theory of Freed and co-workers.^{15,16} These authors moulded the lattice partition function in a double expansion in terms of the inverse lattice coordination number and inverse temperature. The zeroth order term in this expansion is the simple FH result and the higher order contributions constitute systematic corrections over the simple FH result. Several applications of the LC theory, e.g. to mixtures of chemically different polymers¹⁷ and mixtures of linear and branched chain molecules,¹⁸ have indicated the relevance of these theoretical refinements. In the case of athermal linear chains the LC theory provides slightly better predictions of the compressibility factor than the Guggenheim approximation^{7,8} (for athermal chains the Guggenheim theory reduces to the Huggins combinatorial entropy expression). For the chain lengths actually investigated the difference between the Guggenheim and LC theory was only minor but was anticipated to increase in favor of the latter for longer chain lengths.⁸ Despite the importance of the LC theory also some drawbacks should be mentioned. For instance, as a function of chain length, peculiar critical behavior was found in the isomorphic conditions of liquid-liquid coexistence of an incompressible polymer solution and the vapor-liquid coexistence of a compressible pure component.^{8,19,20} Further, as the LC theory relies on a truncated expansion in the inverse lattice coordination number and inverse temperature it is unable to fully account for the long range consequences of the excluded volume effects typical of chain like fluids.

Another line of approach, i.e. the integral equation theory of polymers fluids, was investigated by Curro, Schweizer and collaborators.^{21,22} Integral equation theories were initially developed for simple mono-atomic fluids to study the microscopic structure of fluids.²³ These liquid state theories, employing correlation functions, were extended to simple molecular fluids in the reference interaction site model (RISM) theory by Chandler and co-workers.^{24,25} The RISM theory makes it feasible to predict the inter-molecular correlations among segments or interaction sites on different molecules from information of the intra-molecular correlations, which are set by the molecular architecture, between segments of the same molecule. The application of the RISM theory to flexible chain molecules (Polymer-RISM or PRISM) was initiated by Curro and Schweizer to study the microscopic structure of polymer single components and mixtures.^{21,22} For flexible macromolecules, the intra-molecular structure is not *a priori* known and it must be expected to depend on the inter-molecular correlations which according to the (P)RISM theory are determined by the intra-molecular correlations.

Hence, a complicated interdependence between inter- and intra-molecular correlations exists and, in principle, both types of correlations must be calculated self-consistently. The first attempts to establish this self-consistency have been published only recently and are still a matter of further investigation.²⁶⁻²⁹ Based on the detailed information concerning the correlations in the fluid, the thermodynamic properties can be derived employing exact statistical mechanical relationships.^{23,25,30} Unfortunately, and this is a major drawback of all integral equation theories, these calculations are plagued with so called thermodynamic inconsistencies which are related to the necessary approximations involved in the calculation of the theoretical correlations.²³

Another interesting approach incorporating the conformational degrees of freedom of the chain molecules in the thermodynamics is due to Szleifer.³¹ He considered the chain molecule as a whole in the environment made up by the total system. Note that in the usual FH theory, the influence of the environment is only considered on the segmental level. In evaluating the expression for the partition function, the conformation and translational or configurational degrees of freedom are decoupled. The translational part is assumed to be given by the Flory-Huggins combinatorial entropy and the influence of the conformational degrees of freedom is limited to the internal energy.³¹ Hence for athermal chains the simple FH combinatorial entropy is recovered.

In a more recent theoretical development, Weinhold, Kumar and Szleifer achieved a coupling between translational and conformational degrees of freedom for athermal lattice chains.³² They derived the total entropy in combinatorial and conformational contributions. For the combinatorial entropy a Huggins-Guggenheim like expression was used, depending on the average number of intra-molecular contact which is determined by the conformational degree of freedom.³² The authors found chain dimensions and chemical potentials calculated with this new theory in reasonable agreement with MC simulation data.³²

In this chapter the influence of the excluded volume of the chain molecule is also investigated. We also start from the notion of intra-molecular self-contacts and use this concept to formulate a new theory for athermal and interacting systems. It will be shown that the intra-molecular contacts require the introduction of a new composition variable excluding such contacts and hence fundamentally change the functional dependence of the combinatorial entropy and free energy expressions as formulated by Guggenheim.¹³ In section 4.2 the new theory and expressions for several thermodynamic properties are derived and placed in relation to other existing theories. In section 4.3 the employed MC simulation

algorithms are discussed. In section 4.4 the results for athermal and interacting pure components as well as mixtures are discussed. Finally, section 4.5 summarises the important results and gives directions for future investigations based on the new theory.

4.2 Theory

4.2.1 Partition functions, insertion probabilities and thermodynamics

The present discussion considers the thermal properties of a binary mixture containing N_A s_A -mers, N_B s_B -mers. Thus each $A(B)$ molecule is modeled as a linear sequence of $s_A(s_B)$ consecutive sites on the lattice. For the following general discussion of thermodynamics and statistical mechanics it is convenient to define the following variables

$$\begin{array}{ll} \text{Total number of molecules } N & N = N_A + N_B \\ \text{Number average chain length } s & s = (s_A N_A + s_B N_B) / N \\ \text{Chemical composition } \phi_B (= 1 - \phi_A) & \phi_A = s_A N_A / s N, \phi_B = s_B N_B / s N \end{array}$$

The partition function Q_N of the binary mixture is defined by^{23,33}

$$Q_N(N_A, N_B, N_L, T) = \frac{1}{N_A! N_B!} \sum_{\{\Lambda_N\}} \exp[-\beta U_N(\Lambda_N)] = \frac{1}{N_A! N_B!} Z_N(N_A, N_B, N_L, T) \quad (4.1)$$

with Λ_N is an allowed configuration of the N chain molecules on the lattice; $U_N(\Lambda_N)$ is the internal energy of the system in configuration Λ_N ; the sum runs over all allowed configurations. The factorials in eq 4.1 correct for the indistinguishability of the molecules of components A and B . The normal kinetic contributions to the partition function are not shown since they do not contribute to the density and composition dependence of the thermal properties discussed in this chapter.

A configuration Λ_N is specified by the positions of all segments on the lattice which agree with the constraints of i) at most single occupancy of lattice sites and ii) the connectivity of the segments in each chain molecule. In lattice theories, it is customary to consider only nearest neighbor interactions and the internal

energy of the configuration Λ_N can be written as

$$U_N(\Lambda_N) = -(\mathcal{N}_{AA}(\Lambda_N)\epsilon_{AA} + \mathcal{N}_{BB}(\Lambda_N)\epsilon_{BB} + \mathcal{N}_{AB}(\Lambda_N)\epsilon_{AB}) \quad (4.2)$$

with $\mathcal{N}_{ij}(\Lambda_N)$ the number of contact pairs of the type ij in the configuration Λ_N carrying a corresponding contact energy $-\epsilon_{ij}$. All contacts involving empty lattice sites are assigned a zero contact energy.

The partition function Q_N offers a direct route to the Helmholtz free energy^{23,33}

$$\beta A(N_A, N_B, N_L, T) = -\ln Q_N(N_A, N_B, N_L, T) \quad (4.3)$$

An alternative route is provided by the insertion probabilities of both components, $P_A(N_A, N_B, N_L, T)$ and $P_B(N_A, N_B, N_L, T)$, which are defined by the following ratios of partition functions^{13,34,35}

$$\begin{aligned} P_A(N_A, N_B, N_L, T) &= \frac{Z_{N+1}(N_A + 1, N_B, N_L, T)}{Z_N(N_A, N_B, N_L, T)Z(1, 0, N_L, T)} \\ &= \frac{Z_{N+1}(N_A + 1, N_B, N_L, T)}{Z_N(N_A, N_B, N_L, T)N_L Z_A} \end{aligned} \quad (4.4a)$$

$$\begin{aligned} P_B(N_A, N_B, N_L, T) &= \frac{Z_{N+1}(N_A, N_B + 1, N_L, T)}{Z_N(N_A, N_B, N_L, T)Z(0, 1, N_L, T)} \\ &= \frac{Z_{N+1}(N_A, N_B + 1, N_L, T)}{Z_N(N_A, N_B, N_L, T)N_L Z_B} \end{aligned} \quad (4.4b)$$

The last equalities in Eqs 4.4 are obtained if one realizes that the partition functions of a single chain on the lattice can be written as the product of an intramolecular contribution $Z_A(Z_B)$ and the total number of lattice sites N_L . More specifically, for a single A chain

$$Z(1, 0, N_L, T) = \sum_{\{\Lambda_1\}} \exp[-\beta U_1(\Lambda_1)] = N_L \sum_{\{\Lambda_1'\}} \exp[-\beta U_1(\Lambda_1')] = N_L Z_A \quad (4.5)$$

with Λ_1' the allowed configurations of the chain with the first segment fixed. The summation appearing in the second equality is the intra-molecular partition function of the chain. The first segment can be positioned on each lattice site and N_L identical terms Z_A are obtained.

Eqs 4.4 are called chain insertion probabilities. This interpretation stems from the possibility to rearrange eqs 4.4 as ensemble averages over all configurations of a single s_j -mer, the $N_j + 1$ th molecule, in the mixture of all other molecules.^{5,36} The insertion probabilities were originally introduced by Guggenheim in the study of incompressible lattice mixtures.¹³ More recently, Hall and coworkers employed

the insertion probabilities to derive continuum space analogs of the Flory and the Flory-Huggins lattice theories, the so called generalized Flory and Flory-dimer theories.^{34, 35}

Clearly the chemical potentials of both components are related to the intrinsic insertion probabilities according to

$$\begin{aligned}\beta\mu_A(N_A, N_B, N_L, T) &= \beta(A(N_A + 1, N_B, N_L, T) - A(N_A, N_B, N_L, T)) \\ &= -\ln\left[\frac{Z_{N+1}(N_A + 1, N_B, N_L, T)}{Z_N(N_A, N_B, N_L, T)(N_A + 1)}\right] \\ &= -\ln[Z_A P_A(N_A, N_B, N_L, T)N_L/(N_A + 1)]\end{aligned}\quad (4.6a)$$

$$\begin{aligned}\beta\mu_B(N_A, N_B, N_L, T) &= \beta(A(N_A, N_B + 1, N_L, T) - A(N_A, N_B, N_L, T)) \\ &= -\ln\left[\frac{Z_{N+1}(N_A, N_B + 1, N_L, T)}{Z_N(N_A, N_B, N_L, T)(N_B + 1)}\right] \\ &= -\ln[Z_B P_B(N_A, N_B, N_L, T)N_L/(N_B + 1)]\end{aligned}\quad (4.6b)$$

In the thermodynamic limit, i.e. $N_L, N_A, N_B \rightarrow \infty$ and $sN/N_L = y$ and $s_B N_B/sN = \phi_B$, the chemical potentials and all other intensive thermodynamic functions of state are independent of the extension of the system and depend only on the intensive variables y, ϕ_B and T . Hence, in this limit also the right hand sides of eqs 4.6 can only be functions of these intrinsic variables and one can define limiting chain insertion probabilities according to

$$p_A(y, \phi_B, T) = \lim_{\substack{N_L, N_A, N_B \rightarrow \infty \\ sN/N_L = y, s_B N_B/sN = \phi_B}} P_A(N_A, N_B, N_L, T) \quad (4.7a)$$

$$p_B(y, \phi_B, T) = \lim_{\substack{N_L, N_A, N_B \rightarrow \infty \\ sN/N_L = y, s_B N_B/sN = \phi_B}} P_B(N_A, N_B, N_L, T) \quad (4.7b)$$

Consequently, in the thermodynamic limit, the expressions for the chemical potentials become

$$\beta\mu_A(y, \phi_B, T) = -\ln[s_A p_A(y, \phi_B, T)Z_A/(\phi_A y)] \quad (4.8a)$$

$$\beta\mu_B(y, \phi_B, T) = -\ln[s_B p_B(y, \phi_B, T)Z_B/(\phi_B y)] \quad (4.8b)$$

Furthermore, the chain insertion probabilities can be used to determine the Helmholtz free energy. Applying the definitions of the insertion probabilities, eqs 4.4, recursively to eq 4.1, the partition function can be written as a product of chain insertion probabilities, i.e. the mixture is built up by inserting the chain

molecules one at a time. For example, if the N_A molecules are inserted before the N_B molecules, one finds

$$Q_N(N_A, N_B, N_L, T) = \frac{Z_A^{N_A} Z_B^{N_B} N_L^N}{N_A! N_B!} \prod_{l=1}^{N_A-1} P_A(l, 0, N_L, T) \prod_{m=1}^{N_B-1} P_B(N_A, m, N_L, T) \quad (4.9)$$

On the other hand, if the order of insertion is reversed one obtains

$$Q_N(N_A, N_B, N_L, T) = \frac{Z_A^{N_A} Z_B^{N_B} N_L^N}{N_A! N_B!} \prod_{l=1}^{N_A-1} P_A(l, N_B, N_L, T) \prod_{m=1}^{N_B-1} P_B(0, m, N_L, T) \quad (4.10)$$

Unfortunately, the approximate nature of available theoretical expressions for the insertion probabilities (such as the Huggins approximation discussed in the sequel) may make the partition function dependent on the particular order of insertion.³⁵ The thermodynamic functions, being state functions, must be independent of this order. A possible way to prevent this problem is to average over all distinct ways of constructing the mixture. However, this is a formidable task as, in total, there are $N!/N_A!N_B!$ distinct ways of inserting the chains. A practically useful way, to assure that the intensive thermodynamic functions depend only on the intensive variables, is to insert the molecules at constant chemical composition, ϕ_B . In this case, the density of the mixture is increased to the final density by inserting A and B molecules in the order that attains the mixture composition fixed at the macroscopic composition ϕ_B . The relation between the partition function and the chain insertion probability factors then becomes (to illustrate, the mixture composition is set to $\phi_B = 1/3$, hence, for each B molecule two A molecules must be inserted)

$$Q_N(N_A, N_B, N_L, T) = \frac{Z_A^{N_A} Z_B^{N_B} N_L^N}{N_A! N_B!} \times \dots\dots\dots\{P_A(l+1, m, N_L, T)P_B(l+1, m+1, N_L, T)P_A(l+2, m+1, N_L, T)\}\dots\dots\dots \quad (4.11)$$

where only a typical sequence of insertion factors is shown. The number of insertion factors in a typical sequence depends of course on the composition. In the thermodynamic limit, the chain insertion probabilities are only functions

of the intrinsic variables, as defined in eqs 4.7, and the typical sequence becomes

$$\begin{aligned} & \dots\{P_A(l+1, m, N_L, T)P_B(l+1, m+1, N_L, T)P_A(l+2, m+1, N_L, T)\}\dots = \\ & \dots\{p_A(y'(i), \phi_B, T)p_B(y'(i+1), \phi_B, T)p_A(y'(i+2), \phi_B, T)\}\dots \end{aligned} \quad (4.12)$$

with $y'(i)$ the density, of the mixture under construction, at the insertion of molecule i (either A or B). In the thermodynamic limit, the density does not change in the typical sequence and the insertion factors of A and B molecules can be collected, i.e.

$$\begin{aligned} & \dots\{p_A(y'(l), \phi_B, T)p_B(y'(m+1), \phi_B, T)p_A(y'(l+2), \phi_B, T)\}\dots \\ & = \dots\{p_A(y'(i), \phi_B, T)p_B(y'(i), \phi_B, T)p_A(y'(i), \phi_B, T)\}\dots \\ & = \dots\{[p_A(y'(i), \phi_B, T)^{N_A/N} p_B(y'(i), \phi_B, T)^{N_B/N}]^{\text{Number of molecules in typical sequence}}\}\dots \\ & = \dots\{[p_A(y'(i), \phi_B, T)^{s_{\phi A/s_A}} p_B(y'(i), \phi_B, T)^{s_{\phi B/s_B}}]^{\text{Number of molecules in typical sequence}}\}\dots \\ & = \dots\{[p_e(y'(i), \phi_B, T)]^{\text{Number of molecules in typical sequence}}\}\dots \end{aligned} \quad (4.13)$$

with $y'(i)$ the density of the mixture upon introducing the typical sequence. The last identity can be thought of as the chain insertion probability, $p_e(y, \phi_B, T)$, of a molecule of an *effective* component, determined by the composition of the mixture.

Using the insertion factor of the effective component, defined in eq 4.13, the partition function, eq 4.11, can be written as

$$Q_N(N_A, N_B, N_L, T) = \frac{Z_A^{N_A} Z_B^{N_B} N_L^N}{N_A! N_B!} \prod_{i=1}^{N-1} p_e(y'(i), \phi_B, T) \quad (4.14)$$

Combining eqs 4.3 and 4.14, and making use of the Stirling approximation, $N! = (N/e)^N$, the Helmholtz free energy can be written as

$$\begin{aligned} \beta A = & N_A \ln(\phi_A y) + N_B \ln(\phi_B y) - \sum_{i=1}^{N-1} \ln[p_e(y'(i), \phi_B, N_L, T)] \\ & - N_A \ln(es_A Z_A) - N_B \ln(es_B Z_B) \end{aligned} \quad (4.15)$$

The last two terms in eqs 4.15 are linear in composition and do not contribute to the thermodynamic properties discussed in the following and are therefore omitted in the sequel.

Considering the intensive Helmholtz free energy per segment, and replacing the summation by an integral, we arrive at the following expressions

$$\beta A/sN = (\phi_A/s_A) \ln(\phi_A) + (\phi_B/s_B) \ln(\phi_B) + (1/s) \ln(y) - (N_L/s^2 N) \int_1^{N-1} \ln[p_e(y'(i), \phi_B, N_L, T)] d(si/N_L) \quad (4.16a)$$

$$\beta A/sN = (\phi_A/s_A) \ln(\phi_A) + (\phi_B/s_B) \ln(\phi_B) + (1/s) \ln(y) - (1/sy) \int_0^y \ln[p_e(y', \phi_B, T)] dy' \quad (4.16b)$$

Finally the equation of state can be derived from eq 4.16 by direct differentiation with respect to the volume at constant temperature and composition, or by making use of the thermodynamic identity

$$pV = N_A \mu_A + N_B \mu_B - A \quad (4.17)$$

Both routes lead to the same result, i.e.

$$\beta pV/sN = \beta p v^*/y = (1 - \ln(p_e))/s + (1/sy) \int_0^y \ln[p_e(y', \phi_B, T)] dy' \quad (4.18)$$

Equations 4.8, 4.16 and 4.18 provide relations between the insertion probabilities and the thermodynamic properties considered in this work.

4.2.2 Theoretical expressions for the insertion probabilities of athermal chains

Further progress depends on the development of accurate expressions for the insertion probabilities. It was already mentioned that the limiting chain insertion probabilities as defined in eqs 4.7 are a measure for the success of introducing a test chain in the mixture. For athermal chains, i.e. $\epsilon_{AA} = \epsilon_{BB} = \epsilon_{AB} = 0$, each allowed configuration of the test chain is equally probable and the insertion probability is independent of temperature.

To illustrate the concept, the insertion probabilities typical for the well known Flory and Huggins approximations will be derived. In particular the Huggins approximation will serve as a reference to obtain a more accurate approximation for the insertion probabilities. Both Flory and Huggins derived independently expressions for the entropy of mixing polymer and solvent on a fully occupied lattice.^{2,4} The equivalence of the incompressible polymer solution and the compressible polymer melt was exploited to discuss the equation of state and its

influence on miscibility of compressible polymer systems.^{7,14} In this contribution the Flory and Huggins approximations will be discussed for a compressible binary polymer mixture.

In the Flory approximation it is assumed that each segment can be inserted independently of the other segments in the chain.^{13,34} Consequently, the chain insertion probability can be written as the product of these segmental contributions. The insertion factor of an independent segment (which is the ensemble average over all configurations of the mixture and the test segment) is equal to the fraction of free lattice sites, $(1 - y)$, and the insertion probabilities of a complete j -chain ($j = a$ or b)

$$p_j(y, \phi_B, T) = p_j(y) = (1 - y)^{s_j} \text{ and } p_e = (1 - y)^s \quad (4.19)$$

The chain insertion probability depends only on density and chain length whereas the effective chain insertion probability depends on composition only through the number average chain length s .

In eq 4.19 the insertion problem is oversimplified by completely ignoring the chain connectivity. In particular, for a middle segment two of its z contact positions are taken by covalent bonds. For an end segment one contact position participates in a covalent bond. In fact, the contact positions of a segment involved in covalent bonds are unavailable for contacts with other segments and it is useful to distinguish between covalent and other (external) contacts of a molecule. This distinction leads to the definition of *external contact fractions*^{7,13,14}

$$q_A = \frac{N_A(s_A(z - 2) + 2)}{N_A(s_A(z - 2) + 2) + N_B(s_B(z - 2) + 2) + N_h z} = \frac{\phi_A(1 - \alpha_A)y}{(1 - \alpha y)} \quad (4.20a)$$

$$q_B = \frac{\phi_B(1 - \alpha_B)y}{(1 - \alpha y)} \quad (4.20b)$$

$$q = q_A + q_B = \frac{(1 - \alpha)y}{(1 - \alpha y)} \quad (4.20c)$$

with N_h the number of vacancies on the lattice, α the number of covalent contacts per segment, $\alpha = \alpha_A \phi_A + \alpha_B \phi_B$, $\alpha_j = \gamma(1 - 1/s_j)$ ($j = A$ or B) and $\gamma = 2/z$. The numerator of eq 4.20a denotes the number of inter-segmental contact positions of the N_A chains of type a and the denominator is the total number of contact positions of chain molecules and vacancies. A similar expression, eq 4.20b, is valid for type B molecules. The fraction of inter-segmental contacts, irrespective of being of type A or B , is given by eq 4.20c.

Huggins derived an expression for the entropy of mixing of an incompressible lattice polymer solution, based on the difference between covalent and external contact positions.⁴ The chain insertion probability according to Huggins is also obtained by sequentially inserting the chain segments. As in the Flory approximation, the probability to insert the first segment is equal to the fraction of free lattice sites, $(1 - y)$. To insert the second segment it suffices to find a free contact place, on the first segment. The average probability that a contact position of the first segment is already involved in an external contact pair with other segments in the mixture is equal to the external contact fraction q . The averaged is over all configurations of the molecules already inserted and all configurations of the segment. This estimate of the average probabilities implicitly assumes that the contact positions on each segment can form independently of each other contact pairs; this is called non-interference of pairs. Hence, the probability that a chosen contact position is free equals $(1 - q)$. The insertion of the third and subsequent segments is treated in a similar manner; also for these segments it is assumed that the probability to find a free contact place is equal to $(1 - q)$. Thus, the excluded volume of the chain, resulting from connectivity effects propagated along the chain, is not accounted for. These approximations result in the following expressions for the insertion probabilities

$$\begin{aligned}
 p_A &= (1 - y)(1 - q)^{s_A - 1} = \frac{(1 - y)^{s_A}}{(1 - \alpha y)^{s_A - 1}} \\
 p_B &= (1 - y)(1 - q)^{s_B - 1} = \frac{(1 - y)^{s_B}}{(1 - \alpha y)^{s_B - 1}} \\
 p_e &= \frac{(1 - y)^s}{(1 - \alpha y)^{s(\phi_A(s_A - 1)/s_A + \phi_B(s_B - 1)/s_B)}} = \frac{(1 - y)^s}{(1 - \alpha y)^{s - 1}}
 \end{aligned} \tag{4.21}$$

In addition to the density and chain length dependence already observed in the Flory approximation, the insertion probabilities acquire an extra composition dependence by virtue of the parameter α .

More recently, Bawendi, Freed and Mohanty developed the Lattice Cluster (LC) theory offering systematic corrections to the Flory result.^{15,16} Although the Huggins correction is not a combination of those systematic corrections, it provides a substantial improvement over the Flory result. For instance, the equation of state of athermal lattice polymers obtained from Monte Carlo (MC) simulations, is predicted more accurately by the Huggins approximation than by the Flory expression.⁷ For moderate chain lengths both the LC theory and the Huggins approximation are virtually indistinguishable. However, the quality of the Huggins prediction deteriorates with increasing chain length and the higher order Lattice

Cluster theory offers room for further systematic improvement.⁸ Nevertheless, the Huggins expression can be considered to be an effective and rather accurate expression which was confirmed in further investigations, including interacting lattice polymers and binary polymer mixtures.^{7,14}

The interpretation of the Huggins approximation, given in the derivation of eq 4.21, provides also an opportunity to define an improved insertion probability. Recall the parameter α introduced with the definition of the external contact fraction. The quantity $z\alpha_j$ is the number of covalent contacts of a segment, averaged over all s_j segments in the chain. Hence, the quantity $z(1 - \alpha_j)$ is the average number of free contact positions of a segment. It was shown that a drawback of the Huggins expression is the ignorance of self contacts, intrinsically related to the excluded volume of the chain.^{9-12,14} It should be mentioned that also in the Guggenheim free enthalpy expression, the external contact fractions are used and, hence, the same drawbacks apply to this theory. In addition to the covalent contacts, a chain molecule possesses also *intra-molecular* contacts which are not able to participate in *intermolecular* contacts. For the moment, suppose that the average number of intra-molecular contacts (covalent and non-covalent) of a segment in an s_j -mer is given by $z\omega_j$ (the average is over all configurations of the mixture and the complete s_j -mer and as before ($j = a$ or b)). It is then possible to define *intermolecular contact fractions*

$$\begin{aligned}\theta_A &= \frac{N_A s_A z(1 - \omega_A)}{N_A s_A z(1 - \omega_A) + N_B s_B z(1 - \omega_B) + N_h z} = \frac{\phi_A(1 - \omega_A)y}{(1 - \omega y)} \\ \theta_B &= \frac{\phi_B(1 - \omega_B)y}{(1 - \omega y)} \\ \theta &= \theta_A + \theta_B = \frac{(1 - \omega)y}{(1 - \omega y)} \text{ and } \theta_h = 1 - \theta\end{aligned}\tag{4.22}$$

with $\omega = \omega_A \phi_A + \omega_B \phi_B$.

It is now possible to formulate chain insertion probabilities, which account for the occurrence of intra-molecular contacts, irrespective of the covalent or non-covalent character. Again, the probability to insert the first segment is equal to $(1 - y)$. The next segment can only be added at a free contact place of the first segment. The probability that a contact place in the mixture is involved in an intermolecular contact pair is θ . Hence, the probability that a contact position is free equals $(1 - \theta)$. Taking the same reasoning for the subsequent segments the

following chain insertion probabilities are obtained

$$\begin{aligned}
 p_A &= (1-y)(1-\theta)^{s_A-1} = \frac{(1-y)^{s_A}}{(1-\omega y)^{s_A-1}} \\
 p_B &= (1-y)(1-\theta)^{s_B-1} = \frac{(1-y)^{s_B}}{(1-\omega y)^{s_B-1}} \\
 p_e &= \frac{(1-y)^s}{(1-\omega y)^{s-1}}
 \end{aligned} \tag{4.23}$$

In eqs 4.23, the effect of the chain excluded volume on the nearest neighbor surrounding of the segment is accounted for, provided that the parameter ω_j is known. This is a difficult problem by itself as ω_j depends on density and chain length. In the following theoretical analysis we will also use the probability distribution of ω_j , denoted by $P_{\omega_j}(\Omega_{con}, y)$; the probability that, on average, a segment of the s_j -mer has $z\Omega_{con}$ intra-molecular contact positions. It is easily seen that ω_j can be obtained from $P_{\omega_j}(\Omega_{con}, y)$

$$\omega_j = \frac{\sum_{\Omega_{con}} \Omega_{con} P_{\omega_j}(\Omega_{con}, y)}{\sum_{\Omega_{con}} P_{\omega_j}(\Omega_{con}, y)} \tag{4.24}$$

For the single chain, i.e. ($y = 0$), the probability distribution $P_{\omega_j}(\Omega_{con}, y = 0)$ is easily extracted from a lattice simulation. It suffices to generate a proper sample of the allowed self avoiding walks (SAW's) of the s_j -mer and to inspect each chain configuration for the total number of intra-molecular contacts. From this, the intra-molecular contacts per segment are then easily calculated. For higher chain lengths, it may be necessary to use sophisticated simulation schemes, such as the biased MC algorithm.³⁷ For the chain lengths considered in this chapter, the chain configurations can be produced by straightforward generation of a sufficient number of SAW's on the lattice. For 30- and 16-mers $P_{\omega_j}(\Omega_{con}, y = 0)$ is shown in figure 4.1 (simulation details are found in the section on simulations). The distribution $P_{\omega_j}(\Omega_{con}, y)$ at density y can also be obtained from a simulation. Moreover, if such a simulation is available, other properties of the system are easily extracted. Therefore, we seek an approximate expression to predict the density dependence of ω_j . The zero-density probabilities, $P_{\omega_j}(\Omega_{con}, y = 0)$, reflect the distribution of the allowed single chain configurations according to their intra-molecular surroundings $z\Omega_{con}$. The relative importance of these different intra-molecular surroundings is altered by the density. An estimate of the influence of the density is accomplished along the following lines. The insertion probability p_j refers to the absorption of a chain in a mixture quantified by its density

y and the average number of intra-molecular segmental contacts $z\omega$. Of course, once assimilated, the test chain acquires these mixture characteristics. From eq 4.23, the Flory contribution $(1-y)^{s_j}$ can be isolated which permits an alternative interpretation for p_j . Eqs 4.23 can be viewed as the Flory insertion of independent segments (irrespective of their intra-molecular configuration) and the factor $1/(1-\omega y)^{(s_j-1)}$ which constitutes a measure for the conditional probability that the segments are present with the correct average intra-molecular organization. To this last factor, each segment contributes a factor $1/(1-\omega y)^{((s_j-1)/s_j)}$. Invoking the non-interference of pairs, one can push the interpretation even further and define the contribution of a single intra-molecular contact position

$$\left[\frac{1}{(1-\omega y)^{\frac{(s_j-1)}{s_j}}} \right]^{\frac{1}{z\omega}} \quad (4.25)$$

Recapitulating, eq 4.25 is a measure for the conditional probability to find an intra-molecular contact position in the mixture specified by ω and y . On the other hand, $P_{\omega_j}(\Omega_{con}, y)$ is the conditional probability that a chain-segment in the mixture possesses $z\Omega_{con}$ intra-molecular contact positions. A measure for the probability that a chain has the surrounding $z\Omega_{con}$, in the mixture specified by ω and y , can be calculated from eq 4.25. Each of the $z\Omega_{con}$ intra-molecular contacts of a segment carries a factor, given by eq 4.25. The conditional probability for a complete chain is obtained by subsequent insertion of the s_j independent segments. Putting everything together gives

$$\left(\left[\frac{1}{(1-\omega y)^{\frac{(s_j-1)}{s_j}}} \right]^{\frac{z\Omega_{con}}{z\omega}} \right)^{s_j} \quad (4.26)$$

Eq 4.26 provides a measure for the influence of density on the probability of a chain to have $z\Omega_{con}$ intra-molecular contacts per segment. The probability distribution $P_{\omega_j}(\Omega_{con}, y)$ can then be calculated according to

$$P_{\omega_j}(\Omega_{con}, y) = h_N P_{\omega_j}(\Omega_{con}, y = 0) \left(\frac{1}{(1-\omega y)^{\frac{\Omega_{con}}{\omega}}} \right)^{s_j-1} \quad (4.27)$$

where we have introduced a normalization factor h_N which need not to be known as it cancels in the calculation of ω_j by means of eq 4.24.

The average segmental surrounding of a segment at any density can now be calculated from the simulation data of the single chain, eq 4.27 and eq 4.24. Note that the ω_j 's are also present at the rhs of eq 4.27 and the ω_j 's are obtained iteratively. The predictions for ω_j are compared to simulation data in figure 4.2 and are discussed in 4.4.

Eqs 4.23 and 4.27 are the main theoretical results for athermal chains. The probability distribution $P_{\omega_j}(\Omega_{con}, y)$ can be calculated via eq 4.27 from the distribution $P_{\omega_j}(\Omega_{con}, y = 0)$, obtained from the single chain simulation. Combined with the available relations between the insertion probabilities and thermodynamic properties (eqs 4.8, 4.16 and 4.18) a complete theory for athermal lattice chains is provided. For instance, the Helmholtz free energy of the athermal mixture becomes

$$\begin{aligned} \beta A/sN = & (\phi_A/s_A) \ln(\phi_A) + (\phi_B/s_B) \ln(\phi_B) \\ & + (1/s) \ln(y) - (1/sy) \int_0^y \ln[(1-y')^s / (1-\omega y')^{s-1}] dy' \end{aligned} \quad (4.28)$$

The equation of state is given by

$$\beta pV/sN = \beta p v^*/y = (1 - \ln(p_e))/s + (1/sy) \int_0^y \ln[(1-y')^s / (1-\omega y')^{s-1}] dy' \quad (4.29)$$

with ω defined by eqs 4.27 and 4.24

The complicated density dependence of the insertion probabilities prevents further analytical formulation of the integrals. A detailed comparison to simulation results for pure components and mixtures is postponed to a later section. We will first extend the new theory to mixtures of chains with nearest neighbor segmental interactions.

4.2.3 Theory of interacting chains

For athermal chains, the full microscopic picture entailed in Λ_N (specifying all positions of the segments on the lattice) was reduced to a representation described by the density y and the average number of intra-molecular contacts of a segment $z\omega$. In this representation, the precise type of intermolecular contacts was not relevant. However, assigning contact energies, ϵ_{AA} , ϵ_{BB} and ϵ_{AB} , to the different segmental contacts, configurations with different numbers of AA , BB and AB

inter and intra-molecular contact pairs give rise to a different value of the internal energy $U_N(\Lambda_N)$, which can be appreciated from eq 4.2. Hence, the different configurations must be weighted by their appropriate Boltzmann factors and the evaluation of the insertion probability becomes more complicated.

Therefore, to handle interactions, we resort to the quasi-chemical approach which has been shown to be quite successful.^{7,13,14} The segmental interaction energies influence the formation of segmental contacts and lead to deviations from random mixing. The different types of *intermolecular* contact pairs $n_{ij}(i, j = AA, BB, AB, Ah, Bh, hh)$ in a binary compressible mixture can be expressed in terms of the contact site fractions, θ_j and three extra microscopic parameters, x_{AB} , x_{Ah} and x_{Bh} , according to

$$\begin{aligned} n_{AB} &= T x_{AB} & n_{AA} &= T(\theta_A - x_{AB} - x_{Ah}) \\ n_{Ah} &= T x_{Ah} & n_{BB} &= T(\theta_B - x_{AB} - x_{Bh}) \\ n_{Bh} &= T x_{Bh} & n_{hh} &= T(\theta_h - x_{Ah} - x_{Bh}) \end{aligned} \quad (4.30)$$

with $T = (N_A s_A z(1 - \omega_A) + N_B s_B z(1 - \omega_B) + N_h z)/2 = Ns(1 - \omega)/(\gamma\theta)$ the total number of intermolecular contact pairs in the mixture. In eqs 4.30 and further on, the argument, Λ_N , on these contact pairs is omitted.

The internal energy can be written as a function of the inter and intra-molecular contacts

$$\begin{aligned} U_N(N_A, N_B, N_L, T, x_{AA}, x_{BB}, x_{AB}) = & \\ - \frac{Ns(1 - \omega)}{\gamma\theta} (\epsilon_{AA}(\theta_A - x_{AB} - x_{Ah}) + \epsilon_{BB}(\theta_B - x_{AB} - x_{Bh}) + 2\epsilon_{AB}x_{AB}) & \\ - \frac{Ns}{\gamma} (\epsilon_{AA}(\omega_A - \alpha_A)\phi_A + \epsilon_{BB}(\omega_b - \alpha_B)\phi_B) & \end{aligned} \quad (4.31)$$

with the inter and intra-molecular contributions given by the first and second line respectively of the rhs.

According to eq 4.1, the configurational partition function $Z(N_A, N_B, N_L, T)$ is defined as a sum over allowed configurations. Alternatively, by virtue of the explicit relation of the internal energy to the number of segmental contact pairs which, in turn, are uniquely determined by the parameters x_{AB} , x_{Ah} and x_{Bh} , it is possible to collect all configurations with the same values of x_{AB} , x_{Ah} and x_{Bh} and sum over all possible values of these parameters¹³

$$\begin{aligned} Z(N_A, N_B, N_L, T) = & \sum_{x_{AB}, x_{Ah}, x_{Bh}} C(N_A, N_B, N_L, T, x_{AB}, x_{Ah}, x_{Bh}) \\ & \exp[-\beta U_N(N_A, N_B, N_L, T, x_{AB}, x_{Ah}, x_{Bh})] \end{aligned} \quad (4.32)$$

with $\mathcal{C}(N_A, N_B, N_L, T, x_{AB}, x_{Ah}, x_{Bh})$ the so called configurational factor denoting the number of configurations with the prescribed values of $N_A, N_B, N_L, T, x_{AB}, x_{Ah}$ and x_{Bh} .

If we denote the values of x_{ij} ($ij = ab, ah, bh$) which maximize the partition sum by \bar{x}_{ij} and we replace the complete sum by this maximum term, we have

$$\begin{aligned} Z_N(N_A, N_B, N_L, T) &= \mathcal{C}(N_A, N_B, N_L, T, \bar{x}_{AB}, \bar{x}_{Ah}, \bar{x}_{Bh}) \\ &\exp[-\beta U_N(N_A, N_B, N_L, T, \bar{x}_{AB}, \bar{x}_{Ah}, \bar{x}_{Bh})] \end{aligned} \quad (4.33)$$

where \bar{x}_{ij} are determined by

$$\left. \frac{\partial Z_N(N_A, N_B, N_L, T)}{\partial x_{ij}} \right|_{N_A, N_B, N_L, T, x_{kl} \neq ij} = 0 \quad (4.34)$$

Following Guggenheim, the configurational factor is taken to be¹³

$$\begin{aligned} \mathcal{C}(N_A, N_B, N_L, T, x_{AB}, x_{Ah}, x_{Bh}) &= \\ \mathcal{C}_{ins}(N_A, N_B, N_L, T) &\left\{ \frac{[n_{AB}^*!]^2 [n_{AB}^*!]^2 [n_{Bh}^*!]^2 [n_{AA}^*!] [n_{BB}^*!] [n_{hh}^*!]}{[n_{AB}!]^2 [n_{AB}!]^2 [n_{Bh}!]^2 [n_{AA}!] [n_{BB}!] [n_{hh}!]} \right\} \end{aligned} \quad (4.35)$$

where the starred quantities n_{ij}^* specify the state with all inter-molecular contact pairs equivalent. The n_{ij}^* 's are obtained from eq 4.30 by inserting the values for $x_{ij} = x_{ij}^*$. The first factor, denoted by the \mathcal{C}_{ins} , represents the configurational contribution which arises from the insertion of the chain molecules on the lattice without considering the precise types of contact pairs.

Eq 4.35 was derived by Guggenheim based on the non-interference of pairs which yields the observed factorization. Without going into the detailed arguments of Guggenheim, the following remarks are important for our purpose. The second contribution in eq 4.35, given by the factor in brackets, accounts for the distribution of the intermolecular contact pairs over the lattice. It is explicitly assumed that the contact pairs do not interfere. Hence, they can be independently distributed, regardless of the constraints imposed on the molecules by the first configurational factor, \mathcal{C}_{ins} .

In the case of athermal mixtures, all contact pairs are equivalent and the contact pair numbers n_{ij} acquire the values n_{ij}^* . The parameters x_{ij}^* , necessary to calculate the n_{ij}^* by eq 4.30, are given by the random mixing result, i.e.

$$x_{ij}^* = \theta_i \theta_j \quad (4.36)$$

Moreover, the internal energy is zero and the partition function reduces to the configurational part C_{ins} . Combining eqs 4.1, 4.3 and 4.33 and comparing this to eq 4.28 provides the following assignment for C_{ins}

$$\begin{aligned}
 -\ln[C_{ins}(N_A, N_B, N_L)/(N_A!N_B!)] &= (\phi_A/s_A)\ln(\phi_A) + (\phi_B/s_B)\ln(\phi_B) \\
 + (1/s)\ln(y) - (1/sy) \int_0^y \ln[(1-y')^s/(1-\omega y')^{s-1}] dy' & \quad (4.37)
 \end{aligned}$$

For mixtures involving segmental interactions, the insertion factor C_{ins} as given by eq 4.37 stands for the insertion of the chain molecules with given density, composition and average segmental intra-molecular environment. Although, it must be expected that the intra-molecular surroundings of the chain segments depend not only on density but also on temperature as brought about by the interactions, the parameter ω will be uniquely determined (for given composition density and specified distribution of contact pairs) by the parameters x_{ij} . Thus, eq 4.37 is equally valid for interacting systems with specified composition, density and x_{ij} 's (Note however, C_{ins} is also dependent on temperature. This is an important difference with the original Guggenheim theory where C_{ins} is explicitly independent of temperature for athermal as well as interacting systems). If the anticipated density and temperature dependence of ω_j is known, combination of eqs 4.1, 4.3, 4.30, 4.31, 4.33, 4.35, 4.37 and employing the Stirling approximation for the factorials, the following expression for the Helmholtz free energy is found

$$\begin{aligned}
 \beta A/sN &= (\phi_A/s_A)\ln(\phi_A) + (\phi_B/s_B)\ln(\phi_B) + (1/s)\ln(y) \\
 - (1/sy) \int_0^y \ln[p_e(y', \phi_B, T)] dy' &- \frac{(1-\omega)}{(\gamma\theta)} [2\theta_A \ln(\theta_A) + 2\theta_B \ln(\theta_B) + 2\theta_h \ln(\theta_h) \\
 - 2\bar{x}_{AB} \ln(\bar{x}_{AB}) - 2\bar{x}_{Ah} \ln(\bar{x}_{Ah}) - 2\bar{x}_{Bh} \ln(\bar{x}_{Bh}) \\
 - (\theta_A - \bar{x}_{AB} - \bar{x}_{Ah}) \ln(\theta_A - \bar{x}_{AB} - \bar{x}_{Ah}) \\
 - (\theta_B - \bar{x}_{AB} - \bar{x}_{Bh}) \ln(\theta_B - \bar{x}_{AB} - \bar{x}_{Bh}) \\
 - (\theta_h - \bar{x}_{Ah} - \bar{x}_{Bh}) \ln(\theta_h - \bar{x}_{Ah} - \bar{x}_{Bh})] \\
 - \beta \frac{(1-\omega)}{\gamma\theta} [\epsilon_{AA}(\theta_A - \bar{x}_{AB} - \bar{x}_{Ah}) + \epsilon_{BB}(\theta_B - \bar{x}_{AB} - \bar{x}_{Bh}) + 2\epsilon_{AB}\bar{x}_{AB}] \\
 - \frac{1}{\gamma} [\epsilon_{AA}(\omega_A - \alpha_A)\phi_A + \epsilon_{BB}(\omega_b - \alpha_B)\phi_B] & \quad (4.38a)
 \end{aligned}$$

$$p_e(y, \phi_B, T) = (1-y)^s / (1-\omega(y, \phi_B, T)y)^{s-1} \quad (4.38b)$$

The parameters \bar{x}_{ij} are obtained from eq 4.38 and the general minimization conditions, eqs 4.34. Combining eqs 4.34 and the general thermodynamic relation for the equation of state, $p = -(\partial A/\partial V)_{T,N_A,N_B}$ results in

$$-p = \frac{\partial A}{\partial V} \Big|_{T,N_A,N_B} = \frac{\partial A}{\partial V} \Big|_{T,N_A,N_B,\bar{x}_{ij}} + \sum_{\{\bar{x}_{ij}\}} \frac{\partial A}{\partial \bar{x}_{ij}} \Big|_{T,N_A,N_B,V,\bar{x}_{kl} \neq ij} \frac{\partial \bar{x}_{ij}}{\partial V} \Big|_{T,N_A,N_B} \quad (4.39)$$

where the individual terms in the sum on the rhs equal zero by virtue of the minimization conditions, eqs 4.34. Explicit expressions for the minimization conditions and the equation of state are quite lengthy and are not presented here. Computer code to calculate these quantities is available upon request.³⁸

Finally, the dependence of ω on density and temperature must be determined. The influence of density on the intra-molecular conformations, specified by Ω_{con} , was discussed in the previous paragraph. It was shown that the density imposed by the other molecules in the mixture altered the occurrence of the different single chain conformations (at zero density). On their turn, the interactions perturb the relative importance of the different chain conformations. This can be accounted for by weighting the different conformations with their respective Boltzmann factor, bearing the energy of the chain in that conformation. An $A(B)$ chain in a conformation having $z\Omega_{con}$ intra-molecular contacts per segment possesses an internal energy $u_A(u_B)$

$$u_A = -\frac{s_A(1 - \Omega_{con})}{\gamma\theta_A} [(\theta_A - \bar{x}_{AB} - \bar{x}_{Ah})\epsilon_{AA} + 2\bar{x}_{AB}\epsilon_{AB}] - \frac{s_A}{\gamma}(\Omega_{con} - \alpha_A)\epsilon_{AA} \quad (4.40a)$$

$$u_B = -\frac{s_B(1 - \Omega_{con})}{\gamma\theta_B} [(\theta_B - \bar{x}_{AB} - \bar{x}_{Bh})\epsilon_{BB} + 2\bar{x}_{AB}\epsilon_{AB}] - \frac{s_B}{\gamma}(\Omega_{con} - \alpha_B)\epsilon_{BB} \quad (4.40b)$$

Eqs 4.40 are quite similar to the internal energy of the total mixture. For the single chain, we only look at the total number of inter-molecular contact pairs the chain can make in the conformation with $s_j z\Omega_{con}$ intra-molecular contacts. The average environment of a j -chain, determined by ω_j , is obtained from

$$\omega_j = \frac{\sum_{\Omega_{con}} \Omega_{con} P_{\omega_j}(\Omega_{con}, y, \phi_B, T)}{\sum_{\Omega_{con}} P_{\omega_j}(\Omega_{con}, y, \phi_B, T)} \quad (4.41a)$$

$$P_{\omega_j}(\Omega_{con}, y, \phi_B, T) = P_{\omega_j}(\Omega_{con}, y = 0) \left(\frac{1}{(1 - \omega y)^{\Omega_{con}/\omega}} \right)^{s_j - 1} \exp[-\beta u_j] \quad (4.41b)$$

The intra-molecular contacts per segment of a chain, at given density, composition and temperature, can thus be obtained from the athermal single chain simulation results at zero density. A comparison of ω_j obtained from eq 4.41 with MC simulation data for a 30-mer is shown in figure 4.2. Further detailed comparisons are presented and discussed in section 4.4.

The present theory reduces for specified conditions to previously discussed theories. First of all, the athermal situation is of course recovered. Furthermore, the quasi-chemical theory for binary compressible mixture presented and discussed in an earlier paper is obtained if the complete intra-molecular environment ω_j of a chain is approximated by the covalent bonds, i.e. $\omega_j = \alpha_j$.^{7,14} Also other simplifications, such as the Flory approximation employed in Sanchez-Lacombe theory, are then easily retrieved.^{39,40} It were precisely the limitations of these earlier theories which have led us to introduce this new theory. We are now in a position to compare the theoretical results to MC simulation data which have been collected to support earlier comparison. The new theory also inspired us to extract from the simulation data a new set of properties. The MC simulation techniques and evaluation methods to extract the (exact) results for the model are discussed in the subsequent section.

4.3 Monte Carlo simulations

To verify the proposed theoretical approach we performed Monte Carlo (MC) simulations on a cubic lattice providing thus independent results for the same molecular model as used in the theoretical development. Simulations for homogeneous systems of chain lengths $s = 20, 30$ and 60 were performed in the NpT ensemble and the results on the liquid-liquid phase coexistence were obtained in the isobaric-isothermal semi-grand canonical ensemble.^{9-12,14} For the latter simulations the chain lengths of both components were set equal to $s_A = s_B = 30$. Since these simulations are described in detail in a previous publication we only point out the differences related to the evaluation of the intra-molecular contacts.^{7,14} All details such as the number of chains in the systems, the size of the lattice etc. are the same as in previous publications.^{7,14} To evaluate the effect of chain connectivity we did not analyze the total spatial pair distribution function in the coils but concentrated on nearest neighbor contacts. Specifically, we distinguished in the simulations between intra- and inter-molecular self-contacts. This is the route to obtain the parameter ω , expressing the average intra-molecular

surroundings of a segment, introduced in the theoretical section.

In addition to the multi-chain simulations mentioned above we performed also single chain simulations. Theoretical considerations presented in previous sections rely on the knowledge of the connectivity in the athermal single chain, from which the values for higher concentrations and non-zero interactions can be predicted. We performed single chain simulation for athermal and interacting segments by two methods and obtained the desired factor ω and its distribution. In the first method, growing the relatively short chains, we created configurations with no chain overlap. In the case of interacting chains each non-overlapping configuration was weighted by its proper Boltzmann factor carrying the interaction energy from nearest neighbor contacts. Secondly, we also used the dynamic Monte Carlo method employed in the multi-chain systems, where different self avoiding configurations are created by configurational moves from a previous chain configuration. Both methods yielded identical results for the parameter ω and the distribution $P_\omega(\Omega_{con}, y = 0)$ indicating the correctness of the simulation algorithms.

4.4 Results and discussion

4.4.1 Pure components

In figure 4.1 the probability distribution $P_{\omega_j}(\Omega_{con}, y = 0)$, the probability at zero density that on average a segment in an athermal s -mer has $z\Omega_{con}$ intra-molecular contacts (either covalent bonds or intra-molecular contacts), is depicted for a 16-mer (\bullet), a 30-mer (\blacksquare) and a 60-mer (\blacktriangle). These MC simulation data, collected as explained in section 4.3, are required to calculate the average number of intra-molecular contacts of a chain at any thermodynamic state according to eq 4.27 for athermals and eq 4.41 for interacting chains.

The distributions presented in Figure 4.1 are bounded from above and below, the minimum number of intra-molecular contacts equals the number of covalent bonds, i.e. $\Omega_{con,min} = \alpha_j = \gamma(1 - 1/s)$, and the maximum value of Ω_{con} evidently equals 1. Clearly, this upper bound is very unlikely to occur and is not sampled at all in the finite simulation runs involving 10^6 distinct conformations. The lower bound may substantially contribute to the distribution although the importance of this state decreases with chain length. Furthermore, it can be observed that the most probable value for Ω_{con} shifts to larger values with increasing chain length. Earlier theories, such as the NRM theory,⁷ only operated with this lower

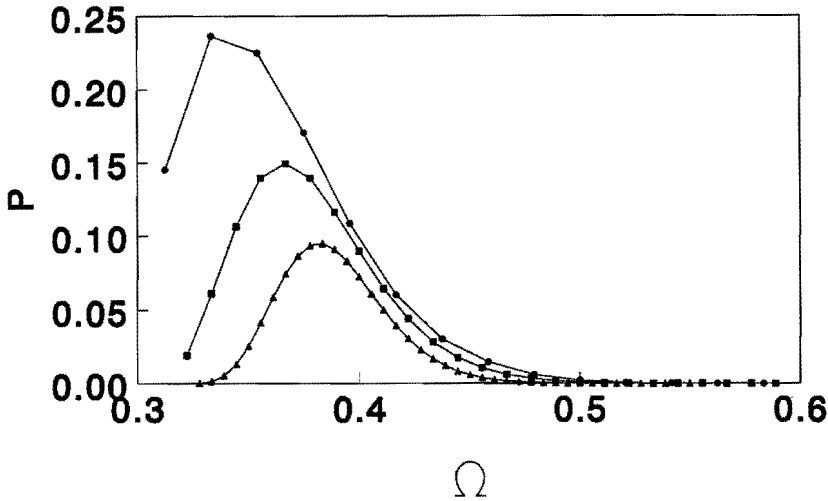


Figure 4.1: Zero-density probability distribution $P_{\omega_j}(\Omega_{con}, y = 0)$ for an athermal 16-mer (\bullet), a 30-mer (\blacksquare) and a 60-mer (\blacktriangle). Line pieces are drawn for convenience.

limiting value $\Omega_{con,min}$ in the calculations. As will become clear in the subsequent discussion, this is an important factor for the remaining discrepancies between theory and simulation observed for the NRM and similar theories.

The simulation data collected for the athermal single chains can immediately be put to use in the calculation of the intra-molecular contacts of athermal chains at any density in the melt, see eqs 4.24 and 4.27. These theoretical predictions (solid lines) are shown in figure 4.2 and compared to MC simulation data for 16-mers (\bullet) and 30-mers (\blacksquare). At zero density ($y = 0$) the calculated and MC results are, by definition, in exact agreement since in this case we are merely calculating the average value of ω according to eq 4.24 over the zero-density distribution $P_{\omega_j}(z\Omega_{con}, y = 0)$. Despite the simple arguments leading to eq 4.27, it is also clear from figure 4.2 that the predicted non-zero density results are in excellent agreement with the MC simulation data. Both theory and simulation show that the fraction of intra-molecular contacts increases with density. Naturally, this increase is intimately connected, although not expressed quantitatively, to the contraction of the average chain dimensions with density. As conjectured in the Flory ideality hypothesis,⁴¹ and quantified in e.g. renormalization group theories, the dimensions of the single chain will change from a self-avoiding walk at low density to a Gaussian random walk at high densities.⁴² These conformational changes are a result of the more efficient screening of intra- and inter-molecular interactions with density and are accompanied by a decrease in the coil dimen-

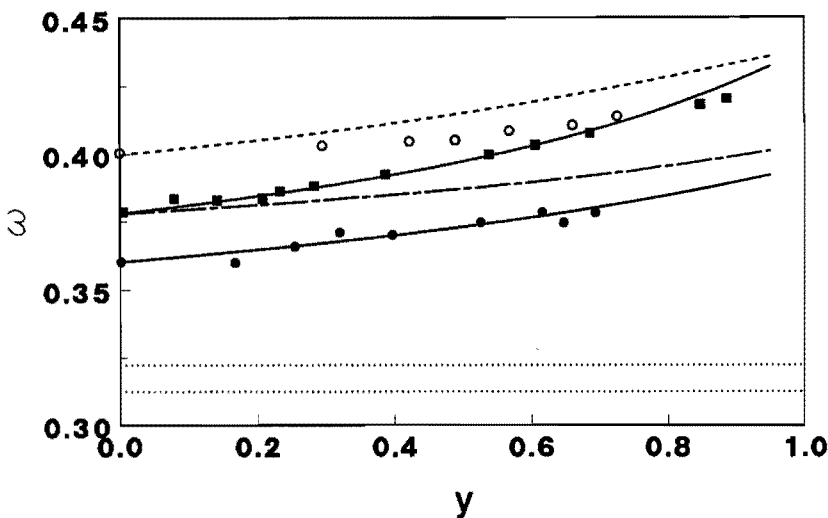


Figure 4.2: Average intra-molecular contacts per segment for athermal 16-mers (\bullet), athermal 30-mers (\blacksquare) and interacting 30-mers (\circ) ($e = 0.2$) as a function of density y . Solid lines indicated the predictions according to eq 4.27, the dashed line the prediction according to eq 4.41. The dotted lines indicate the value of ω used in the NRM theory. The dash-dotted line is the prediction for athermal 30-mers according to the theory of Weinhold, Kumar and Szleifer.

sions.

As a reminder the value of ω employed in the NRM theory, i.e. $\omega = \alpha$, is shown in figure 4.2 by the dotted lines (α increases with chain length). It becomes clear that the number of covalent bonds is a poor (under)estimate for the total number of intra-molecular contacts. Furthermore, since α is independent of density and segmental interactions it is unable to capture the subtle changes with density and interactions found for the true ω . One may anticipate that properties depending directly or indirectly on the intra-molecular contacts will be poorly predicted by the NRM theory. In the sequel, several examples of this will be presented.

At this point a comparison with the recent theory of Weinhold, Kumar and Szleifer is at place.³² These authors presented a theoretical derivation of the total entropy of an athermal polymer solution, composed of combinatorial and conformational parts. Also in their theory a coupling between conformational and translational degree of freedoms is established. Thus coupling results in a concentration dependence of the intra-molecular contacts of the chain molecule, which are directly connected to its conformational properties. Making use of the

similarity between an athermal incompressible polymer solution and an athermal compressible pure component the density dependence of the number of intramolecular contacts for athermal 30-mers according to their theory is depicted by the dash-dotted line in figure 4.2. Clearly, the predicted density dependence of this theory is too weak. This is in agreement with their results on the variation of the radius of gyration and the solvent chemical potential in athermal incompressible solutions.³²

Similar calculations, but now based on eq 4.41, can be done for interacting chains. The results for 30-mers interacting with a nearest neighbor contact energy $e = \epsilon/k_B T = 0.2$ are also presented in figure 4.2 (MC data (\circ), theory (dashed line)).

Although at intermediate densities the predictions are not as accurate as for the athermals, theory and simulations still agree reasonably well for these interacting chains. Another interesting point in figure 4.2 is the convergence at higher densities to the same value of ω for athermal and interacting chains. Again this may be viewed as a consequence of Flory's ideality assumption, i.e. the effective screening of intra- and inter-molecular interactions at these high densities. It is important to realize that we are not *invoking* the ideality hypothesis; the theory *predicts* that effective screening indeed occurs! However, judging from the MC simulation results, the screening already appears to be quite effective starting at densities $y \sim 0.75$. In the theory, this cancelling of inter- and intra-molecular interactions is only complete at full packing. But also at intermediate densities the incomplete screening is properly accounted for by the theory. It should be appreciated that these results for the interacting chains can only be obtained from the simultaneous set of equations given by the minimization condition, eq 4.34, and the equation of state, eq 4.39 (in eq 4.41 the interaction energies of the chains, defined by eqs 4.40, enter. These interaction energies depend on the microscopic parameters \bar{x}_{ij} which can only be determined by solving the equation of state and the minimization condition).

In figure 4.3 the compressibility factor $pV/Nk_B T$ for athermal s -mers is plotted as a function of density. The theoretical predictions of the new theory (solid lines) are compared to MC simulation data (symbols).

In addition, the NRM theory, presented in previous publications, serves as a reference.⁷ As already discussed in some detail and confirmed in figure 4.3, the NRM theory gives a quantitative prediction of the compressibility factor of 20-mers (\bullet) and 30-mers (\blacksquare). However, it was already anticipated that the accuracy of the prediction should deteriorate with increasing chain length.⁸ Therefore, we

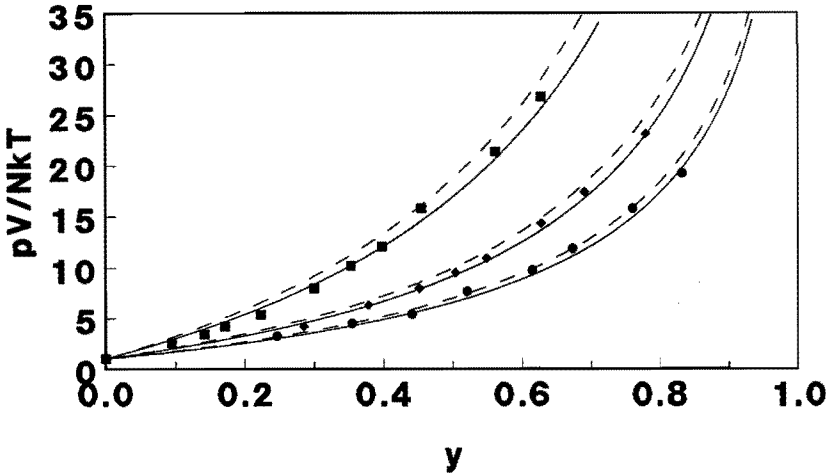


Figure 4.3: Compressibility factor $pV/Nk_B T$ as a function of packing fraction γ for different chain lengths $s = 20$, (\bullet); $s = 30$, (\blacksquare); $s = 60$, (\blacktriangledown). Full lines represent the ω -theory and long dashed lines the NRM theory.

present additional simulation data for athermal 60-mers (\blacktriangledown). In figure 4.3 it can indeed be observed that the NRM predictions overestimates these new MC results. On the other hand, the predictions according to the new theory (solid lines) are in excellent agreement with the MC data for all investigated chain lengths. Actually, for all chain lengths the new predictions are systematically lower than the NRM predictions. Hence, for a given temperature, pressure and chain length the new theory predicts in all cases a slightly higher density. For these athermals the physical explanation is quite clear. The insertion probability depends on the average number of intra-molecular contacts of the chain molecules according to eq 4.23. At a given density and chain length the insertion of a molecule in an environment with a higher number of intra-molecular contacts is easier than in an environment with a smaller number of intra-molecular contacts. Whence, in order to reach a certain density a lower pressure is required or, alternatively, at a given pressure the density can become higher if the molecules have a larger number of intra-molecular contacts. In the new theory the number of intra-molecular contacts of chain segments exceed the number of covalent bonds, i.e. the minimal number of intra-molecular contacts used in the NRM theory. This higher value of ω leads to a higher insertion probability and hence to a higher density at a selected pressure and temperature.

In figures 4.4-4.5 some results are shown for interacting 30-mers. In figure 4.4

the density at zero pressure is shown as a function of reduced interaction energy $e = \epsilon/k_B T$. Both theoretical results for the NRM theory (dashed lines) and the

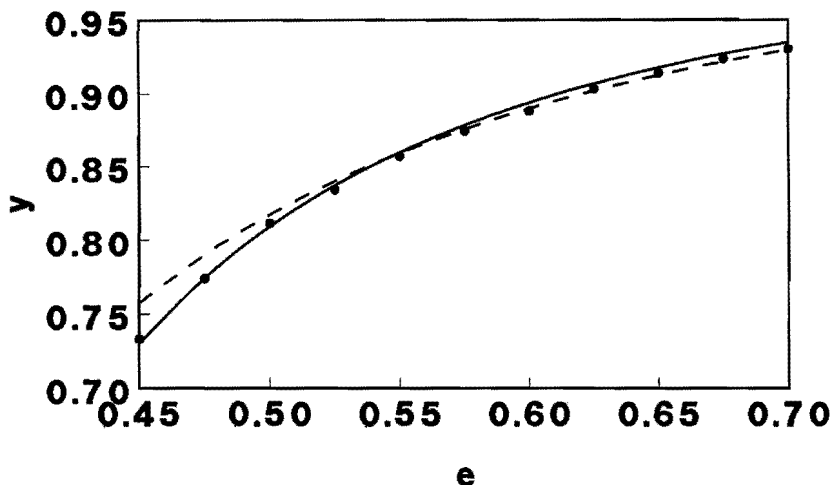


Figure 4.4: Packing fraction y vs inter-segmental interaction e at $\bar{p} = 0$ for $s = 30$. MC results (\bullet). Full line represents the ω -theory prediction and dashed line the NRM theory.

new theory (solid lines) are shown. At high densities, obtained at the higher values of the interactional energies, the difference between both theories is only minor. However, at the lower interactional energies the new theory quantitatively predicts the MC simulation results whereas the NRM theory systematically gives a too high density. Previously, it was argued but not proven that this deficiency was related to the improper modeling of the intra-molecular contacts in the NRM theory.⁷ This is corroborated by the predictions of the new theory.

In figure 4.5 the corresponding segment-vacancy and segment-segment contacts are plotted as a function of density. Once more the new theory provides a quantitative prediction of both types of contacts. In contrast, the NRM theory shows deviations at the low density side. These deviations, closely connected to the observed overestimate of the density in figure 4.4, are nicely remedied by the new theory.

Although not explicitly shown, the pressure dependence of the equation of state is predicted accurately with the new theory. The differences with the NRM theory are not very pronounced although also in this case the new theory provides a consistently better prediction of the lower density states.

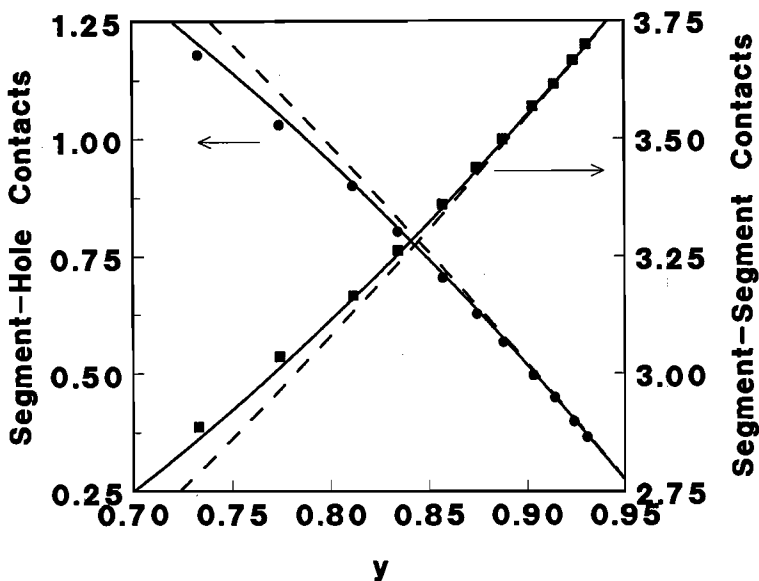


Figure 4.5: Segmental contacts vs packing fraction y corresponding to interactions ϵ in Figure 4.4. Segment-segment (■) and segment-vacancy (●) contacts MC results. Full line represents the ω -theory prediction and dashed line the NRM theory.

4.4.2 Mixtures

The deficiencies related to the use of a homogeneous segment distribution in the NRM theory are most clearly demonstrated for mixtures. (The deficiencies of theories operating with a homogeneous density assumption become clear in the prediction of the different type of contacts. In such theories, the number of intramolecular self-contacts, due to the chain connectivity, are ignored, which results in an underestimation of the total number of self-contacts and an accompanying overestimation of the cross-contacts.)

A simple but nevertheless very illustrative example is provided by a (hypothetical) binary mixture in the athermal limit ($e_{AA} = e_{BB} = e_{AB} = 0$) where both components have equal chain lengths. In the case of equal chain lengths, chosen here to be $s_A = s_B = s = 30$, the equation of state is truly independent of composition (A and B are indistinguishable) and identical to that of a single component with the same chain length. In figure 4.3 it is demonstrated that the athermal equation of state is accurately predicted by the new as well as the NRM theory.⁷ However, a detailed comparison of the different contacts in the mixture clearly reveals the deficiencies of the NRM theory. In Figure 4.6 the

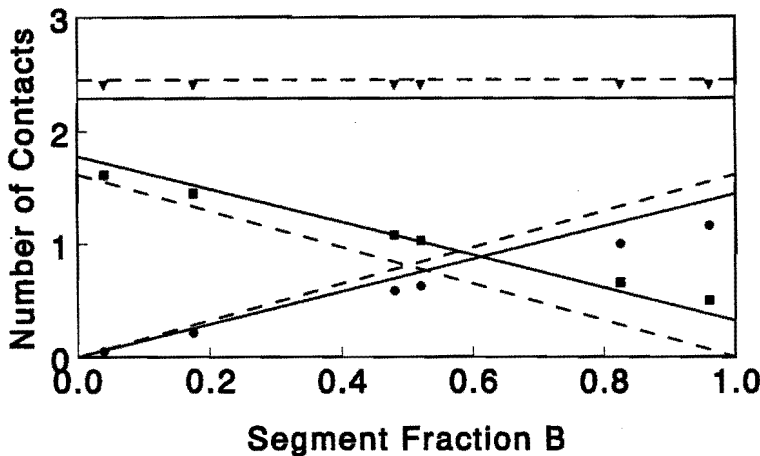


Figure 4.6: Number of contacts of A segments as a function of composition for athermal mixtures ($\epsilon_{AA} = \epsilon_{BB} = \epsilon_{AB} = 0$) at the reduced pressure $\tilde{p} = 0.16$: AA contacts (■), AB contacts (●), and Ah contacts (▼). the full lines represent the ω -theory prediction and dashed lines the NRM theory.

different types of contacts of A segments are shown as a function of the mixture composition given by ϕ_B . The NRM predictions at a reduced pressure $\tilde{p} \equiv pv^*/k_B T = 0.16$ are depicted by the dashed lines. The number of contacts involving vacancies (▼) is predicted quite accurately, in agreement with the quality of prediction of overall density. However, the situation is different for the contacts involving other segments. For instance, the number of (AA) contacts (■) is predicted to decrease with ϕ_B and in (nearly) pure B the number of (AA) contacts equals zero. However, the simulation shows a decrease in (AA) contacts to a limiting value at $\phi_B = 1$, which is due to the chain connectivity. Even at infinite dilution, A segments remain surrounded by intra-molecular A segments that result in a non-zero number of (AA) contacts in (almost) pure B . The number of (AB) contacts (●), starting in pure A from zero, is predicted to increase with ϕ_B . The simulation shows the same limiting behavior since (AB) contacts only involve intermolecular contacts that vanish if one of the components is infinitely diluted. The value of (AB) contacts with increasing ϕ_B is overestimated, which is a direct consequence of the inaccurate limiting behavior of the (AA) contacts and the constraint on the total number of contacts a type A segment can make. The latter is for a 30-mer, $s_A = 30$, given by

$$AA + AB + Ah = (s_A(z - 2) + 2)/s_A = z(1 - \alpha_A) = 4.06667 \quad (4.42)$$

Figure 4.6 applies equally well to B contacts if the following changes are made $\phi_B \rightarrow \phi_A$, $(AA) \rightarrow (BB)$, $(AB) \rightarrow (BA)$ and $(Ah) \rightarrow (Bh)$. From this comparison it is clear that the assumption of a homogeneous segment distribution is not really fulfilled.

Turning our attention to the new theory, it can be observed that all types of contacts are accurately predicted. For contacts involving different molecules, i.e. AB and Ah contacts, the predictions are quite similar for both the NRM and the new theory. It might appear that the NRM theory provides a somewhat better prediction of the Ah contacts. However, both predictions are well within the accuracy of the MC simulation data and the slightly worse result for the new theory may be attributed to this 'experimental' uncertainty. The new theory clearly performs better than the NRM theory in the prediction of the AA contacts, involving both intra- and intermolecular contributions. Evidently, the new theory correctly accounts for the limiting behavior of the AA contacts in pure B . This limiting behavior is completely due to the intra-molecular contacts which are taken care of by the parameter ω in the theory. Clearly, the improved prediction of the AA contacts also leads to an improved prediction of the AB contacts as the total number of contacts (excluding covalent bonds) remains fixed by the constrained, eq 4.42.

Further evidence of the importance of the intra-molecular self-contacts can be found in the equation of state of interacting mixtures. The density as a function of composition or effective interaction parameter $\langle e \rangle = \phi_A^2 e_{AA} + \phi_B^2 e_{BB} + 2\phi_A\phi_B e_{AB}$ is shown in Figure 4.7. The contact energies are set to the following values $e_{AA} = 0.5$, $e_{BB} = 0.7$ and $e_{AB} = 0.6$. The cross-interaction parameter is set such that the Flory-Huggins exchange energy parameter $\Delta W = -(2\varepsilon_{AB} - \varepsilon_{AA} - \varepsilon_{BB})$ equals zero. Both NRM and the new theory give fair predictions of the equation of state behavior of these mixtures although the accuracy is not as high as for pure components. These differences have been discussed in a previous publication and the conclusions presented there remain valid.¹⁴

Additional interesting information is obtained from the different types of contacts. In Figure 4.8 the contacts of A segments are shown as a function of composition and effective interaction parameter. Just as in the athermal mixtures, the number of segment-vacancy contacts (\blacktriangledown) is accurately predicted over the whole composition and/or interaction range. However, (AA) contacts and (AB) contacts show deviations with varying composition. For the (AA) contacts (\blacksquare) the number of contacts is predicted well at small concentrations of component

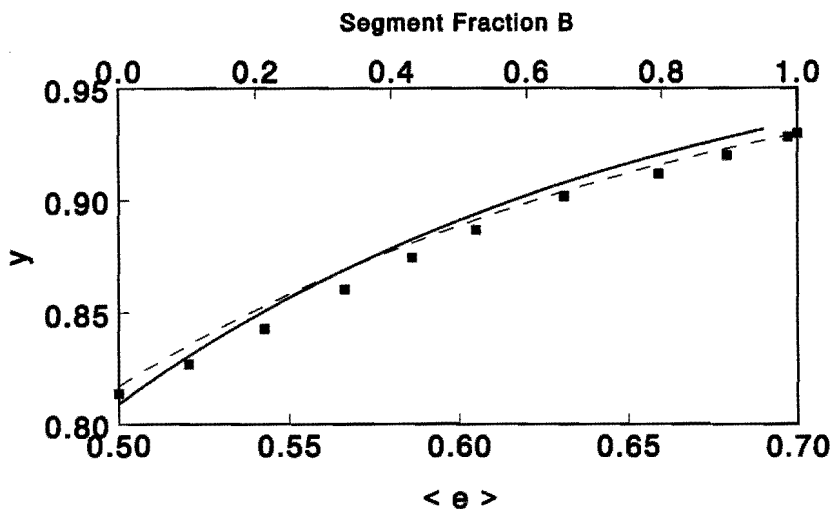


Figure 4.7: Density y as a function of the effective interaction parameter $\langle e \rangle$ (bottom axis) and blend composition (top axis) for polymer blends ($e_{AA} = 0.5, e_{BB} = 0.7, e_{AB} = 0.6$). MC simulation results (■) and theoretical predictions according to the new theory (solid lines) and the NRM theory (dashed lines).

B , but the predictions deteriorate with increasing B content. Again, the NRM result approaches zero in pure B whereas the simulation results show a finite number of (AA) contacts. These remaining contacts are of intra-molecular origin caused by chain connectivity. For the number of (AB) contacts (\bullet) a similar observation is made. In pure A both theory and simulation show no hetero-contacts, whereas approaching pure B too many contacts are predicted. The reason for these differences has already been addressed in the discussion of Figure 4.6. Due to chain connectivity, B segments experience more B contacts, relative to the overall blend composition, than predicted in the mean field theory. Taking into account the constraint, eq 4.42, the (AB) contacts are over-predicted.

Once again, proper theoretical modeling of the intra-molecular self-contacts leads to very accurate predictions (solid lines) of the different types of contacts as can be appreciated in figure 4.8. Similar reasoning applies to the contacts made viewed from an B segment, but this is not repeated here.

Another important aspect of the thermodynamic properties of chain molecule mixtures is found in the liquid-liquid ($L - L$) miscibility behavior. As discussed previously, the NRM theory so far provided the best prediction of the upper critical miscibility (UCST) behavior found in the symmetric binary mixture ($s_A = s_B = 30, \epsilon_{AA} = \epsilon_{BB} = 200K$ and $\epsilon_{AB} = 188.77542K$).¹⁴ In figure 4.9

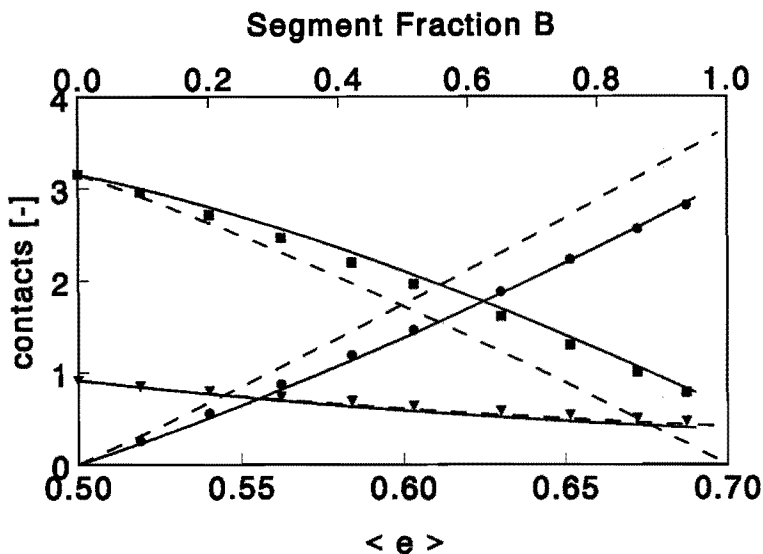


Figure 4.8: Number of contacts of A segments as a function of effective interaction parameter $\langle e \rangle$ (bottom axis) or composition (top axis) for the parameters used in Figure 4.7. MC results for AA contacts (■), AB contacts (●), and Ah contacts (▼). Full lines represent the ω -theory prediction and dashed lines the NRM theory.

the MC simulation data for these symmetric mixtures are shown and are compared to the predictions according to the NRM (dashed lines) and the new theory (solid lines). The energetically driven UCST miscibility gap found in this system is due to the unfavorable cross-interactions. Previously, it was demonstrated that, taking the simple incompressible Flory-Huggins-Staverman theory as a reference, the introduction of vacancies on the lattice resulted in a dramatic lowering and broadening of the predicted UCST miscibility gap.¹⁴ A further significant reduction of the predicted UCST critical temperature and corresponding L-L binodal was obtained for the NRM theory. This further enlargement of the homogeneous one-phase region could be ascribed to the preference in the NRM theory of self-contacts over cross-contacts.¹⁴ By avoiding the unfavorable cross-contacts the miscibility gap is substantially lowered in comparison with theories which assume a random mixing of contacts, i.e. proportional to the overall composition.

Nevertheless, substantial deviations between theory and MC simulation data remained. The NRM miscibility gap was still some 60-80 K too high in temperature. It was already anticipated that an important cause for these deviations might be the ignorance of the intra-molecular contacts in the theoretical considerations.¹⁴ This is indeed confirmed in this study. In figure 4.11 the effect of the

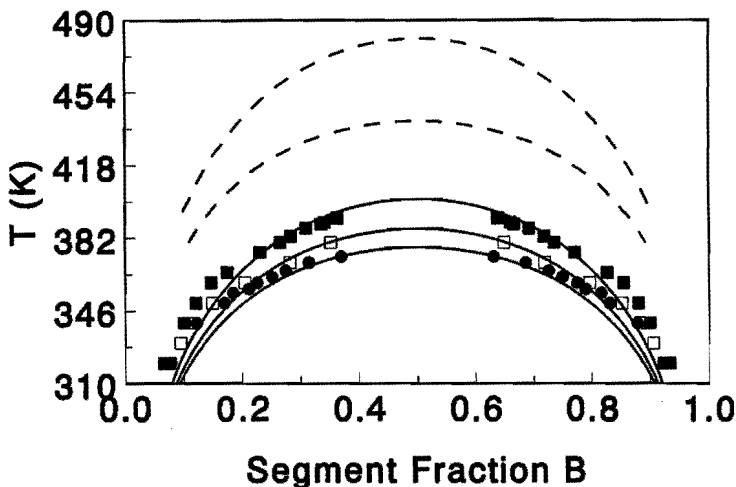


Figure 4.9: Binodal temperature as a function of composition at $p = 0$ bar (\bullet), $p = 10$ bar (\square) and $p = 30$ bar (\blacksquare). Full lines represent the ω -theory prediction and dashed lines the NRM theory at 10 bar and 30 bar.

intra-molecular contacts on the $L-L$ phase behavior is clearly demonstrated. The new theory provides a prediction which is in accurate agreement with the simulation data. Nevertheless, the predicted binodal is somewhat narrower than the MC binodal. For the relatively short chains considered here, Sariban and Binder showed that the coexistence curve in the critical region has not the parabolic shape predicted by the mean field theories but is significantly flatter as a consequence of non-classic critical behavior characterized by the Ising critical exponent $\beta = 0.325$ opposed to the classic mean field value $\beta = 0.5$.⁹ They argued that this flattened critical region could also lead to a substantial broadening of the complete coexistence curve even far away from the critical region.⁹

In figure 4.10 we also show the density along the binodal curve. The predicted composition dependence of the density is somewhat too steep, corresponding to the narrow binodal found in figure 4.9. Apart from this, the quality of the prediction of the density along the binodal is similar to that of the equation of state of homogeneous mixtures with similar interactions.

In figure 4.11 the different types of A contacts along the binodal are shown. Here also the differences between the NRM (dashed lines) and the new theory (solid lines) can be clearly observed. The number of Ah contacts (\blacktriangledown) is accurately predicted. On the other hand the predictions of the number of AA contacts (\blacksquare) is only reasonable for compositions rich in A . The agreement between the NRM

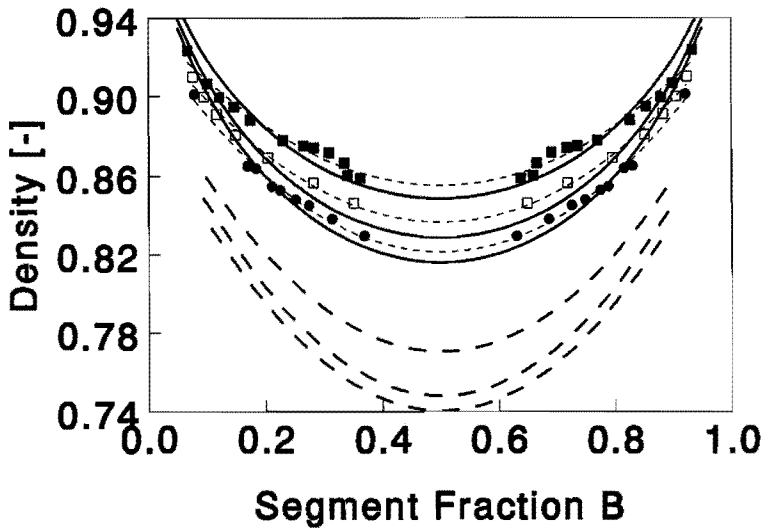


Figure 4.10: Density as a function of composition at binodal curve for $p = 0$ bar (●), $p = 10$ bar (□) and $p = 30$ bar (■). Full lines represent the ω -theory prediction and dashed lines the NRM theory. The thin dashed lines are drawn for convenience.

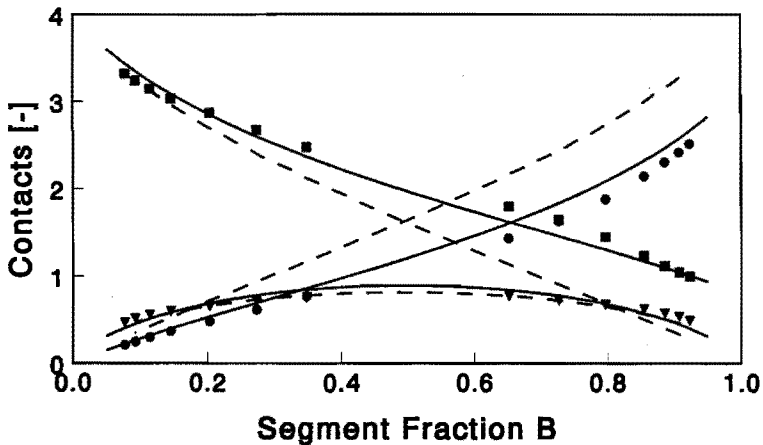


Figure 4.11: Number of contacts of A segments as a function of composition along the binodal, shown in Figure 4.9 at $p = 0$ bar. MC data for AA contacts (■), AB contacts (●) and Ah contacts (▼). Full lines represent the ω -theory prediction and dashed lines the NRM theory.

theory and the MC simulation data deteriorates with increasing B content of the mixture. In agreement with the discussions presented above, the NRM theory predicts a decreasing number of AA contacts effectively becoming zero in pure

B. The MC simulation data also show a decrease in *AA* contacts but in pure *B* a finite fraction of *AA* contacts remains. This finite fraction is of course a consequence of the chain connectivity making the number of *AA* contacts higher than the overall blend composition. The underestimation of the *AA* contacts leads also here to an inevitable overestimate of the *AB* contacts (\bullet), as the total number of contacts is fixed by the constrained, eq 4.42. This overestimate increases with ϕ_B . This should be contrasted with the predictions of the new theory. Again, the predictions of NRM and the new theory are virtually identical for the number of *Ah* contacts (\blacktriangledown). However, for the number of *AA* contacts (\blacksquare) a very accurate prediction is provided, including the limiting behavior at $\phi_B = 1$. Furthermore, an accurate prediction of the number of *AB* contacts (\bullet) is also given.

Finally, some microscopic information about the mean square end-to-end distance $\langle r^2 \rangle$ of both components along the binodal is given in figure 4.12. For

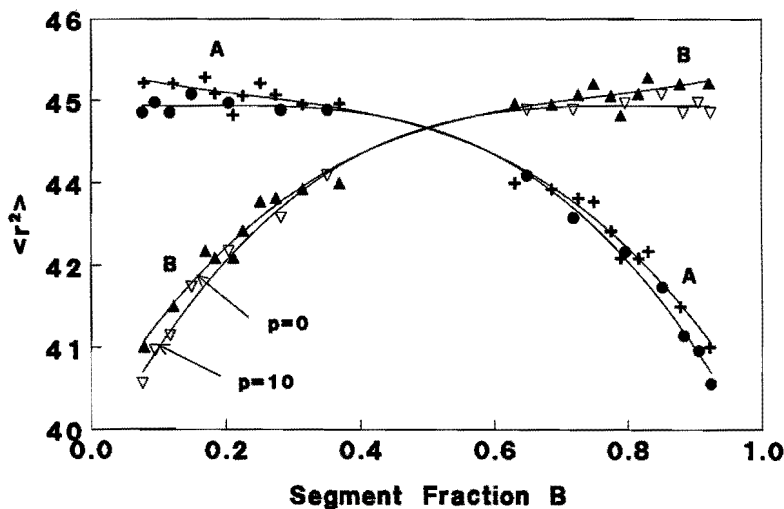


Figure 4.12: Mean square end-to-end distance $\langle r^2 \rangle$ of component A (\bullet , \circ) and B (\blacksquare , \square) along the coexistence curve at $p=0$ bar (\bullet , \blacksquare) and 10 bar (\circ , \square), shown in Figure 4.9, as a function of the composition of the coexisting phase.

asymmetric compositions, the chains of the minority component have smaller dimensions. This is due to the unfavorable environment provided by the majority component. On the other hand the chains of the majority component do not significantly change coil dimensions and behave practically as in its own melt. A slight decrease with pressure of the coil dimensions can be observed related to the higher density.

Evidently, a decrease in chain dimensions as given by the end-to-end distance $\langle r^2 \rangle$ will be accompanied by an increase in the number of intra-molecular contacts and vice versa. Therefore, we present in figure 4.13 for the same conditions as in figure 4.12 the variation with pressure and mixture composition of the fraction of intra-molecular contacts as entailed in ω_A (ω_B). Although figure 4.12 and

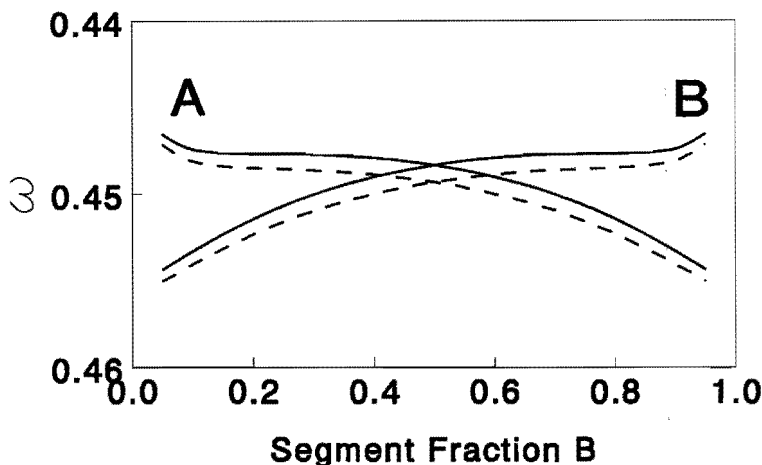


Figure 4.13: Average number of intra-molecular contacts ω of component *A* and *B* along the coexistence curve at $p=0$ bar (dashed line) and $p=10$ bar (solid line), shown in Figure 4.9, as a function of the composition of the coexisting phase.

4.13 cannot be compared directly, obvious similarities are observed. For asymmetric compositions, the chains of the minority component have a larger number of intra-molecular contacts indicating a smaller end-to-end distance. Also in the theory this change in ω is caused by the unfavorable environment provided by the other component. Consequently, the chains of the minority component ‘react’ to this by making more intra-molecular contacts. On the other hand, the majority component behaves practically as in its own melt only leading to a small variation if the number of intra-molecular contacts.

The small variations in $\langle r^2 \rangle$ found with pressure in the MC simulation data are not reflected in the variation of the number of intra-molecular contacts ω . The subtle balance between density and interactions governing the variations in $\langle r^2 \rangle$ and ω is not reproduced by the theory.

4.5 Conclusions

Starting from the definition of the insertion probabilities a new theory for compressible binary mixtures was defined. Due to the approximate nature of the theoretical expressions for the insertion probability the partition function and the thermodynamic state functions may depend on the particular order of insertion. We therefore define a practically useful insertion order which assures that the intensive thermodynamic state functions are functions of the appropriate thermodynamic variables, i.e. density, temperature and composition. Subsequently, theoretical expressions for the insertion probabilities were derived which depend on the presence of intra-molecular self-contacts related to the long range excluded volume of the chain molecules. These theoretical developments automatically resulted in a dependence on density, i.e. the environment of the chain molecule, of the intra-molecular contacts. Eqs 4.23 and 4.27 are the main theoretical results for athermal chains. From eq 4.27, the influence of density on the distribution $P_{\omega_j}(\Omega_{con}, y)$ can be obtained. Employing eq 4.24 the average molecular environment, expressed in ω_j , can be computed. The insertion probability at any density can be found by employing ω_j in eq 4.23. The Helmholtz free energy and the equation of state can be calculated by inserting $p_e(y)$ in eqs 4.16 and 4.18 respectively. For the interacting chains, the influence of the density and interaction on the distribution $P_{\omega_j}(\Omega_{con}, y, \phi_B, T)$ and the average environment ω_j is given by eq 4.41. The insertion probability at a given density and given values of ϵ_{ij} and \bar{x}_{ij} is then easily calculated from eq 4.38b. The equation of state and the maximized parameters x_{ij} are obtained by simultaneously solving eqs 4.34 and 4.39 at a given density and temperature. The Helmholtz free energy at any density and temperature can be obtained invoking eq 4.38.

Employing the new theory, predictions for the equation of state of pure components and binary mixtures as well as the liquid-liquid coexistence as a function of pressure were provided and compared to MC simulation results. Furthermore, detailed microscopic information on the different types on segmental contacts were collected in the MC simulations and compared to the theoretical predictions. It was found that the new theory successfully predicts all presented data. For example, the compressibility factor of athermal chains is accurately predicted even for the highest investigated chain lengths ($s = 60$). The prediction of the new theory were systematically better than those of the NRM theory and are even better than those provided by the LC theory for linear chains. An extensive comparison of the new theory to the LC theory and some other theoretical

approaches will be the subject of chapter 5.

The effects of the intra-molecular self-contacts is most clearly demonstrated for mixtures. The most clarifying example is provided by the predicted non-zero number of intra-molecular contacts even for the most asymmetric mixture compositions. It was further observed that the incorporation of the intra-molecular contacts also resulted in an almost quantitative prediction of the liquid-liquid miscibility behavior. The remaining deviations being most likely due to the non-classical critical scaling behavior.⁹

In conclusion, the present theory has been shown to be very accurate in comparison with MC simulation data. The new theory also opens the way to the thermodynamics of more complex chain architectures such as branched chains etc. Furthermore, the theory is equally applicable to compressible polymers solutions by assigning a chain length of unity to one of the chain molecules.

References

- [1] Flory, P. J., *J. Chem. Phys.* **9**, 660, 1941.
- [2] Flory, P. J., *J. Chem. Phys.* **10**, 51, 1942.
- [3] Huggins, M. L., *J. Chem. Phys.* **9**, 440, 1941.
- [4] Huggins, M. L., *Ann. N.Y. Acad. Sci.* **43**, 1, 1942.
- [5] Allen, M. P., Tildesley, D. J., *Computer Simulation of Liquids*. Clarendon, Oxford, 1987.
- [6] Binder, K., *Ann. Rev. Phys. Chem.* **43**, 33, 1992.
- [7] Nies, E., Cifra, P., *Macromolecules* **27**, 6033, 1994.
- [8] Madden, W. G., Pesci, A. I., Freed, K. F., *Macromolecules* **23**, 1181, 1990.
- [9] Sariban, A., Binder, K., *J. Chem. Phys.* **86**, 5859, 1987.
- [10] Sariban, A., Binder, K., *Macromolecules* **21**, 711, 1988.
- [11] Sariban, A., Binder, K., *Macromol. Chem.* **189**, 2537, 1988.
- [12] Sariban, A., Binder, K., *Colloid Polym. Sci.* **266**, 389, 1988.
- [13] Guggenheim, E. A., *Mixtures*. Oxford University Press, London, 1952.
- [14] Cifra, P., Nies, E., Broersma, J., *Macromolecules* **29**, 6634, 1996.
- [15] Bawendi, M. G., Freed, K. F., Mohanty, U., *J. Chem. Phys.* **84**, 7036, 1986.
- [16] Bawendi, M. G., Freed, K. F., *J. Chem. Phys.* **88**, 2741, 1988.
- [17] Dudowicz, J., Freed, K. F., *Macromolecules* **24**, 5112, 1991.
- [18] Freed, K. F., Dudowicz, J., *Macromolecules* **29**, 625, 1996.

- [19] Yan, Q., Jian, J., Liu, H., Hu, Y., *J. Chem. Ind. Eng. (China)* 46, 517, 1995.
- [20] Yan, Q., Liu, H., Hu, Y., *Macromolecules* 29, 4066, 1996.
- [21] Curro, J. G., Schweizer, K. S., *Macromolecules* 20, 1928, 1987.
- [22] Schweizer, K. S., Curro, J. G., *Advances in Polymer Science* 116, 321, 1994.
- [23] Hansen, J. P., McDonald, I. R., *Simple theory of liquids*. Academic Press, London, UK, second edn., 1986.
- [24] Chandler, D., Andersen, H. C., *J. Chem. Phys.* 57, 1930, 1972.
- [25] Chandler, D., in E. W. Montroll, J. L. Lebowitz (eds.), *Studies in Statistical Mechanics VIII*, p. 275. North - Holland, Amsterdam, 1982.
- [26] Grayce, C. J., Schweizer, K. S., *J. Chem. Phys.* 100, 6846, 1994.
- [27] Grayce, C. J., Yethiraj, A., Schweizer, K. S., *J. Chem. Phys.* 100, 6857, 1994.
- [28] Melenkevitz, J., Schweizer, K. S., Curro, J. G., *Macromolecules* 26, 6190, 1993.
- [29] Melenkevitz, J., Curro, J. G., Schweizer, K. S., *J. Chem. Phys.* 99, 5571, 1993.
- [30] Dickman, R., Hall, C. K., *J. Chem. Phys.* 89, 3168, 1988.
- [31] Szleifer, I., *J. Chem. Phys.* 92, 6940, 1990.
- [32] Weinhold, J. D., Kumar, S. K., Szleifer, I., *Europhysics Letters* 35, 695, 1996.
- [33] McQuarrie, D. A., *Statistical Mechanics*. Harper and Row Publishers, New York, 1976.
- [34] Dickman, R., Hall, C. K., *J. Chem. Phys.* 85, 4108, 1986.
- [35] Honell, K. G., Hall, C. K., *J. Chem. Phys.* 95, 4481, 1991.
- [36] Widom, B., *J. Chem. Phys.* 39, 2808, 1963.
- [37] Frenkel, D., Smit, B., *Understanding Molecular Simulation from Algorithm to Applications*. Academic Press, Inc., San Diego, 1996.

- [38] Computer codes can be requested from Erik Nies by e-mail(tgpken@chem.tue.nl).
- [39] Sanchez, I. C., Lacombe, R. H., *J. Phys. Chem.* 80, 2352, 1976.
- [40] Lacombe, R. H., Sanchez, I. C., *J. Phys. Chem.* 80, 2568, 1976.
- [41] Flory, P. J., *Principles of Polymer Chemistry*. Cornell University Press, Ithaca, 1953.
- [42] Freed, K. F., *Renormalization Group Theory of Macromolecules*. John Wiley and Sons, New York, 1987.

Chapter 5

Thermodynamic properties of compressible lattice polymers: A comparison of MC simulation data and theories. Pure components

5.1 Introduction

Since the independent works of Flory and Huggins, more than half a century ago, on the thermodynamics of (incompressible) polymer solutions a great number of theories are available to predict and describe the thermodynamic behavior of incompressible and compressible polymer solutions and polymer blends. In most cases the improvements on the classic Flory-Huggins (FH) theory set forth in a new theory are clearly illuminated. However, a detailed comparison of different improved theories is much scarcer, while, we believe, it could be of interest to investigators in polymer thermodynamics, in need of an improved theory to describe or interpret some of their experimental data. At least partly, we would like to fill this gap and make a comparison of a number of improved theories to 'experimental' data obtained from Monte Carlo (MC) simulation studies on the same molecular model.

Clearly it is impossible to consider all theories and it is necessary to make some selection. Here we chose theories based on the lattice model and in particular we will discuss the Lattice Cluster (LC) theory of Freed and coworkers, the confor-

mational theory of Szeifer, the recent theory of Weinhold, Kumar and Szeifer (WKS) for athermal polymers, the ω -theory developed in our laboratory and the non-random mixing (NRM) theory based on the quasi-chemical approximation of Guggenheim.

Since all the suggested theories are based on the lattice model a direct comparison to experimental data for real polymer systems will not be attempted. It has been demonstrated quite convincingly that the accuracy of any theory is much easier to verify in a comparison to thermodynamic data of the molecular model used in the theoretical developments. With the advent of computer simulations, it has now become possible to obtain the exact thermodynamic data for any molecular model. Hence, we will compare the theoretical results to Monte Carlo simulation results for the lattice model. Here, we will limit us to the equation of state behavior, including the vapor-liquid coexistence region, of pure compressible lattice chain fluids. The technologically more important polymer solutions and blends will be discussed in a forthcoming contribution. However, also for these solutions and blends the equation of state properties of the pure components are of interest as they are known to control the behavior of the mixtures. As a reminder, it should be mentioned that the lattice model is not an adequate model for the liquid state. In effect, these inadequacies can be nicely demonstrated by confronting off-lattice simulations with the theoretical predictions of the lattice model. Subsequently, hybrid theories, combining lattice and off-lattice aspects, were proposed to alleviate the deficiencies of the original lattice model.¹⁻⁴ It should be pointed out that these deficiencies were already recognized much earlier and were also removed along different lines in cell theories^{5,6} and in hole theories.⁷⁻¹²

The organization of the rest of this chapter is as follows: in section 2 we introduce the different theories and present briefly the relations amongst them, if any, and the relation to the Flory-Huggins theory. In section 3 the thermodynamic conditions that will be discussed are introduced. In section 4, the theoretical predictions for the thermodynamic properties are compared to MC simulation data. Finally, section 5 presents the conclusions and some remarks.

5.2 Model and theories

5.2.1 The lattice model for a compressible pure component

Consider N linear s -mers each occupying s consecutive sites on a cubic lattice of N_L sites. The lattice coordination number is denoted by z . The overall fraction of filled lattice sites or the segmental packing fraction $y = sN/N_L$ with $N_L = sN + N_h$ and N_h the number of vacant lattice sites. The total volume is given by $V = N_L v^*$ with v^* the lattice site volume. Non-covalently bonded polymer segments are assigned a nearest neighbor interaction potential $-\epsilon$, ($\epsilon \geq 0$).

The lattice model has been, and still is, frequently used to discuss the thermodynamic properties of chain fluids. Consequently, a great number of theories has been presented. In the following subsections we summarize the different theories that will be discussed in this chapter and give the theoretical expressions for Helmholtz free energy. Moreover, the EoS is given whenever a simple explicit expression can be derived.

5.2.2 The Flory-Huggins theory

The Flory-Huggins mean field theory¹³⁻¹⁹ represents a convenient reference point in the history of polymer theory and plays an important role in the understanding and development of the statistical thermodynamics of polymers. However, in this simple theory the influence of the long range chain connectivity is completely ignored. Nevertheless, the FH theory at least qualitatively explains a number of features of the thermodynamic properties of polymers, such as the influence of chain length on the location and shape of the liquid-liquid miscibility gap of polymer solutions.¹³ The FH expression for the Helmholtz free energy of a compressible pure component reads

$$\frac{\beta A}{sN} = \frac{1-y}{y} \ln(1-y) + \frac{1}{s} \ln y - \gamma \beta \epsilon y \quad (5.1)$$

with $\gamma = 2/z$. The equation of state of the system can be obtained from the Helmholtz free energy, A , according to

$$p = - \left. \frac{\partial A}{\partial V} \right|_{N,T} \quad (5.2)$$

and the equation of state of FH theory is given by

$$\frac{\beta pV}{sN} = -\frac{\ln(1-y)}{y} - \left(1 - \frac{1}{s}\right) - \gamma z \beta \epsilon y \quad (5.3)$$

where p is the pressure, $\beta = 1/(k_B T)$ is the reciprocal of the temperature multiplied by the constant of Boltzmann and z is the coordination number.

5.2.3 The Huggins theory

Already in the original publication Huggins derived an approximate correlation for the chain connectivity up to nearest neighbors. The Huggins theory provides a substantial improvement over the FH theory. For instance, the equation of state (EoS) of athermal lattice polymers predicted by the Huggins theory is much more accurate than the FH result. The Huggins Helmholtz free energy is given by

$$\frac{\beta A}{sN} = \frac{1-y}{y} \ln(1-y) + \frac{1}{s} \ln y - \frac{1-\alpha y}{\gamma y} \ln(1-\alpha y) - 2\beta \epsilon \frac{(1-\alpha)^2 y}{(1-\alpha y)} \quad (5.4)$$

where the first two terms on the rhs of eq 5.4 represent the FH entropy, also found in eq 5.1, $\alpha = \gamma(1 - 1/s)$ is the probability that a nearest neighbor lattice site is taken by the next segment in the s -mers. The equation of state of the Huggins theory reads

$$\frac{\beta pV}{sN} = -\frac{\ln(1-y)}{y} - \left(1 - \frac{1}{s}\right) + \frac{\alpha}{\gamma} + \frac{\ln(1-\alpha y)}{\gamma y} - 2\beta \epsilon \frac{(1-\alpha)^2 y}{(1-\alpha y)^2} \quad (5.5)$$

The FH theory can be recovered by formally assuming an infinite coordination number, i.e. $z \rightarrow \infty$. Then, $\alpha = 0$ and the inter-segmental contact fraction q reduces to the occupied site fraction, i.e. $q = y$.

5.2.4 The NRM theory

Both Flory and Huggins assumed that nearest neighbor contacts are made at random. The effects of the interactions on the formation of the different segmental contacts can be accounted for by the quasi-chemical approximation of Guggenheim.²⁰ The NRM theory for compressible chain molecules, discussed in previous publications, is the compressible analogue of the Guggenheim theory for incompressible polymer solutions.^{21,22} The interactions influence the mixing of molecules at the segmental level and lead to deviations from random mixing. The different types of contacts in a compressible pure component are uniquely

determined in terms of the contact site fractions and extra microscopic parameter x . The NRM theory provides accurate predictions of the equation of state behavior of pure components as well as the liquid-liquid miscibility behavior of polymer blends.^{21,22} The NRM equation for the free energy of interacting pure component is given by²¹

$$\begin{aligned} \frac{\beta A}{Ns} = & \frac{1-y}{y} \ln(1-y) + \frac{1}{s} \ln y - \frac{1-\alpha y}{\gamma y} \ln(1-\alpha y) \\ & + \frac{1-\alpha}{\gamma q} [2q \ln(q) + 2(1-q) \ln(1-q)] \\ & - (q - \bar{x}) \ln(q - \bar{x}) - 2\bar{x} \ln(\bar{x}) - (1-q - \bar{x}) \ln(1-q - \bar{x}) \\ & - \frac{\beta \epsilon}{\gamma q} (1-\alpha)(q - \bar{x}) \end{aligned} \quad (5.6)$$

where q is the inter-segmental contact fraction defined as

$$q = \frac{(1-\alpha)y}{(1-\alpha y)} \quad (5.7)$$

and \bar{x} is obtained by minimization of the Helmholtz free energy

$$\left. \frac{\partial A}{\partial \bar{x}} \right|_{N, N_L, T} = 0 \quad (5.8)$$

The minimization condition eq 5.8 can be solved for \bar{x}

$$\bar{x} = \frac{1 - [(1 - 4q(1-q)(1 - e^{\epsilon/k_B T}))^{1/2}]}{2(1 - e^{\epsilon/k_B T})} \quad (5.9)$$

The equation of state is given by

$$\begin{aligned} \frac{\beta p V}{sN} = & -\frac{\ln(1-y)}{y} - \left(1 - \frac{1}{s}\right) + \frac{\alpha}{\gamma} + \frac{\ln(1-\alpha y)}{\gamma y} \\ & - \left(\frac{\beta \epsilon}{\gamma}\right) \frac{\bar{x}}{y} + \frac{1}{\gamma y} [(\bar{x} - 1) \ln(1 - \bar{x} - q) + \bar{x} \ln(q - \bar{x})] \\ & - 2\bar{x} \ln(\bar{x}) + 2 \ln(1 - q) \end{aligned} \quad (5.10)$$

The non-random mixing in eqs 5.6 and 5.10 effects the terms between square brackets and energetic term. For athermal system the NRM theory is identical to the Huggins result. Moreover, if random mixing is enforced, $\bar{x} = q(1 - q)$, the Huggins theory is also obtained. The predictions of the NRM theory have extensively been compared to MC simulation data in previous publications and will serve as a reference in the current comparisons.^{21,22}

5.2.5 The ω -theory

In the theories of Flory-Huggins, Huggins and NRM, the intra-molecular correlations are either completely ignored or, at best, approximately accounted for up to nearest neighbors. In order to include the long range intra-molecular correlations, we recently formulated a theory employing the information of a single chain.²³

Expressions for the partition function, the Helmholtz free energy and other thermodynamic properties of athermal and interacting compressible lattice polymers are derived from the definition of the insertion probability. The insertion probability approach was initially introduced by Guggenheim.²⁰ More recently, Hall and co-workers also employed the insertion probabilities to derive continuum space analogs of the Flory-Huggins and the Huggins lattice theories, the so-called Flory and Flory-dimer theories.^{1,24} In the ω -theory the Helmholtz free energy A and EoS for athermal components are given by

$$\beta A/sN = (1/s) \ln(y) - (1/sy) \int_0^y \ln[(1-y')^s/(1-\omega y')^{s-1}] dy' \quad (5.11)$$

$$\begin{aligned} \beta pV/sN = \beta p v^*/y &= (1 - \ln[(1-y')^s/(1-\omega y')^{s-1}])/s \\ &+ (1/sy) \int_0^y \ln[(1-y')^s/(1-\omega y')^{s-1}] dy' \end{aligned} \quad (5.12)$$

where ω accounts for the occurrence of intra-molecular contacts that a chain can make, irrespective of the covalent or non-covalent character. The average number of intra-molecular contacts (covalent and non-covalent) of a segment in an s -mer is given by $z\omega$ and can be calculated from

$$\omega_j = \frac{\sum_{\Omega_{con}} \Omega_{con} P_{\omega_j}(\Omega_{con}, y)}{\sum_{\Omega_{con}} P_{\omega_j}(\Omega_{con}, y)} \quad (5.13)$$

with $P_{\omega_j}(\Omega_{con}, y)$ the probability that, averaged over all conformations, a segment of the s -mer has $z\Omega_{con}$ intra-molecular contact positions. For the single chain, i.e. $y = 0$, the probability distribution $P_{\omega_j}(\Omega_{con}, y = 0)$ is easily extracted from a single chain simulation. Details are given in chapter 4. Explicit expressions for the density dependence are given by eqs 24, 27 in chapter 4.

The evaluation of the partition function for interacting chains is performed invoking the quasi-chemical approximation. The final result for the Helmholtz

free energy of interacting polymers is given by²³

$$\beta A/sN = (1/s) \ln(y) - (1/sy) \int_0^y \ln[p_e(y', T)] dy' - \frac{(1-\omega)}{(\gamma\theta)} [2\theta \ln(\theta) + 2(1-\theta) \ln(1-\theta) - 2\bar{x} \ln(\bar{x})] \quad (5.14a)$$

$$- (\theta - \bar{x}) \ln(\theta - \bar{x}) - (1 - \theta - \bar{x}) \ln(1 - \theta - \bar{x}) - \frac{\beta\epsilon}{\gamma\theta} (1-\omega)(\theta - \bar{x}) - \frac{\beta\epsilon}{\gamma} (\omega - \alpha) p_e(y, T) = (1-y)^s / (1-\omega y)^{s-1} \quad (5.14b)$$

where $p_e(y, T)$ is the chain insertion probability and θ is the inter-molecular contact fraction defined as

$$\theta = \frac{(1-\omega)y}{(1-\omega y)} \quad (5.15)$$

The last two terms in eq 5.14a stem from the internal energy. The parameter \bar{x} is obtained by minimization of the Helmholtz free energy according to eq 5.8. Explicit expressions for the minimum condition and the equation of state are quite lengthy and are not presented here.²⁵ For interacting chains, the average number of intra-molecular contacts, ω , is a function of density and temperature given by eq 41b of chapter 4. There is a subtle difference between the inter-molecular contact fraction θ and the inter-segmental contact fraction q (compare eq 5.7 and eq 5.15). In eq 5.7 only the contacts occupied by covalent bonds are excluded from inter-segmental contacts. In the inter-molecular contact fraction θ also the contact positions of a segment taken by segments of the same chain (i.e. long range effects of chain connectivity) are excluded in counting the number of intermolecular contacts.

From the ω -theory all previously discussed theories can be obtained as limiting cases. For example, if the complete intra-molecular environment ω is approximated by the covalent bonds only, i.e. $\omega = \alpha$, the NRM theory is obtained. Further reduction to the Huggins and Flory-Huggins theories has been discussed in the previous subsection.

5.2.6 The conformational theory of Szleifer

Szleifer presented a new mean field theory for polymer solutions that explicitly accounts for the conformational degrees of freedom of the chain molecules.²⁶ This is established by considering the *chain molecule* in the environment made up by the

total system. Note that in the usual mean field theory of Flory and Huggins the influence of the environment is only considered on the *segmental level*. In evaluating the partition function the conformational and translational degrees of freedom are decoupled. The translational part of the partition function is assumed to be given by the Flory-Huggins combinatorial entropy. The internal energy contribution of the partition function is expressed in the *internal partition function* of the polymer molecules $q_f(y, T)$, which depends on the conformational properties of the chain. Combining both contributions the reduced excess Helmholtz free energy per segment for a compressible pure s -mer was shown to be

$$\frac{\beta\Delta A}{sN} = \frac{1-y}{y} \ln(1-y) + \frac{1}{s} \ln y - \frac{1}{s} \ln q_f(y, T) \quad (5.16)$$

with $q_f(y, T)$ given by

$$q_f(y, T) = \sum_{\nu} \exp\left[-\frac{\beta\epsilon}{2} n_e(\nu)(1-y)\right] \quad (5.17)$$

$n_e(\nu)$ is the total number of external contacts of a chain in conformation ν and the sum runs over all possible conformations.

From the Helmholtz free energy the equation of state can be derived and is given by

$$\frac{\beta pV}{sN} = -\frac{1}{y} \ln(1-y) - \left(1 - \frac{1}{s}\right) - \frac{y}{s} \beta\epsilon \langle n_e \rangle \quad (5.18)$$

where $\langle n_e \rangle$ is the average number of external contacts of a chain

$$\langle n_e \rangle = \frac{\sum_{\nu} n_e(\nu) \exp\left[-\beta\frac{\epsilon}{2} n_e(\nu)(1-y)\right]}{\sum_{\nu} \exp\left[-\beta\frac{\epsilon}{2} n_e(\nu)(1-y)\right]} \quad (5.19)$$

The first two terms in the Helmholtz free energy equation, eq 5.16, are the Flory-Huggins combinatorial entropy of mixing polymer segments and vacancies. If a polymer molecule is viewed as s unconnected segments, $n_e(\nu) = sz$, the Flory-Huggins theory is recovered. The same simplification is obtained if athermal condition ($\epsilon = 0$) is explored. Therefore, the internal partition function or the external contact number of neighbors of a chain is an important factor in the Szeifer theory. As soon as the single chain probability distribution $n_e(\nu)$ is obtained, $q_f(y, T)$ and other thermodynamic properties can be computed. Just as in the ω -theory this number of contacts is obtained employing a single chain Monte-Carlo simulation. In fact $n_e(\nu)$ and $P_{\omega_j}(\Omega_{con}, y = 0)$ can be related. The

number of external contacts $n_e(\nu)$ in a particular conformation ν is related to the number of intra-molecular contacts $\Omega_{con}(\nu)$ in that conformation by

$$n_e(\nu) = sz(1 - \Omega_{con}(\nu)) \quad (5.20)$$

The chain conformations can be grouped according to their number of external contacts or equivalently to their number of intra-molecular contacts and a probability distribution $P_{n_e}(n_e, y = 0)$ related to $P_{\omega_j}(\Omega_{con}, y = 0)$ can be defined

$$P_{n_e}(n_e, y = 0) = P_{\omega_j}(1 - \Omega_{con}, y = 0) \quad (5.21)$$

Thus, eq 5.17 and hence eqs 5.18 and 5.19 can be written in terms of the intra-molecular contact probability $P_{\omega_j}(\Omega_{con}, y = 0)$.

5.2.7 The theory of Weinhold, Kumar and Szleifer

As already mentioned in the previous paragraph, for athermal conditions ($\epsilon = 0$) the Szleifer theory reduces to the simple FH theory combinatorial entropy. Clearly this is a consequence of the imposed decoupling of configurational and conformational contributions to the partition function. To remedy this shortcoming, Weinhold, Kumar and Szleifer proposed another mean field theory so far only applied to athermal systems.²⁷ The total entropy was split in configurational and conformational contributions. The configurational entropy S_{pack} was assumed to be given by a Huggins-Guggenheim-type combinatorial expression²⁷

$$\frac{S_{pack}}{k_B N s} = -\frac{1-y}{y} \ln(1-y) - \frac{\ln y}{s} + \frac{1-\omega'y}{\gamma y} \ln(1-\omega'y) + \frac{1}{s} \ln s \quad (5.22)$$

with $\omega' = 1 - \langle n_e(\nu) \rangle / zs = 1 - q'/s$ and q' is also an external contact fraction as defined by Weinhold et.al.²⁷ The conformational entropy S_{conf} is

$$\frac{S_{conf}}{k_B} = -N \sum_{\nu} P(\nu) \ln P(\nu) \quad (5.23)$$

where the $P(\nu)$ denotes the probability of the chains being in conformation ν . The total entropy of the system, $S = S_{pack} + S_{conf}$, is now maximized subject to the constraint that

$$\sum_{\nu} P(\nu) = 1 \quad (5.24)$$

to produce the final result for the probability of the chain being in conformation ν ,

$$P(\nu) = \frac{P_0(\nu)}{h_{sc}} \exp[\chi_{pack} n_e(\nu)] \quad (5.25)$$

where h_{sc} is a normalization factor, $P_0(\nu)$ is the probability of a single athermal chain in conformation ν and χ_{pack} is the 'interaction parameter' which originates exclusively from entropic packing considerations and is given by

$$\chi_{pack} = \frac{1}{2} + \frac{1}{2\omega'y} \ln(1 - \omega'y) \quad (5.26)$$

For the athermal chain fluid the entropy equals to the Helmholtz free energy and only in this case the EoS can be obtained.

5.2.8 The lattice cluster theory

Freed and co-workers developed the lattice cluster theory yielding a formally exact solution of the lattice model. Initially, the LC theory was derived employing mathematical methods used in field theory and particle physics.^{28,29} Later an algebraic derivation of the LC theory, more transparent to polymer scientists, has been presented.³⁰ The LC theory not only offers an exact solution of the lattice model but also provides systematic corrections to the Flory-Huggins theory when the formal solution is expanded in terms of the inverse of the lattice coordination number $1/z$ and the reduced energy $\beta\epsilon$. However, the lattice cluster expansion must be truncated at a certain order. Therefore, in actual application the LC theory is also an approximate theory, but at least a formal route to device systematic improvements is provided. Recently, Dudowicz and Freed extended the LC theory to compressible multi-component polymer blends allowing for an internal structure of monomer and solvent.³¹ The excess Helmholtz free energy ΔA of mixing per segment is given by³¹

$$\beta\Delta A/sN = \left(\sum_{i=1}^4 A_i + \sum_{i=1}^4 B_i + \sum_{i=1}^4 C_i \right) (1-y) - \frac{\Delta S}{k_B s N} \quad (5.27)$$

where A_i , B_i and C_i are known parameters containing the energetic corrections defined with cluster expansion: A_i corresponds to the $z\epsilon^i$ contributions, B_i to the ϵ/z terms and C_i to the ϵ^2 terms. Further, ΔS is the non-combinatorial athermal limit of entropy of mixing for a polymer-vacancy system ($s > 2$). For linear chains discussed here the coefficients A_i , B_i and C_i and the entropy of mixing ΔS are

$$\frac{\beta \Delta A_m}{Ns(1-y)} = \sum_{i=1}^4 A_i + \sum_{i=1}^4 B_i + \sum_{i=1}^4 C_i - \frac{S}{kNs(1-y)}$$

$$\frac{\beta \Delta E_m}{Ns(1-y)} = \sum_{i=1}^4 i A_i + \sum_{i=1}^4 B_i + 2 \sum_{i=1}^4 C_i$$

$$A_1 = \frac{ez}{2}$$

$$A_2 = -\frac{e^2 z}{4} y(1-y)$$

$$A_3 = -\frac{e^3 z}{12} y(1-y)(1-2y)^2$$

$$A_4 = -\frac{e^4 z}{48} y(1-y)(1-6y(1-y)(3y^2-3y+2))$$

$$B_1 = -e^{\frac{s-1}{s}}(1-y)$$

$$B_2 = \frac{e}{z}(1-y)\left(\frac{3-s}{s}\right)$$

$$B_3 = -\frac{2e}{z} \frac{s-1}{s} y(1-y)\left(\frac{3-s}{s}\right)$$

$$B_4 = -\frac{4e}{z} \left(\frac{s-1}{s}\right)^3 y^2(1-y)$$

$$C_1 = -\frac{e^2}{2} \frac{s-1}{s} (1-y)(1-2y)^2$$

$$C_2 = -e^2 \frac{s-2}{s} (1-y)^2$$

$$C_3 = -e^2 \left(\frac{s-1}{s}\right)^2 y(1-y)^2(1-3y)$$

$$C_4 = -\frac{e^2}{2} \frac{5-3s}{s} (1-y)^3$$

$e = \epsilon/k_B T$ in this table.

Table 5.1: *Free energy of mixing and internal energy of mixing for a polymer-void (solvent) system.*

taken from a paper of Dudowicz and Freed³¹ and are summarized in Tables 5.1 and 5.2.

The LC expansion is quite different from the theories described above which are all based on a direct, although approximate, evaluation of the partition function. Some details are presented in the chapter 2. Eq 5.27 can also be applied to pure compressible polymer systems by invoking the similarity between polymer-void system and compressible pure polymer. The EoS of the system can directly be obtained from the excess free energy, ΔA , according to the eq 5.2

In the subsequent comparison of the average number of external nearest neighbor contacts will be discussed. Note that in the NRM theory the external contact number is calculated from the external contact fraction q and in the ω -theory

$$\frac{-\Delta S - \frac{y}{s+1} \ln y - (1-y) \ln(1-y)}{kNs(1-y)}$$

$$= \frac{1}{z} A_1^2 + \frac{1}{z^2} [\sum_{i=2}^9 A_i + y \sum_{i=10}^{12} A_i + y^2 A_{13}]$$

$$A_1 = \frac{s-1}{s}$$

$$A_2 = -4 \frac{(s-1)(s-2)}{s^2}$$

$$A_3 = \frac{8}{3} \left(\frac{s-1}{s}\right)^3$$

$$A_4 = -2 \frac{(s-1)(s-3)}{s^2}$$

$$A_5 = \left(\frac{s-2}{s}\right)^2$$

$$A_6 = -2 \frac{(s-1)(10-4s)}{s^2}$$

$$A_7 = 2 \left(\frac{s-1}{s}\right)^4$$

$$A_8 = \frac{2}{s} \left(\frac{s-1}{s}\right)^2 (5-3s)$$

$$A_9 = 0$$

$$A_{10} = \frac{8}{3} \left(\frac{s-1}{s}\right)^3$$

$$A_{11} = 2 \left(\frac{s-1}{s}\right)^4$$

$$A_{12} = 2 \frac{(s-1)^2 (5-3s)}{s^3}$$

$$A_{13} = 2 \left(\frac{s-1}{s}\right)^4$$

Table 5.2: *Non-combinatorial athermal limit of entropy of mixing for a polymer-void (solvent) system.*

from θ and ω . For the LC theory the average number of external contacts can be computed from the internal energy E of the compressible pure polymer. For the nearest neighbor pair potentials considered here the internal energy can be written without approximation as

$$E = \frac{sNC_{ss}}{2} \epsilon \quad (5.28)$$

with C_{ss} the number of contact positions neighboring a segment occupied by other non-covalently bonded segments.

The excess internal energy of mixing polymer-void can be derived from the excess

Helmholtz free energy according to

$$\Delta E = -sNT^2 \left. \frac{\partial(\Delta A/sNT)}{\partial T} \right|_{N,y} \quad (5.29a)$$

$$\Delta E = E - E_s - E_h \quad (5.29b)$$

where $E_s = Nsz/2(1 - \alpha)\epsilon$ is the internal energy of pure polymer without holes and $E_h = 0$ is the internal energy of pure holes. Combining eqs 5.28 and 5.29 the number of external segment-segment contacts, C_{ss} , and the number of segment-hole contacts, C_{sh} , are obtained

$$C_{ss} = \frac{2\Delta E}{Ns\epsilon} + z(1 - \alpha) \quad (5.30a)$$

$$C_{sh} = C_{tot} - C_{ss} \quad (5.30b)$$

where C_{tot} is the total number of non-covalent contact sites available for a segment, for a 30-mer $C_{tot} = z(1 - \alpha) = 4.0666 \dots$

5.3 Thermodynamic properties

Quite generally, pure components may exhibit liquid-vapor coexistence although in practice these thermodynamic conditions are not always attainable for long chains. In the pV -plane of a pure component, a stable, a meta-stable and an unstable region can be defined. In the stable region the fluid remains in one phase. Whereas in the unstable and meta-stable regions, a fluid will ultimately phase separate into two phases. These three regions are separated by the binodal and spinodal curves. The liquid-gas binodal curve defines the coexistence between a liquid and a vapor phase and delineates the stable and meta-stable regions. Coexisting liquid and vapor phases obey the thermodynamic equilibrium criteria for chemical potential, pressure and temperature

$$\mu_l = \mu_v \quad (5.31a)$$

$$p_l = p_v \quad (5.31b)$$

$$T_l = T_v \quad (5.31c)$$

In the next section the theoretical predictions of the equation of state of pure lattice chain fluids in the homogeneous region as well as vapor-liquid coexistence will be compared to MC data of the lattice model.

5.4 Results and discussions

5.4.1 Equation of state behavior

a. Athermal chains.

In figures 5.1 and 5.2 the compressibility factor $pV/Nk_B T$ versus packing fraction y , calculated from different theories, is compared to Monte-Carlo simulation results for athermal chains with chain length $s = 20, 60$ (figure 5.1) and 30 (figure 5.2). The Monte Carlo simulation results are denoted by the symbols and the

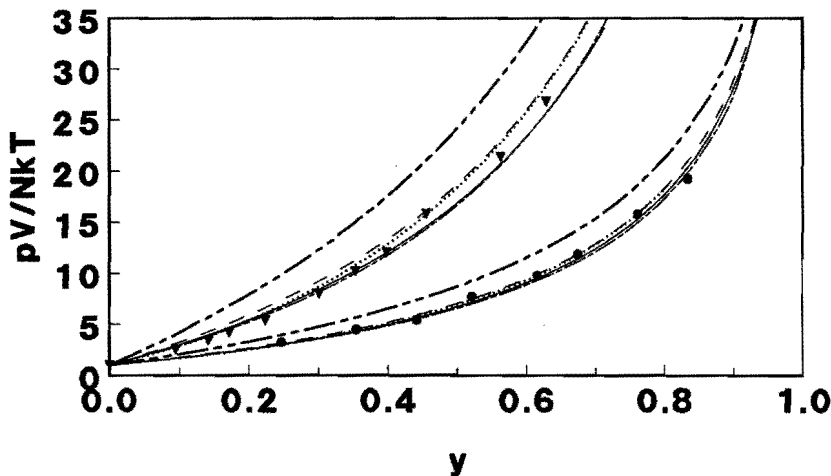


Figure 5.1: Compressibility factor of athermal chains as a function of packing fraction y . $s=20$ (\bullet), $s=60$ (\blacktriangledown); Full lines represent the ω -theory; dotted lines the LC theory; long dashed lines the NRM theory and dot-dot-dashed lines the Szeifer theory.

theoretical results are depicted by the lines. The simulation data, employing a NpT MC simulation algorithm, were collected in a previous contribution.²¹ Although we have not calculated the ‘experimental’ uncertainties on the simulation data they are thought to be small (about the size of the symbol).

Clearly the Szeifer theory (— · — · —) overestimates the compressibility factor in the whole density range. In fact, the influence of the conformational properties on the thermodynamic behavior is limited to the contribution involving the interactional energy ϵ (see eqs 5.16 and 5.18 and compare to eqs 5.1 and 5.3). Hence, the Szeifer theory reduces to the Flory-Huggins theory for athermal chains and provides no improvement on the simple FH result.

In the case of athermal chains the NRM theory reduces to the Huggins result for the entropy of mixing segments and holes.²¹ In figures 5.1 and 5.2, it can

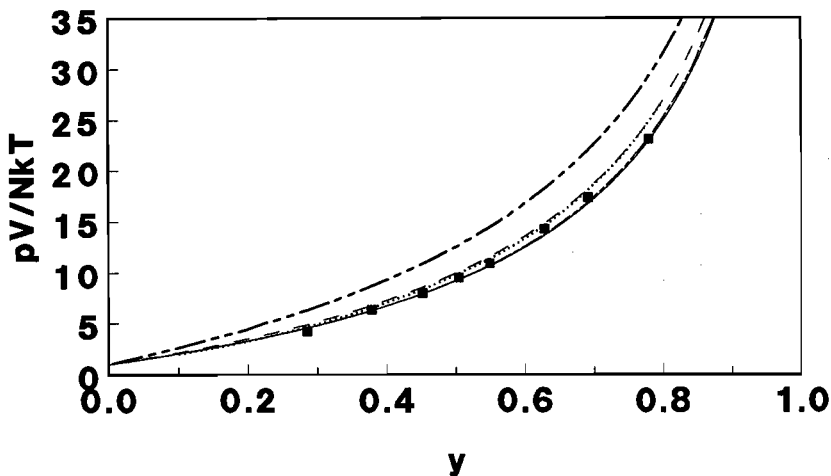


Figure 5.2: *Caption as in figure 5.1 for $s=30$.*

be observed that the NRM theory (- - - -) provides a good but slightly too high prediction of the compressibility factor. The discrepancy between theory and simulation worsens with increasing chain length.

In the high density range the NRM result is practically indistinguishable from the predictions of the LC theory ($\cdots\cdots$). In the low density range the LC theory is systematically lower and closer to the MC simulation result. This difference between LC and NRM theory becomes more pronounced with increasing chain length. Although the LC theory is in better agreement with MC simulation data; the predicted compressibility factor remains systematically too high especially at intermediate and high densities. Also in the case of the LC theory the deviations between theory and simulation increase with chain length. Although formally the lattice cluster theory incorporates the effect of all correlations, the necessary truncation of the cluster expansion implies that only local correlations are accounted for. Since long range correlation effects become more important with increasing chain length, the predictions of the LC theory also deteriorate with chain length.

Finally, both the WKS theory (- - - -)²⁷ and the ω -theory (—) give an accurate prediction of the compressibility factor for all investigated chain lengths and can be considered to be the best theories of the investigated set available for the equation of state behavior of athermal linear chains. Apparently, the long range correlations are, although approximate, quite effectively incorporated in both theories. Both theories start from a single chain simulation, monitoring

the number of intra-molecular contacts over the different conformational states. Although, it has already been shown in the previous chapter that the predicted density dependence of the intra-molecular contacts is quite different,²³ the predicted equation of state behavior is almost identical.

b. Interacting chains.

Unfortunately, the WKS theory is not (yet) applicable to interacting systems and hence cannot be considered in the discussion of interacting systems. In figures 5.3 and 5.4 the MC equation of state data²¹ of interacting 30-mers are presented and compared to theoretical predictions. The densities at zero pressure

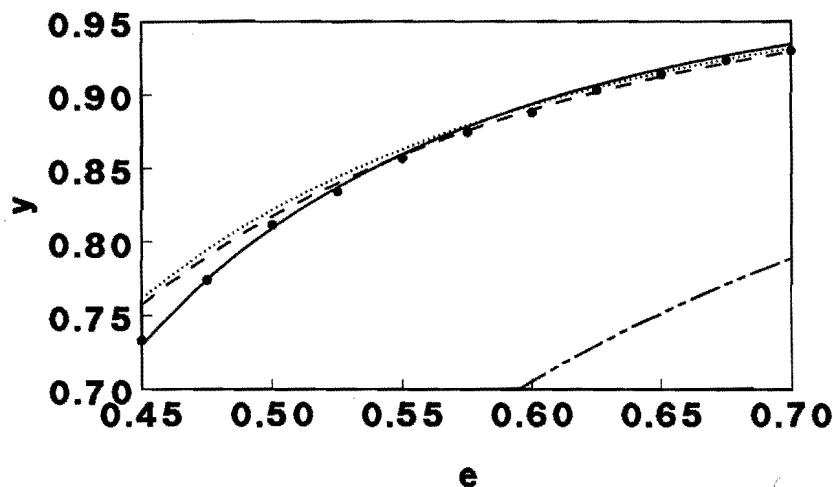


Figure 5.3: Packing fraction y vs inter-segmental interaction e for $s = 30$ and $\bar{p}=0$. MC results (\bullet); Notation is the same as figure 5.1.

as a function of reduced interaction potential $e = \epsilon/k_B T$ are shown in figure 5.3. The densities versus reduced pressure, $\bar{p} = (pv^*)/(\epsilon/\gamma k_B T)$, at given reduced interaction potential are shown in figure 5.4. It should be noted that the reduced interaction energy e can also be interpreted as an inverse reduced temperature.

In both figures it can be observed that the Szleifer theory (---) predicts extremely low densities at all investigated values of the interaction potentials and pressures. In the theoretical section it was discussed that the Szleifer theory reduces to the FH result if the polymer molecules are viewed as unconnected segments. It has previously been shown that the simple FH theory systematically predicts too high densities for all investigated interaction energies and pressures.²¹ From an energetical point of view this can be understood as follows: although the contact positions involved in covalent bonds are effectively excluded from inter-

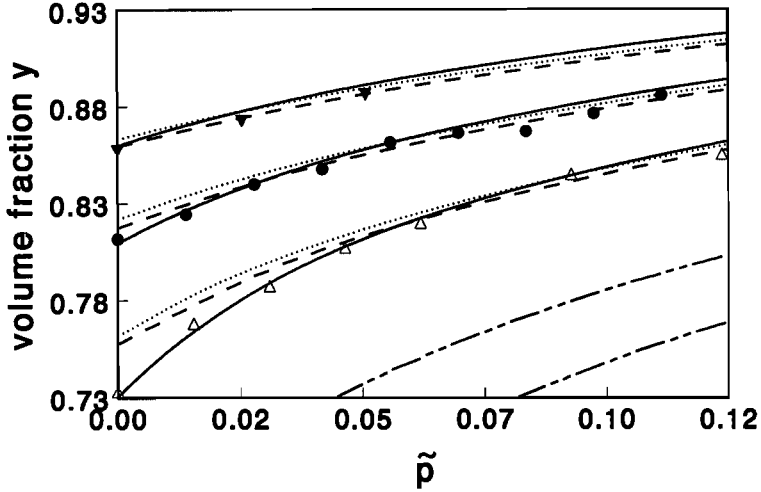


Figure 5.4: Density as a function of reduced pressure for different interactions: $e = 0.45(\Delta)$, $0.5(\bullet)$, $0.55(\blacktriangledown)$. Full lines represent the ω -theory prediction; Dotted lines the LC theory; dashed lines the NRM theory and dot-dot-dashed lines the Szleifer theory.

segmental interactions, in the FH approximation the difference in covalent and inter-segmental contact positions is ignored and all z contact positions of a chain segment contribute to the internal energy. Consequently, the internal energy is predicted to be too high, leading to a too high density at a given interaction energy in the FH theory. As can be seen from eq 5.18 the correction suggested by Szleifer operates on the internal energy and evidently results in an over-correction towards lower densities. Clearly, the combination of the FH entropy contribution (derived from the unconnected segments) and a more accurate estimate of the internal energy (excluding the intra-molecular contacts) produces an in-balance between both contributions in the equation of state. Accordingly, the predictions of the Szleifer theory are in fact worse than those of the original FH theory it sets out to improve.

Turning now to the LC ($\cdots\cdots$) and NRM ($-\ - - -$) theories in figures 5.3 and 5.4, it can be seen that they show good agreement with MC data in the high density range. However, at low densities the LC theory predicts densities slightly higher than the NRM theory and further away from the MC data. Apparently, to reach results similar or even better than these provided by the NRM theory the cluster expansion in the LC theory should be pushed even further to higher order contributions. Again, the ω -theory produces accurate predictions for the equation of state behavior of interacting polymer chains in the whole investigated

range of temperatures and pressures. Especially at low densities, the ω -theory yields substantial improvement over the NRM and LC theories. It is in this low density range where an inhomogeneous segment density exists that the influence of the chain connectivity is most noticeable. One might agree that this is almost trivial since information on the athermal single chain is introduced in the theory. However, the same single chain information is introduced in the conformational theory of Szleifer for which improvement is not observed.

In figure 5.5 more detailed information on the different type of contacts is depicted for the equation of state data presented in figure 5.3. Here, the numbers of segment-hole and segment-segment contacts are presented as a function of density. From figures 5.3 and 5.4 it is evident that the Szleifer theory needs a significantly larger reduced inter-segmental energy e to reach a given density. In

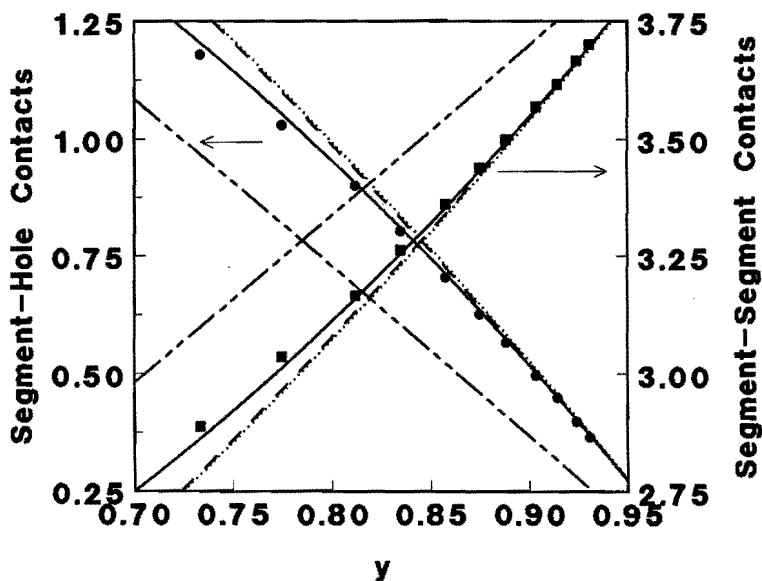


Figure 5.5: Segmental contacts vs packing fraction y corresponding to interactions e in Figure 2 and at $\bar{p} = 0$. (■) segment-segment contacts; (●) segment-hole contacts. Full lines represent the ω -theory prediction; Dotted lines the LC theory and dashed lines the NRM theory.

figure 5.5 it can be perceived that a larger value of e also lead to a significantly larger number of segment-segment contacts and of course a smaller number of segment-vacancy contacts.

The same argument appears to apply to the NRM and the LC theory to obtain a low density, e.g. $y = 0.75$, a lower value of reduced interaction energies is

required (see figure 5.3). Whence, a smaller number of segment-segment contacts and a larger number of segment-hole contacts is produced. In conclusion it can be seen in figure 5.5 that only the ω -theory provides a correct prediction of both equation of state data (figure 5.3) and the number of contacts (figure 5.5).

In figure 5.3 we noticed that the difference between the different theories was most noticeable at low densities. Hence in figure 5.6 the equation of state and the number of segment-hole contact at even lower densities than in figures 5.3 and 5.4 are investigated. This can only be accomplished by employing smaller values of the reduced interactional energy e . In figure 5.6 the e is fixed at $e = 0.3$ and variations in density are brought about by changing pressure. In figure 5.6

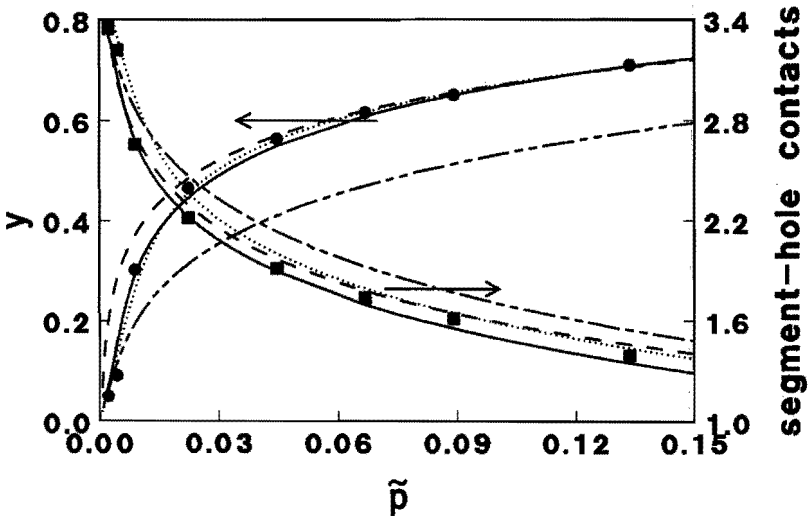


Figure 5.6: Segmental-hole contacts (■) and density y (●) vs pressure for $e = 0.3$. Full lines represent the ω -theory prediction, dotted lines the LC theory, dashed lines the NRM theory and dot-dot-dashed lines the Szeifer theory.

it can be observed that the LC theory, the NRM theory and the ω -theory all provide satisfactory predictions of the variation in density with pressure. It can also be observed that the LC theory is, especially at low and high densities, closer to the ω -theory than to the NRM theory. At the smaller value of the reduced energy, $e = 0.3$, compared to the values shown in figure 5.3 and 5.4, the truncated cluster expansion is much more adequate and the LC theory also yields better results. The same can be seen for the number of segment-hole contacts. Especially at higher densities the three theories produce acceptable results. At low densities both the ω - and NRM theories are in good agreement with MC

data. Whereas the LC theory tends to overestimate the number of segment-hole contacts. As already mentioned, at these low densities the full chain connectivity becomes important in determining the number of segment-hole contacts. Due to the truncation in the LC theory only local correlations are accounted for leading to a too high number of segment-hole contacts.

In agreement with the previous result, it can be observed that the Szleifer theory yields a poor prediction of the equation of state as well as the number of segment-hole contacts.

5.4.2 The liquid-vapor coexistence

The prediction of coexistence curves is a sensitive test for all theories, since an accurate prediction of the chemical potentials and the equation of state behavior of the polymer in both phases is required. In figures 5.7, 5.4.2, 5.9 and 5.10 the liquid-vapor binodal curves for chain length $s = 1, 2, 4, 8, 16, 32, 64, 100$, calculated for the different theories, are presented in comparison with the Monte-Carlo simulation data taken from the paper of Yan et.al.^{32,33}

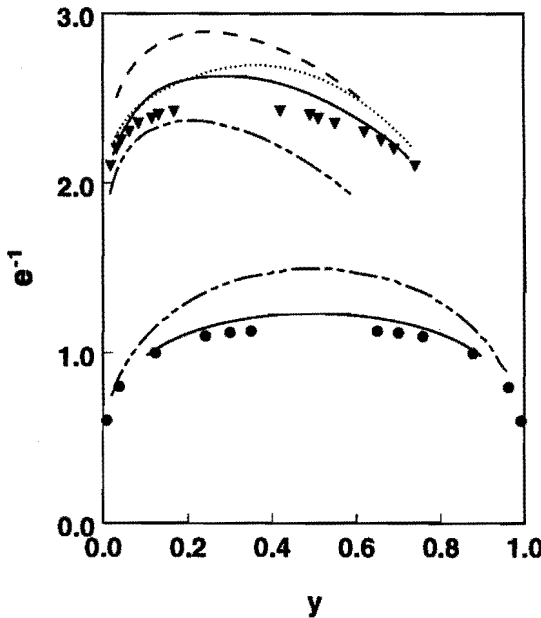


Figure 5.7: liquid-vapor coexistence binodal curves for $s=1$ (\bullet) and 16 (\blacktriangledown). Full lines represent the ω -theory prediction, dotted lines the LC theory, dashed lines the NRM theory and dot-dot-dashed lines the Szleifer theory.

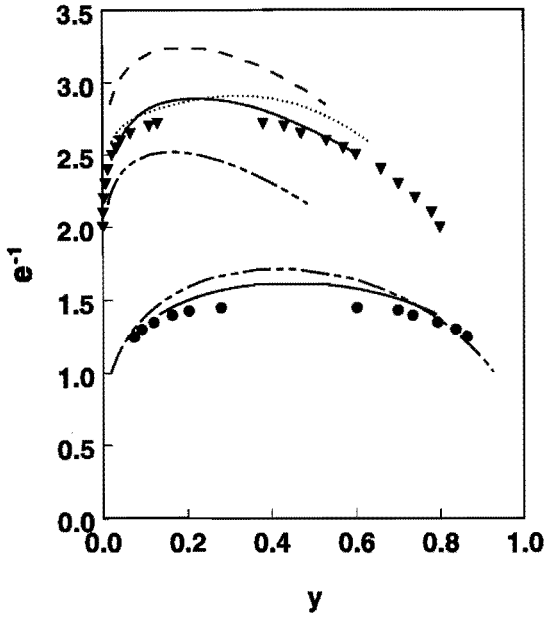


Figure 5.8: *Caption is the same as figure 5.7, but for $s=2$ (\bullet) and 32 (\blacktriangledown).*

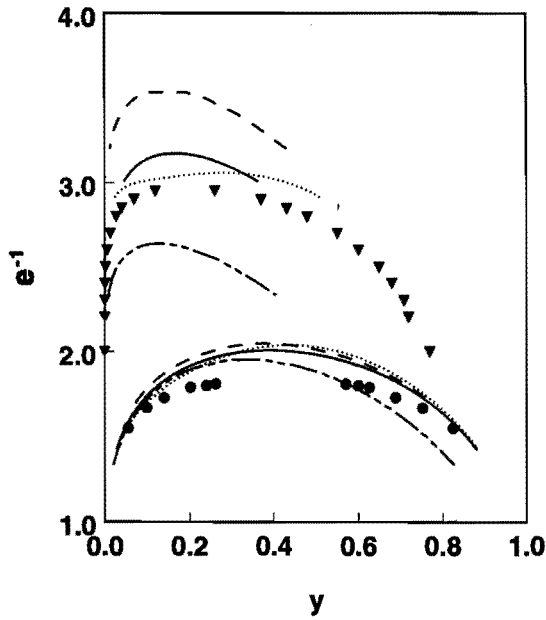


Figure 5.9: *Caption is the same as figure 5.7, but for $s=4$ (\bullet) and 64 (\blacktriangledown).*

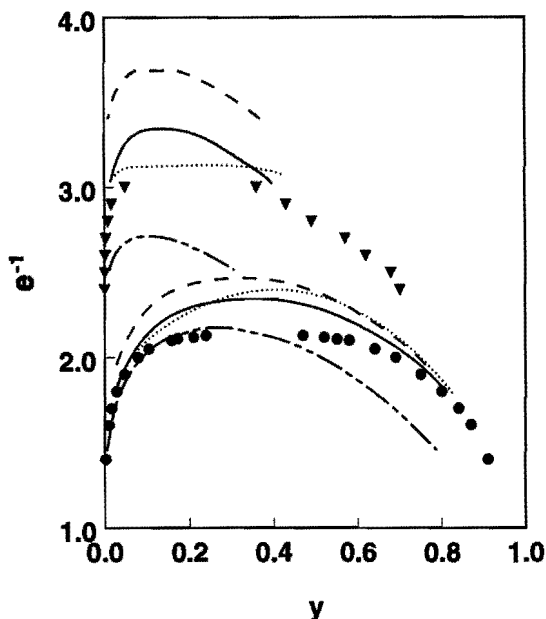


Figure 5.10: *Caption is the same as figure 5.7, but for $s=8$ (\bullet) and 100 (\blacktriangledown).*

The liquid-vapor binodals calculated from eqs 5.31, 5.16 and 5.18 for the Szleifer theory (— — — —) are the narrowest of all theories although they are wider than those of the Flory theory as shown by Szleifer.²⁶ The figures also show that the predicted coexistence curves are located at too high temperatures for short chains whereas for higher chain lengths the opposite can be observed. The chain conformational correction, embodied in the internal partition function $q_f(y, T)$, becomes more important with increasing chain length. In fact, for monomers, the Szleifer theory reduces to the Flory theory and the predicted coexistence curve is located at too high temperatures.²⁰ With increasing chain length the internal partition function $q_f(y, T)$ gains in importance and the predicted coexistence curve shifts to lower temperatures in comparison to the Flory predictions. However, increasing the chain length further the influences of the internal partition function becomes too strong and already for moderate chain lengths, $s \geq 16$, the predicted coexistence curves shift below the MC simulation data.

In figures 5.12 and 5.11 the density and inverse of the reduced critical temperature are plotted as a function of chain length. The reduced critical temperature, $k_B T / \epsilon = e^{-1}$, is plotted versus $s^{-1/2} + (2s)^{-1}$.

If the FH theory were exact this plot should result in a straight line. Clearly,

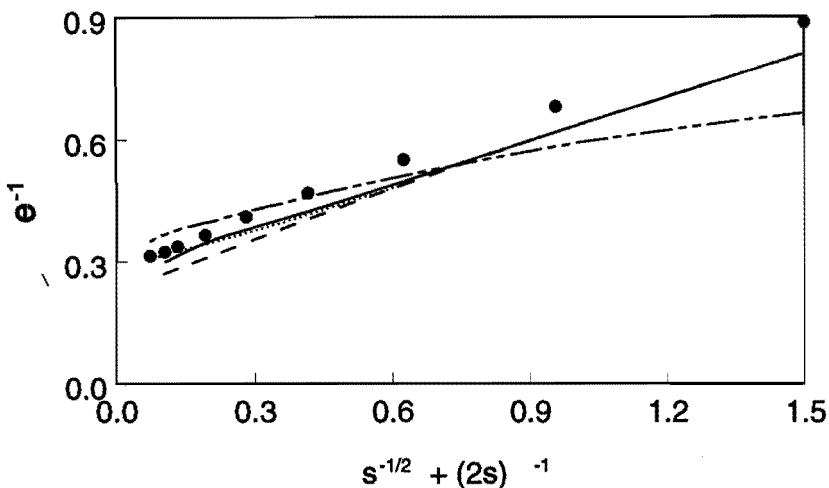


Figure 5.11: Critical temperatures as a function of chain length. MC data (\bullet). Full lines represent the ω -theory prediction, dotted lines the LC theory, dashed lines the NRM theory and dot-dot-dashed lines the Szleifer theory.

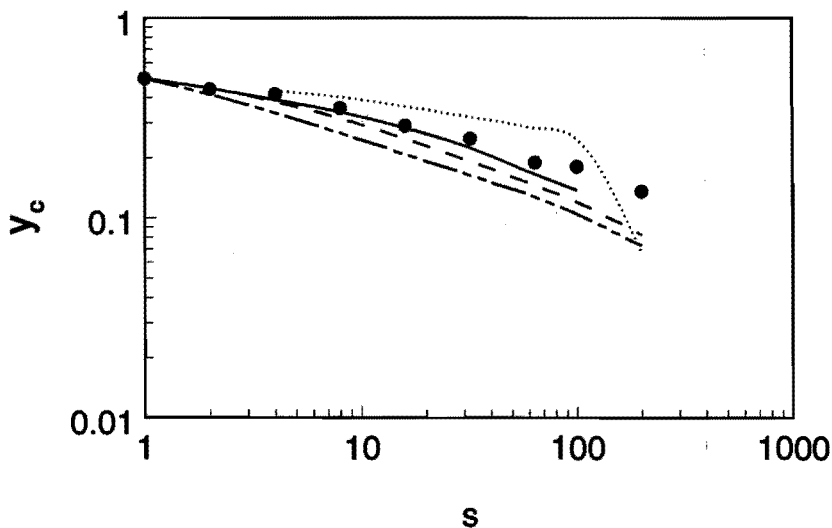


Figure 5.12: Critical composition vs chain length. Notation is the same as figure 5.11.

all theories and the simulation data show some curvature in this representation. In agreement with the discussion on the coexistence curve it can be observed that the Szleifer theory provides too high critical temperatures at small chain lengths and too low temperatures at large chain length. Consequently the overall slope

of the reciprocal critical temperature versus chain length is too small. The chain length dependence of the critical density is shown in figure 5.12. For the monomer, all theories predict a critical density $y_c = 0.5$ which is a direct consequence of the particle-vacancy symmetry on the lattice.²⁰ However, with increasing chain length the critical density is predicted to be too low according to the Szleifer theory.

The predicted liquid-vapor coexistence curves according to the LC theory (.....) and NRM theory (- - - -) are quite broad and are located for all chain lengths at higher temperatures than the MC data. For the smallest chain lengths ($s = 1, 2$) the LC theory, eq 5.27, is not applicable and the L-V coexistence curve cannot be calculated. For the short chain lengths ($s = 4, 8$) the predictions of the LC theory and the NRM theory are somewhat different at the low density side but the high density branches coincide. For the larger chain lengths, the differences between the LC and the NRM theories become more pronounced. Although the two theories still tend to similar results at high densities the differences at low densities are quite significant. The LC predictions are closer to the MC data than the NRM theory. However, the overall shape of the LC theory is quite peculiar, the more so, at higher chain lengths. In figure reffig:criticaltem it can be observed the predicted critical temperature of NRM and LC theories are practically identical at smaller chain lengths but at higher chain lengths the LC theory is closer to the MC data. Considering the critical densities as a function of chain length (figure 5.12) the NRM theory performs somewhat better than the Szleifer theory but the densities remain too small. On the other hand the critical densities of LC theory are systematically higher than the MC results. Furthermore, a peculiar sudden drop below the MC data occurs for chain lengths $s \geq 100$. For even higher chain lengths the predictions of LC theory even drop below the Szleifer results. The unconventional behavior of the LC theory (peculiar shape of the coexistence curve and the unusual chain length dependence of the critical densities) has been observed previously and has been attributed to the truncated cluster expansion but is not really understood.³²

Finally the ω -theory predictions are presented by the full lines. Especially for small and intermediate chains length $s \leq 32$ the results of the ω -theory are better than those obtained from the LC theory. For higher chain lengths the coexistence curves predicted by the ω -theory are at somewhat too high temperatures. However, the broadness of the curves is close to the MC data and no peculiar shape as for the LC theory can be observed. Furthermore, the predicted critical temperatures according to the ω -theory are similar to those of the LC

theory as can be observed in figure 5.11. In figure 5.12 it can be observed that the predicted critical densities are in quite satisfactory agreement with the MC simulation results.

5.5 Conclusions

a. Equation of state

The equation of state and vapor-liquid coexistence of compressible pure components have been investigated employing a number of recently published lattice theories. The theoretical results are compared to Monte-Carlo simulation data for the lattice model.

The ω -theory accurately predicts the equation of state for all investigated densities and pressures. This demonstrates the successful incorporation of the chain connectivity in the ω -theory. At high densities the LC theory, truncated at a certain order, and the NRM theory also give fair predictions of equation of state behavior of interacting polymers. At low densities the LC theory and the NRM theory show some deviation from the MC simulation data. These deviation can be attributed to the limited account of the chain connectivities in both the NRM theory and the LC theory. However, in principle the LC theory can be pushed to higher order approximation, thus, providing a route to systematic improvements. The Szleifer theory results in poor predictions of the equation of state, certainly in comparison with the other theories. It was made plausible that the poor results of the Szleifer theory are mainly due to an improper balance between entropy and energy. The theory of Weinholt, Kumar and Szleifer, which incorporates the influence of the conformational properties also in the combinatorial entropy, gives an accurate prediction of the equation of state properties of athermal chains virtually indistinguishable from the ω -theory. At present the theory is not yet extended to interacting systems.

b. The Liquid-vapor coexistence

The Szleifer theory produces narrow binodal curves. The critical density predicted by the Szleifer theory is lower than the MC data and the critical temperatures do not agree with the MC data either. Again the main reason is due to an in-balance between entropy and energy. The NRM theory produces too high critical temperatures and the deviation becomes worse with increasing chain length. The critical densities of the NRM theory are also lower than the MC data but are better than those of the Szleifer theory. The LC theory gives an accurate prediction for the critical temperature, but produces a peculiar shape of the coexistence

curves and an incorrect course of the critical densities versus chain length. The ω -theory yields acceptable critical temperatures but not quantitative agreement with the MC simulation data. Nevertheless, considering the shape of the coexistence curve and the chain length dependence of both critical temperature and density, the ω -theory provides the best agreement of all theories considered. Of course all theories predict classical critical exponents and should not be used if one is especially interested in the critical phenomena. However, away from the critical region, the ω -theory has proven to be quite successful in prediction both the equation of state behavior of homogeneous system as well as the liquid-vapor coexistence. In a subsequent chapter, we will study the equation of state and liquid-liquid demixing phase separation of polymer blends via the theories studied here.

References

- [1] Dickman, R., Hall, C. K., *J. Chem. Phys.* 85, 4108, 1986.
- [2] Dickman, R., Hall, C. K., *J. Chem. Phys.* 89, 3168, 1988.
- [3] Honnell, K. G., Hall, C. K., *J. Chem. Phys.* 90, 1841, 1988.
- [4] Yethiraj, A., Hall, C. K., *J. Chem. Phys.* 95, 8494, 1991.
- [5] Lennard-Jones, J. E., Devonshire, A. F., *Proc. Roy. Soc., A* 163, 63, 1937.
- [6] Prigogine, I., Bellemans, A., Mathot, V., *The Molecular Theory of Solutions*. North-Holland Publishing Co, Amsterdam, 1957.
- [7] Simha, R., Somcynsky, T., *Macromolecules* 2, 341, 1969.
- [8] Simha, R., Carri, G., *J. Polymer Sci, Polym. Phys.* 32, 2645, 1994.
- [9] Nies, E., Stroeks, A., *Macromolecules* 23, 4092, 1990.
- [10] Nies, E., Xie, H., *Macromolecules* 26, 1683, 1993.
- [11] Stroeks, A., Nies, E., *Macromolecules* 23, 4088, 1990.
- [12] Xie, H., Nies, E., *Macromolecules* 26, 1689, 1993.
- [13] Flory, P. J., *Principles of Polymer Chemistry*. Cornell University Press, Ithaca, 1953.
- [14] Flory, P. J., *J. Chem. Phys.* 9, 660, 1941.
- [15] Flory, P. J., *J. Chem. Phys.* 10, 51, 1942.
- [16] Flory, P. J., *Proc. R. Soc. London, A* 234, 60, 1956.
- [17] Flory, P. J., *Proc. Natl. Acad. Sci. U. S. A.* 79, 4510, 1941.

- [18] Huggins, M. L., *Ann. N.Y. Acad. Sci* 43, 1, 1942.
- [19] Huggins, M. L., *J. Chem. Phys.* 9, 440, 1941.
- [20] Guggenheim, E. A., *Mixtures*. Oxford University Press, London, 1952.
- [21] Nies, E., Cifra, P., *Macromolecules* 27, 6033, 1994.
- [22] Cifra, P., Nies, E., Broersma, J., *Macromolecules* 29, 6634, 1996.
- [23] Wang, S., *PhD - thesis, Chapter 4*. Eindhoven University of Technology, The Netherlands, 1997.
- [24] Honell, K. G., Hall, C. K., *J. Chem. Phys.* 95, 4481, 1991.
- [25] Computer codes can be requested from Erik Nies by e-mail(tgpkem@chem.tue.nl).
- [26] Szleifer, I., *J. Chem. Phys.* 92, 6940, 1990.
- [27] Weinhold, J. D., Kumar, S. K., Szleifer, I., *Europhysics Letters* 35, 695, 1996.
- [28] Freed, K. F., *J. Phys. A* 18, 871, 1985.
- [29] Bawendi, M. G., Freed, K. F., Mohanty, U., *J. Chem. Phys.* 84, 7036, 1986.
- [30] Freed, K. F., Bawendi, M. G., *J. Phys. Chem.* 93, 2194, 1989.
- [31] Dudowicz, J., Freed, K. F., Madden, W. G., *Macromolecules* 23, 4830, 1990.
- [32] Yan, Q., Liu, H., Hu, Y., *Macromolecules* 29, 4066, 1996.
- [33] Yan, Q., Jian, J., Liu, H., Hu, Y., *J. Chem. Ind. Eng. (China)* 46, 517, 1995.

Chapter 6

Thermodynamic properties of compressible lattice polymers: A comparison of MC simulation data and theories. Polymer blends

6.1 Introduction

In the previous chapter we investigated in more detail the predictions of several theories concerning the thermodynamic behavior of pure components. In this chapter the theoretical predictions involving binary mixtures of lattice chain molecules are discussed. It should be a matter of course to review the theories that have been studied for the pure components. Unfortunately, not all these theories have been worked out for mixtures and the extensions to mixtures require further assumptions which we prefer to leave to the designers of the pure component theories. In fact, from the theories considered in the previous chapter only the FH and Huggins theories, the lattice cluster (LC) theory, the non-random mixing (NRM) theory and the ω -theory have been expanded for mixtures. Hence, in the following discussion we are limited to this smaller set of theories.

We are not only restricted in the number of theories but also in the information that can be studied. For the NRM theory and the ω -theory we have information on the different types of contacts present in the system. For pure components the number of different segment contacts in the LC theory could easily be worked

out from the internal energy. However, for mixtures the internal energy does not suffice to reveal the contributions of the different types of contacts. Hence, in this comparison we will also limit the comparison to sheer thermodynamic properties, i.e. the equation of state and the liquid-liquid miscibility behavior. Despite these strong limitations in theories and in experimental data we feel it is still useful to present this comparison.

The rest of this chapter is organized as follows. In Section 2 we introduce the different theories. In Section 3 the thermodynamic conditions are introduced. The results for equation of state and the liquid-liquid demixing phase diagram are presented in Section 4. Concluding remarks are drawn in Section 5.

6.2 Model and theories

6.2.1 The lattice model for a compressible polymer blend

Consider a binary mixture of linear chains, which contains N_A s_A -mers and N_B s_B -mers on a lattice of N_L sites, each of volume v^* . Thus each $A(B)$ molecule occupies $s_A(s_B)$ consecutive sites on the lattice. The non-covalent nearest neighbors are assigned attractive interaction potentials, i.e. $-\epsilon_{AA}$, $-\epsilon_{AB}$ and $-\epsilon_{BB}$ ($\epsilon_{ij} > 0$, i, j is A or B). The effective interactional parameter $\langle \epsilon \rangle$ and exchange energy ΔW are defined as

$$\langle \epsilon \rangle = \epsilon_{AA}\phi_A^2 + \epsilon_{BB}\phi_B^2 + 2\epsilon_{AB}\phi_A\phi_B \quad (6.1a)$$

$$\Delta W = \epsilon_{AA} + \epsilon_{BB} - 2\epsilon_{AB} \quad (6.1b)$$

The exchange energy ΔW and the effective interaction $\langle \epsilon \rangle$ are not independent but are related according to

$$\langle \epsilon \rangle = \epsilon_{AA}\phi_A + \epsilon_{BB}\phi_B - \Delta W\phi_A\phi_B \quad (6.2)$$

6.2.2 The Flory-Huggins theory

The original Flory-Huggins (FH) mean field theory, obtained for the incompressible lattice model, provided a rationalization for the frequently occurring UCST miscibility behavior in polymer solutions. Later the FH theory was extended to compressible systems thus providing a molecular explanation for the occurrence of LCST miscibility behavior in polymer solutions and blends. It was found that a possible cause for the LCST miscibility is a difference in the compressibility of

the mixture constituents.¹

The FH expression for the Helmholtz free energy of a binary polymer mixtures reads

$$\frac{\beta A}{sN} = (\phi_A/s_A) \ln(\phi_A) + (\phi_B/s_B) \ln(\phi_B) + \frac{1-y}{y} \ln(1-y) + (1/s) \ln(y) - \frac{z}{2} \beta \langle \epsilon \rangle y \quad (6.3)$$

And the equation of state is given by

$$\frac{\beta pV}{sN} = -\frac{1}{y} \ln(1-y) - (1 - \frac{1}{s}) - \frac{z}{2} \beta \langle \epsilon \rangle y \quad (6.4)$$

The Flory-Huggins theory was, and still is, frequently employed to study the thermal behavior of polymer solutions and blends. However, in the FH theory random mixing on a segmental level is assumed and the long range correlations caused by chain connectivity are completely ignored. According to the FH theory the equation of state of a binary mixture is identical to that of a single equivalent component with an effective chain length, $s = (s_A N_A + s_B N_B)/N$, and an effective interaction parameter $\langle \epsilon \rangle$. Note that in the case of compressible mixture $\langle \epsilon \rangle$ is the appropriate effective energy parameter and not ΔW . It was shown by Madden that the latter is the only energy parameter necessary to describe an incompressible binary lattice mixture with nearest neighbor contact energies.² For compressible mixture the pure component interaction constant ϵ_{AA} and ϵ_{BB} are also important.

6.2.3 The NRM theory

The NRM theory has been suggested^{3,4} to improve upon the simple Flory-Huggins theory. In essence this theory is the compressible analogue of the quasi-chemical theory of Guggenheim for incompressible systems. It was shown that the NRM theory indeed gives better agreement with the simulation data for the equation of state and liquid-liquid coexistence conditions.

The Helmholtz free energy of a binary blend is given by⁴

$$\begin{aligned}
\beta A/sN &= (\phi_A/s_A) \ln(\phi_A) + (\phi_B/s_B) \ln(\phi_B) + \frac{(1-y)}{y} \ln(1-y) + (1/s) \ln(y) \\
&- \frac{(1-\alpha y)}{\gamma y} \ln(1-\alpha y) - \frac{(1-\alpha)}{(\gamma q)} [2q_A \ln(q_A) + 2q_B \ln(q_B) + 2q_h \ln(q_h)] \\
&- 2\bar{x}_{AB} \ln(\bar{x}_{AB}) - 2\bar{x}_{Ah} \ln(\bar{x}_{Ah}) - 2\bar{x}_{Bh} \ln(\bar{x}_{Bh}) \\
&- (q_A - \bar{x}_{AB} - \bar{x}_{Ah}) \ln(q_A - \bar{x}_{AB} - \bar{x}_{Ah}) - (q_B - \bar{x}_{AB} - \bar{x}_{Bh}) \ln(q_B - \bar{x}_{AB} - \bar{x}_{Bh}) \\
&- (q_h - \bar{x}_{Ah} - \bar{x}_{Bh}) \ln(q_h - \bar{x}_{Ah} - \bar{x}_{Bh}) \\
&- \beta \frac{(1-\alpha y)}{\gamma y} [\epsilon_{AA}(q_A/y - \bar{x}_{AB} - \bar{x}_{Ah}) + \epsilon_{BB}(q_B/y - \bar{x}_{AB} - \bar{x}_{Bh}) + 2\epsilon_{AB}\bar{x}_{AB}]
\end{aligned} \tag{6.5}$$

where q_j is the external contact fraction (excluding covalent bonds) of component j , $q_j = (1-\alpha_j)\phi_j y / (1-\alpha y)$ and $q = q_A + q_B$, $q_h = 1-q$ and $\alpha = \alpha_A \phi_A + \alpha_B \phi_B$, $\alpha_j = 2/z(1-1/s_j)$ is the fraction of intra-molecular contacts of a segment in an s_j -mer.

The segmental interaction energies influence the formation of segmental contacts and lead to deviations from random mixing. The different types of contacts in a binary compressible mixture are uniquely determined in terms of the contact site fractions, q_j , and three extra microscopic parameters, \bar{x}_{AB} , \bar{x}_{Ah} and \bar{x}_{Bh} . These microscopic parameters are obtained by minimizing the Helmholtz free energy, according to

$$-\left. \frac{\partial A}{\partial x_{ij}} \right|_{N_A, N_B, N_L, T, x_{kl} \neq ij} = 0, \text{ for } x_{ij} = x_{AB}, x_{Ah} \text{ and } x_{Bh} \tag{6.6}$$

The equation of state can be obtained by a straightforward differentiation yielding

$$\begin{aligned}
\frac{\beta p v^*}{y} &= -\frac{\ln(1-y)}{y} - 1 + \frac{1}{s} + \frac{\ln(1-\alpha y)}{\gamma y} \\
&+ \frac{\alpha}{\gamma} + \frac{1}{\gamma} [2q_A \ln(q_A) + 2q_B \ln(q_B) + 2q_h \ln(q_h)] \\
&- (q_A - \bar{x}_{AB} - \bar{x}_{Ah}) \ln(q_A - \bar{x}_{AB} - \bar{x}_{Ah}) \\
&- (q_B - \bar{x}_{AB} - \bar{x}_{Bh}) \ln(q_B - \bar{x}_{AB} - \bar{x}_{Bh}) \\
&- (q_h - \bar{x}_{Ah} - \bar{x}_{Bh}) \ln(q_h - \bar{x}_{Ah} - \bar{x}_{Bh}) - 2\bar{x}_{AB} \ln(\bar{x}_{AB}) \\
&- 2\bar{x}_{Ah} \ln(\bar{x}_{Ah}) - 2\bar{x}_{Bh} \ln(\bar{x}_{Bh}) \\
&- \frac{\beta}{\gamma y} [\epsilon - (\epsilon_{AA}(q_{AA}/y)^2 + \epsilon_{BB}(q_{BB}/y)^2)q]
\end{aligned} \tag{6.7}$$

The NRM theory is quite successful in the prediction of the equation of state and phase behavior of pure components³ and polymer blends.⁴ The residual

deviations from MC data that were shown to exist are likely related to the chain connectivity and critical behavior.⁴

6.2.4 The ω -theory

The ω -theory⁵ was recently formulated in an effort to introduce the complete effect of chain connectivity. As explained in detail in chapter 4, the special status of the non-covalently bonded intra-molecular contacts of a segment and the influence of the density and interaction on them was recognized. In ω -theory the Helmholtz free energy A of a binary mixture is given by⁵

$$\begin{aligned}
 \beta A/sN = & (\phi_A/s_A) \ln(\phi_A) + (\phi_B/s_B) \ln(\phi_B) + (1/s) \ln(y) \\
 & - (1/sy) \int_0^y \ln[p_e(y', \phi_B, T)] dy' - \frac{(1-\omega)}{(\gamma\theta)} [2\theta_A \ln(\theta_A) + 2\theta_B \ln(\theta_B) + 2\theta_h \ln(\theta_h) \\
 & - 2\bar{x}_{AB} \ln(\bar{x}_{AB}) - 2\bar{x}_{Ah} \ln(\bar{x}_{Ah}) - 2\bar{x}_{Bh} \ln(\bar{x}_{Bh}) \\
 & - (\theta_A - \bar{x}_{AB} - \bar{x}_{Ah}) \ln(\theta_A - \bar{x}_{AB} - \bar{x}_{Ah}) - (\theta_B - \bar{x}_{AB} - \bar{x}_{Bh}) \ln(\theta_B - \bar{x}_{AB} - \bar{x}_{Bh}) \\
 & - (\theta_h - \bar{x}_{Ah} - \bar{x}_{Bh}) \ln(\theta_h - \bar{x}_{Ah} - \bar{x}_{Bh})] \\
 & - \beta \frac{(1-\omega)}{\gamma\theta} [\epsilon_{AA}(\theta_A - \bar{x}_{AB} - \bar{x}_{Ah}) + \epsilon_{BB}(\theta_B - \bar{x}_{AB} - \bar{x}_{Ah}) + 2\epsilon_{AB}\bar{x}_{AB}] \\
 & - \frac{Ns}{\gamma} [\epsilon_{AA}(\omega_A - \alpha_A)\phi_A + \epsilon_{BB}(\omega_b - \alpha_B)\phi_B]
 \end{aligned} \tag{6.8a}$$

$$p_e(y, \phi_B, T) = (1-y)^s / (1-\omega(y, \phi_B, T)y)^{s-1} \tag{6.8b}$$

where $\omega = \omega_A\phi_A + \omega_B\phi_B$ and the external contact fraction θ_j is defined as

$$\theta_j = \frac{\phi_j(1-\omega_j)y}{(1-\omega y)} \tag{6.9a}$$

$$\theta_h = 1 - \theta_A - \theta_B = \frac{1-y}{(1-\omega y)} \tag{6.9b}$$

The microscopic parameters, \bar{x}_{ij} , are obtained by minimizing the Helmholtz free energy according to eq 6.6. The equation of state (EoS) of the binary mixture can be obtained from the Helmholtz free energy by differentiation with respect to volume. Because explicit expressions for the minimization condition and the equation of state are quite lengthy they are not repeated here.⁶ The average number of intra-molecular contacts (covalent and other) of a segment is given by $z\omega_j$. The average is over all segments in the chain and all the conformations that

the chain may have in the mixture. The ω_j for a single athermal chain can be extracted from a single chain simulation. From the ω_j of a single chain, the intramolecular contacts $z\omega_j$ at certain density and temperature can be calculated.⁵ The exact procedure is outlined in chapter 4 .

6.2.5 The lattice cluster theory

The lattice cluster theory formulated by Freed and co-workers⁷⁻¹⁰ is an important achievement in the development of the lattice polymer theory. The LC theory not only offers a formally exact theory for the lattice model in terms of a double expansion in the inverse temperature and the inverse lattice coordination number, but also makes it possible to predict the thermodynamic properties of polymers with different structures.

In the first theoretical discussions and practical applications Bawendi and Freed limited the cluster expansion to so-called first-order corrections.¹¹ More recently, Freed and co-workers defined a second generation LC theory by including higher order corrections in the cluster expansion. This second generation LC theory was employed for pure components, dealt with in the previous chapter. Unfortunately, we have not been able to apply this higher order theory to binary mixtures and are forced to adopt the first order LC theory of Bawendi and Freed¹²

In this version of the LC theory, the free energy of mixing is given by

$$\beta A/Ns = \frac{\phi_A}{s_A} \ln(\phi_A y) + \frac{\phi_B}{s_B} \ln(\phi_B y) + \frac{1-y}{y} \ln(1-y) + g_{01}(1-y)\phi_A + g_{02}(1-y)\phi_B + g_{12}\phi_A\phi_B y \quad (6.10)$$

where g_{01} , g_{02} and g_{12} are known functions of ϵ_{ij} and $1/z$, tabulated in Appendix B.

From the Helmholtz free energy the equation of state can be derived

$$\beta PV/sN = \beta P v^*/y = -\frac{1}{y} \ln(1-y) - \left(1 - \frac{1}{s}\right) + \phi_A \frac{\partial g_{01}}{\partial y} y(1-y) - \phi_A y g_{01} + \phi_B \frac{\partial g_{02}}{\partial y} y(1-y) - \phi_B y g_{02} + \frac{\partial g_{12}}{\partial y} \phi_A \phi_B y^2 + g_{12} \phi_A \phi_B y \quad (6.11)$$

6.3 Thermodynamic properties

The equation of state can directly be put to use in the comparison with MC data of homogeneous mixtures. The binary mixture may also possess, for certain

condition, a liquid-liquid miscibility gap. The liquid-liquid coexistence curve obeys the equilibrium conditions

$$\mu'_A = \mu''_A \quad (6.12a)$$

$$\mu'_B = \mu''_B \quad (6.12b)$$

$$p' = p'' \quad (6.12c)$$

$$T' = T'' \quad (6.12d)$$

For the binary mixture the chemical potential μ_j may be calculated from the Gibbs free energy $G(= A + pV)$

$$\mu_A/s_A = (G/sN) - \phi_B \frac{\partial(G/sN)}{\partial\phi_B} \Big|_{p,T} \quad (6.13a)$$

$$\mu_B/s_B = (G/sN) + \phi_A \frac{\partial(G/sN)}{\partial\phi_B} \Big|_{p,T} \quad (6.13b)$$

Eqs 6.12 are completely general; for the symmetric chain mixtures considered in the miscibility study ($s_A = s_B = 30, \epsilon_{AA} = \epsilon_{BB}$) the coexistence condition $\mu'_j = \mu''_j$ ($j = A, B$) is also given by

$$\frac{\partial(G/sN)}{\partial\phi_A} \Big|_{p,T} = 0 \quad (6.14a)$$

$$\frac{\partial(G/sN)}{\partial\phi_B} \Big|_{p,T} = 0 \quad (6.14b)$$

In the present calculations we used the simpler conditions, eqs 6.14, instead of the more general equilibrium conditions, eqs 6.12a and 6.12b. For a binary mixture, the critical state is located at the top of the binodal curve and obeys the following set of conditions

$$\frac{\partial^2(G/sN)}{\partial\phi_b^2} \Big|_{p,T} = 0 \quad (6.15a)$$

$$\frac{\partial^3(G/sN)}{\partial\phi_b^3} \Big|_{p,T} = 0 \quad (6.15b)$$

For the symmetric systems considered here a perfectly symmetrical binodal curve is obtained and the critical composition is $\phi_b = 0.5$.

6.4 Results and discussions

Definitely, the mixture theories are applicable to all possible combinations of chain lengths. However, so far the available simulation results have been limited to one particular combination of chain lengths, i.e. $s_A = s_B = 30$. Hence, the comparison is also restricted to this particular system.

6.4.1 Homogeneous mixtures.

In the portrayal of the results we will make use of the effective reduced interaction parameter $\langle e \rangle$ defined by

$$\langle e \rangle = e_{AA}\phi_A^2 + e_{BB}\phi_B^2 + 2e_{AB}\phi_A\phi_B \quad (6.16)$$

with $e_{ij} = \epsilon_{ij}/k_B T$.

The definition of effective reduced interactions, eq 6.16, stems from the Flory-Huggins theory. According to the FH theory the equation of state of a binary mixture is identical to that of a single equivalent component with an effective chain length, $s = (s_A N_A + s_B N_B)/N$, and an effective reduced interaction parameter $\langle e \rangle$.

Deviations from this principle of an effective component have already been found in previous studies both in MC simulations and in the NRM theory. For instance, it has been demonstrated that the equation of state of the mixture explicitly depends on the different interaction constants ϵ_{AA} , ϵ_{BB} , ϵ_{AB} and on the mixture composition.⁴ Also in the present comparison these explicit dependencies will become apparent.

In a first set of calculations we analyze mixtures with a zero exchange energy ΔW , i.e. $\Delta W = \epsilon_{AA} + \epsilon_{BB} - 2\epsilon_{AB} = 0$. For such mixtures the exchange of AA and BB contacts for AB contacts is not accompanied by a change in interaction energy for the specific contacts. Consequently, for an incompressible system there is also no change in internal energy. However, a compressible mixture is not only marked by an exchange of contacts upon mixing but also by a change in density, hence, yielding a change in internal energy. The variation in density with composition, mainly caused by the pure component interaction parameters ϵ_{AA} and ϵ_{BB} , in mixtures having $\Delta W = 0$ are shown in figures 6.1 and 6.2. The density is shown as a function of the composition of the mixture (top x-axis) and as a function of the effective interaction parameter (bottom x-axis) defined by eq 6.16. The actual values of the individual interaction constants are $\epsilon_{AA} = 0.5$, $\epsilon_{BB} = 0.9$ and $\epsilon_{AB} = 0.7$ (figure 6.1) and $\epsilon_{AA} = 0.5$, $\epsilon_{BB} = 0.7$ and $\epsilon_{AB} = 0.6$ (figure 6.2). The MC simulation data for the mixtures (■) and for the pure component (○) with the same value of the interaction parameter are compared to the theoretical results for the pure component (thin lines) and mixtures (thick lines) of the NRM (---), the ω -theory (—) and the LC theory (- - - -). If the principle of the effective component would be valid the densities as shown in figures 6.1 and 6.2 should be independent of the details of the interaction constants and should coincide for mixtures and the pure component.

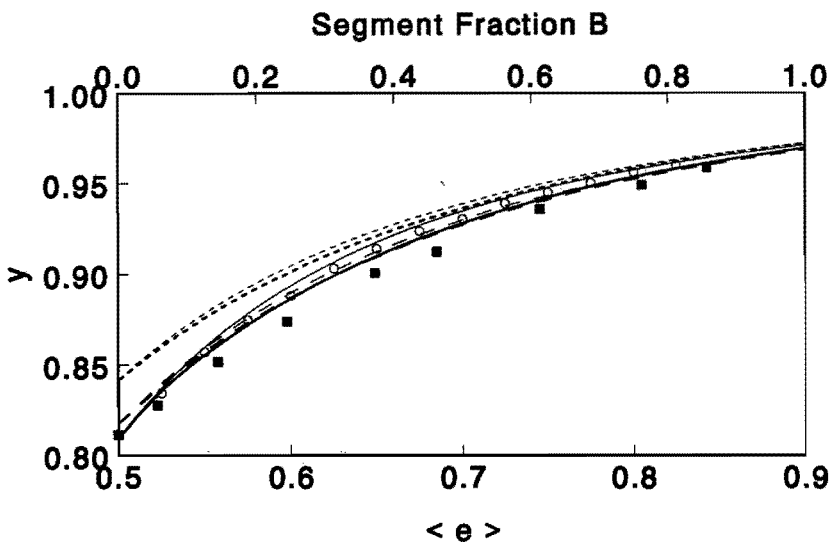


Figure 6.1: Density y as a function of the effective interaction parameter $\langle e \rangle$ (bottom axis) or composition ϕ_B (top axis) for polymer blends (■) for $e_{AA} = 0.5$, $e_{BB} = 0.9$, $e_{AB} = 0.7$. For comparison also the density of a pure component (○) as a function of interaction energy $e = \langle e \rangle$ is presented. The theoretical predictions for the pure component and the mixtures are depicted by thin and thick lines respectively: ω -theory (solid lines); LC theory (dotted lines) and NRM theory (dashed lines).

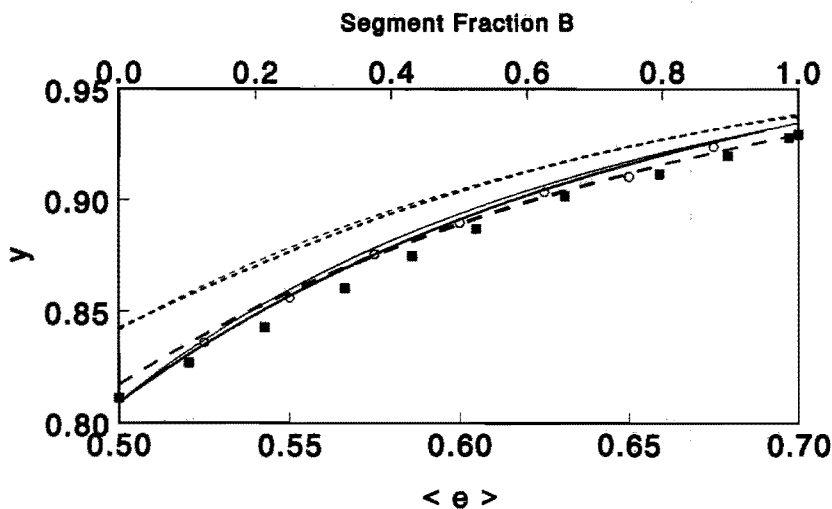


Figure 6.2: Caption as in figure 6.1 for $e_{AA} = 0.5$, $e_{BB} = 0.7$, $e_{AB} = 0.6$.

Clearly, small but systematic deviations from the effective component principle are observed both in the simulations and in the theories. Although we have not calculated the ‘experimental’ uncertainties on the simulation data they are thought to be small (about the size of the symbol) and the difference between mixtures and pure component are expected to be significant. It can be seen that the densities of the mixtures are systematically lower than those of the pure component. This is confirmed by all the theories although the effects are much smaller. Both NRM and ω -theories are much alike in their prediction and are closest to the MC simulation data. The LC theory shows the largest deviations from the MC simulation data.

In figure 6.3 a mixture of fixed composition ($\phi_B \simeq 0.5$) and fixed pure component interaction constants $\epsilon_{AA} = \epsilon_{BB} = 0.5$ is presented. The effective interaction parameter is varied in this case by varying the cross interaction parameter in the interval $[0.5 \leq \epsilon_{AB} \leq 1]$.

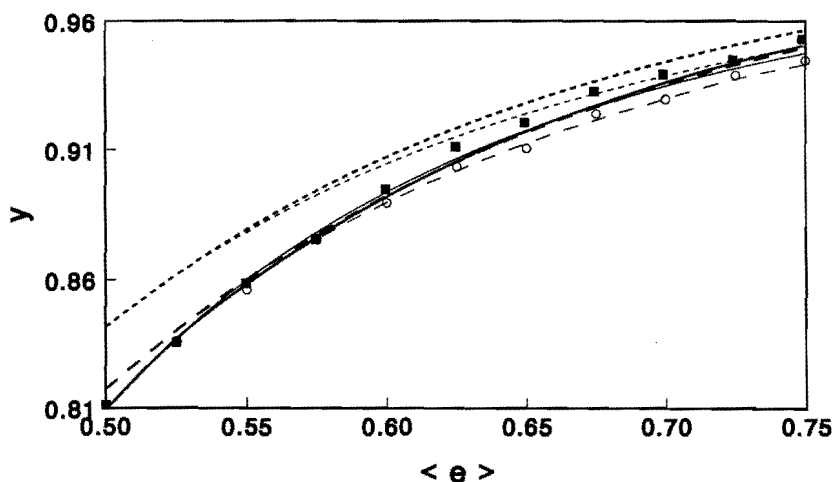


Figure 6.3: Density y as a function of the effective interaction parameter $\langle e \rangle$ for polymer blends at fixed components $\phi_B \simeq 0.5$. The interaction constants $e_{AA} = e_{BB} = 0.5$ and $e_{AB}(0.5 \leq e_{AB} \leq 1)$. For comparison also the density of a pure component (\circ) as a function of interaction energy $e = \langle e \rangle$ is presented. The theoretical predictions for the pure component and the mixtures are depicted by thin and thick lines respectively: ω -theory (solid lines); LC theory (dotted lines) and NRM theory (dashed lines).

In this mixture, the pure component densities are lower than the mixture densities. This qualitative trend is nicely confirmed by the NRM theory and the LC

theory, although the quantitative agreement for the latter is poor. Surprisingly, the ω -theory predicts virtually the same density for this pure component and the mixtures. At present, it is thought that this is attributed to an improper dependence of the intra-molecular contacts with composition and interactions in these mixtures. To gain more insight in this discrepancy a further and more detailed study is required.

6.4.2 Liquid-liquid coexistence

It has been ascertained that coexistence conditions are quite susceptible to small variations in theories and constitute a rather sensitive test for a theory. For instance, the critical conditions obey second and third order derivatives of the free enthalpy with composition. Hence small differences in the composition dependence of the Gibbs free energy may become important in determining the exact location of the critical state and hence the complete binodal curve.

In figure 6.4 the binodal temperatures of the binary mixtures are shown as a function of composition at 0 and 30 bar. The critical temperature and hence

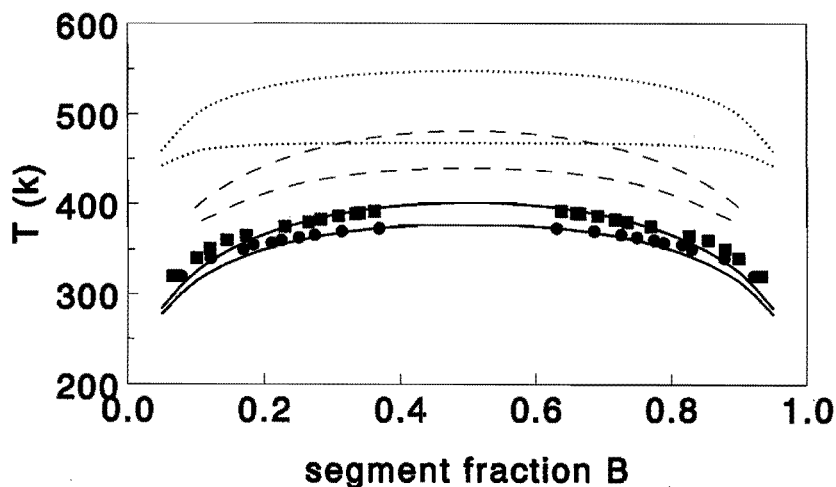


Figure 6.4: Binodal temperatures as a function of composition at $p = 0$ bar (\bullet) and $p = 30$ bar (\blacksquare). Prediction according to the ω -theory (solid lines), the NRM theory (dashed lines) and the LC theory (dotted lines).

complete binodals of the LC theory ($\cdots\cdots$) are located approximately 100K too high and the pressure dependence is obviously too large. The zero pressure binodal curve possesses an extremely flat shape and is definitely too broad in

comparison with the MC data. The shape of the 30 bar binodal is much closer to the correct shape. However, these qualitative changes in binodal shape with pressure are not confirmed by the 'experimental' binodal curves. For the MC data the application of these moderate pressures only results in a shift of the binodal to higher temperatures. Furthermore, both LCT binodals show an almost abrupt change in slope at the extremes of the composition scale not in agreement with the smoother variation in shape shown by the MC data. Although the zero pressure binodal is extremely flat, it still has the typical mean field parabolic shape reminiscent of classic critical scaling behavior.¹³⁻¹⁶

The binodals according to the ω -theory (—) are in excellent agreement with the simulation data. Both the predicted temperature location as well as the pressure dependence are in excellent agreement. Nevertheless, the binodal curves are still somewhat too narrow and, just as in the case of the LC theory, a typical parabolic shape is found in the critical region, the fingerprint of classic critical scaling behavior. For these relatively small chain lengths the critical behavior is typified by a non classic critical behavior and the true binodal curves have a more cubic shape.¹³⁻¹⁶ It was suggested by Sariban and Binder that the extra flattening in the critical region, although the extent of this region was not quantified, might also lead to a broadening of the complete binodal curves.¹³⁻¹⁶ Another, or additional, cause for the slightly too narrow binodals is the existence of fluctuations in the local densities or composition, related to the chain connectivity, in the extreme composition regions. It has been shown that such fluctuations represent an extra destabilization in solutions and blends possibly resulting in a broader binodal curve.¹⁷⁻¹⁹

The results of the NRM theory (- - -) are very similar to the result of the ω -theory if one is concerned with the shape of the binodal curves. However, the critical temperature and hence the complete binodal curve are located approximately 60 K too high. This higher (critical) temperature leads to a lower density, a higher compressibility and thus a larger pressure dependence. Nevertheless compared to the LC theory a gratifying prediction of the liquid-liquid coexistence is obtained. However, in comparison with the ω -predictions the agreement is rather poor.

6.5 Conclusions

The equation of state behavior of homogeneous mixtures has been investigated employing theory and MC simulations. Deviations from the principle of the ef-

fective component and the effective interaction parameter $\langle e \rangle$, valid in the Flory-Huggins theory, are found for all theories in agreement with the MC simulation results.

The LC theory systematically predicts too high densities for all investigated mixtures, the more so at smaller values of the interactional parameter $\langle e \rangle$. The changes in density with variations in composition and in actual values of the interaction constants ϵ_{AA} , ϵ_{BB} and ϵ_{AB} are in qualitative agreement with the MC simulation results.

Overall, the NRM theory provides the best agreement with the MC simulation data. Both the changes in density with variations in composition and interactional constants as well as the absolute values of the densities are in gratifying agreement with the MC data. The ω -theory is also in good agreement with the simulation results for the mixtures with zero exchange energy ΔW . In the situation that the interactions favor the formation of cross contacts, the ω -theory fails to correctly capture the changes in density. It is suggested that this is caused by an interplay between the variations in the intra-molecular contacts due to the mixture environment, embodied in ω , and the non-random formation of self- and hetero-contacts utilized in the quasi-chemical approximation.

The liquid-liquid phase behavior is very accurately predicted by the ω -theory. The predicted temperature location of the binodal curves and the influence of pressure on the liquid-liquid coexistence curve are in excellent agreement with MC results. The theoretical binodal curves are somewhat too narrow at the extremes of the composition interval.

The NRM predictions are qualitatively similar to those of the ω -theory but are located approximately 60K too high in temperature. Concomitantly, this high temperature results in a lower density, a higher compressibility and hence a slightly too large pressure dependence. The LC theory binodals and critical temperatures are ca. 100K too high and hence are very sensitive to pressure. Furthermore, the qualitative changes with pressure in binodal shape are not in agreement with the MC simulation results.

To summarize, the ω -theory provides excellent predictions of the liquid-liquid miscibility behavior and the equation of state behavior of mixtures possessing a zero exchange energy ΔW . The density of mixtures with favorable cross interactions, i.e. $\Delta W < 0$, are not accurately predicted. The cause for this discrepancy is most likely related to an interplay between the quasi-chemical approximation, represented by the microscopic parameters \bar{x}_{ij} and the chain environment, represented by ω . A further and more detailed study of this discrepancy is necessary.

References

- [1] Lacombe, R. H., Sanchez, I. C., *J. Phys. Chem.* *80*, 2568, 1976.
- [2] Madden, W. G., Pesci, A. I., Freed, K. F., *Macromolecules* *23*, 1181, 1990.
- [3] Nies, E., Cifra, P., *Macromolecules* *27*, 6033, 1994.
- [4] Cifra, P., Nies, E., Broersma, J., *Macromolecules* *29*, 6634, 1996.
- [5] Wang, S., *PhD - thesis, Chapter 4*. Eindhoven University of Technology, The Netherlands, 1997.
- [6] Computer codes can be requested from Erik Nies by e-mail(tgpkcn@chem.tue.nl).
- [7] Freed, K. F., *J. Phys. A* *18*, 871, 1985.
- [8] Bawendi, M. G., Freed, K. F., Mohanty, U., *J. Chem. Phys.* *84*, 7036, 1986.
- [9] Freed, K. F., Bawendi, M. G., *J. Phys. Chem.* *93*, 2194, 1989.
- [10] Dudowicz, J., Freed, K. F., Madden, W. G., *Macromolecules* *23*, 4830, 1990.
- [11] Bawendi, M. G., Freed, K. F., *J. Chem. Phys.* *88*, 2741, 1988.
- [12] The second generation LC theory was introduced by Jacek Dudowicz and Karl F. Freed. The equations in that paper do not yield the correct thermodynamic behavior and do not reduce upon simplification to the first order LC theory. We have discussed these problems with Prof. Karl F. Freed and dr. Jacek Dudowicz and have already been able to correct some typing errors in the theoretical expressions given in the original publication. However, including these corrections the predictions are still not correct. Currently, we are still in discussion with dr. Dudowicz about possible problems in the theory.
- [13] Sariban, A., Binder, K., *Colloid Polym. Sci.* *266*, 389, 1988.

- [14] Sariban, A., Binder, K., *Macromolecules* 21, 711, 1988.
- [15] Sariban, A., Binder, K., *Macromol. Chem.* 189, 2537, 1988.
- [16] Sariban, A., Binder, K., *J. Chem. Phys.* 86, 5859, 1987.
- [17] Muthukumar, M., *J. Chem. Phys.* 85, 4722, 1986.
- [18] Koningsveld, R., Stockmayer, W. H., Kennedy, J. W., Kleintjens, L. A., *Macromolecules* 7, 73, 1974.
- [19] Bates, F. S., Muthukumar, M., Wignall, G. D., Fetters, L. J., *J. Chem. Phys.* 89, 535, 1988.

Chapter 7

Outlook: Possible extensions and applications

7.1 PRISM applications

In the previous chapters we have discussed the influence of the chain connectivity, found in flexible linear chain molecules, on the structure and thermodynamics of pure and mixed fluids. As a first contribution, a new intra-molecular correlation function ω_{excl}^{intr} for the isolated chain has been derived. The correlation function ω_{excl}^{intr} has been inserted in the (lattice)-PRISM theory to obtain the intermolecular correlations and the thermodynamic properties of the chain fluid. It was demonstrated that ω_{excl}^{intr} and the combination ω_{excl}^{intr} /PRISM yield predictions closer to MC simulation data than the results acquired from an ideal chain intra-molecular correlation function. However, the suggested approach does not come to meet the fundamental problem that for flexible molecules intra- and inter-molecular correlations should be determined self-consistently. Such an approach does not only require extensive mathematical manipulations but also important approximations. Only recently, a self-consistent PRISM calculation has been put forward and the accuracy of this is a matter of current investigations.

As an application, the new single chain intra-molecular correlation function can be invoked in the PRISM theory to study properties of polymers blends and solutions. For these systems the liquid-liquid miscibility behavior can be explored. However, in these applications one may anticipate that the mutual influence of intra- and inter-molecular correlations will become quite significant and a self-consistent PRISM theory is more appropriate.

Possible further applications of the (P)RISM theory in combination with a

predetermined intra-molecular correlation function can be envisioned when the intra-molecular architecture is chiefly responsible for the observed physical behavior. For instance, it may be profitable to investigate in the PRISM concept the qualitatively different solution behavior of dendrimers and linear chain molecules built of the same chemical units.¹ Other applications may be found in the thermodynamics of branched and linear chain molecules and their mixtures. Furthermore, the integral equation approach is also very suited to study the behavior of chain fluids at surfaces. The interfacial predictions of the PRISM theory in combination with an ideal chain intra-molecular correlation function were shown to be quite interesting, although, also in this case, the ideal chain intra-molecular correlations limited the quantitative success. With the new correlation function ω_{excl}^{intr} the study of interfacial problems could yield more quantitative insights. Evidently, with some additional computational effects all PRISM development presented in this thesis can be extended to off-lattice systems.

7.2 ω -theory

The other approach that was pursued in this thesis employed insertion probabilities to establish the effects of the chain connectivity on the thermodynamics and the nearest neighbor structure of polymer fluids. All activity was focused on linear flexible polymers and mixtures thereof. A self-consistent prediction of inter and intra-molecular contacts was accomplished and the predicted thermodynamic properties were found to be in excellent to good agreement with MC simulation results. Although, it should be mentioned that the equation of state of mixtures with favorable cross interactions were not accurately predicted. Possibly, this is related to a less fortunate 'interaction' between the quasi-chemical approximation and the variation in the intra-molecular contacts, represented by ω in the theory. A further and more detailed study of this problem is required.

Nevertheless, the suggested approach is believed to be sufficiently versatile for further applications. As a possible extension mixtures of linear and short chain branched polymers, mentioned in the General Introduction, comes to mind. Clearly, the insertion probability will depend on the structure of the chain molecule. As a first intuitive but, as it turns out, too naive procedure one can collect the distribution of the number of intra-molecular contacts in a single branched chain simulation and inject this information into the main equations of the ω -theory presented in chapter 4, eqs 4.41. However, a feasibility study revealed that this approach is too simple and the predicted effect of branching on the equation

of state of the pure component is opposite to that found in MC simulations. It should be appreciated that the different segments in the backbone and in the branches of the chain molecule have different 'flexibilities' and a different response to density and composition. A more consistent view is to conceive the branched polymer as a copolymer of different types of segments.

This brings us to the more general problem of the thermodynamic properties of (random) copolymers. In order to treat such systems the theory must be extended to copolymers. In a first step one has to define the insertion probability of a copolymer and establish the relation of this insertion probability to the chemical composition (distribution). Once this more general frame for copolymers is established, branched polymers can be treated in the copolymer theory.

As an application, the ω -theory can be used to predict the thermodynamics of polymer solution. Clearly, in this case the chain length of one component of polymer blends can be assigned unity.

The study of interfacial problems is another possible choice. Szleifer outlined the procedures to extend his (bulk) conformational theory to interfacial problems.² Considerations along similar lines can be applied to the ω -theory. In this way one can investigate the shape, orientation of the molecules and their influence on e.g. the interfacial tension and the width of the interface. Alternatively, the present theory could perhaps be of use in the self-consistent field scheme as devised by Scheutjens and Fleer.³ Along this path a wide range of applications, paved by these authors, can be explored. Also the ω -theory can be extended to off-lattice polymer systems. For instance, this can be established by defining the off-lattice insertion probability following the work of Dickman, Hall and coworkers.⁴ These authors combined FH-like combinatorial argument with off-lattice results for hard sphere or hard dumbbells and derived the so-called Generalized Flory theory and dimer equations of state for off-lattice fluids. Similar argument can be employed to derive an off-lattice ω -theory. Another possible approach to off-lattice system is to extend ω -theory to the cell and hole theories as developed by Lennard-Jones, Devonshire,⁵ Prigogine,⁶ Simha⁷ and others.⁸

References

- [1] Baars, M., Meijer, E. W., *Private communication*. Vakgroep Organische Chemie, TUE.
- [2] Szleifer, I., *J. Chem. Phys.* *92*, 6940, 1990.
- [3] Fleer, G. J., Cohen-Stuart, M. A., Scheutjens, J. M. H. M., Cosgrove, T., Vincent, B., *Polymer at Interfaces*. Chapman and Hall, London, 1993.
- [4] Dickman, R., Hall, C. K., *J. Chem. Phys.* *85*, 4108, 1986.
- [5] Lennard-Jones, J. E., Devonshire, A. F., *Proc. Roy. Soc., A* *163*, 63, 1937.
- [6] Prigogine, I., Bellemans, A., Mathot, V., *The Molecular Theory of Solutions*. North-Holland Publishing Co, Amsterdam, 1957.
- [7] Simha, R., Somcynsky, T., *Macromolecules* *2*, 341, 1969.
- [8] Nies, E., Stroeks, A., *Macromolecules* *23*, 4092, 1990.

Appendix A

The t_{ij} 's calculated from cluster expansion

Curro, Blatz and Pings have derived an approximation for the end point distribution function of an athermal chain in continuous space. Here, we use this distribution function to calculate the intra-molecular correlation function of an athermal chain on a cubic lattice. For an athermal chain the interaction potential of covalently and non-covalently bonded segments are given by eqs 3.2 and 3.3 with $u_{attr} = 0$. The total potential energy $\epsilon(l, m, n)$ can be written as the sum of pair potentials between covalent bonds (w_{ii+1}) and non-covalent bonds (u_{ij})

$$\epsilon(l, m, n) = \sum_{i=1}^{s-1} w_{ii+1}(l, m, n) + \sum_{i=1}^{s-2} \sum_{j=i+2}^s u_{ij}(l, m, n) \quad (\text{A.1})$$

The end point $(1 - s)$ distribution function on the cubic lattice is given by:

$$Z_{1s}(l, m, n) = \sum_{l_2, m_2, n_2} \sum_{m_2, \dots, s-1} \sum_{n_2, \dots, s-1} \exp\left(\frac{\epsilon(l, m, n)}{kT}\right) \quad (\text{A.2})$$

Making use of eqs 3.2 and 3.3 the distribution function of an athermal polymer chain can be written as

$$Z_{1s}(r_{1s}) = \sum_{l_2, m_2, n_2} \dots \sum_{l_{s-1}, m_{s-1}, n_{s-1}} \prod_{i=1}^{s-1} \delta(r_{ii+1} - 1) \prod_{i=1}^{s-2} \prod_{j=i+2}^s (1 - h_{ij}) \quad (\text{A.3})$$

with $h_{ij} = 1 - \exp(-\beta u_{ij})$. The $Z_{1s}(r_{1s})$ can be presented as a graph expansion with an expansion parameter λ . After some manipulation the following expression is obtained

$$Z_{1s}(r_{1s}; \lambda) = (1 + \lambda h_{1s}) \sum_{i=0}^{\frac{s-3}{2}} \xi_i(r_{1s}) \lambda^i \quad (\text{A.4})$$

There are two types of graphs in $Z_{1s}(r_{1s}; \lambda)$, i.e. nodal and elementary graphs. The function $Z_{1s}(r_{1s}; \lambda)$ can be written as the sum of the nodal graphs $N_{1s}(r_{1s}; \lambda)$ and the elementary graphs $E_{1s}(r_{1s}; \lambda)$, viz.

$$Z_{1s}(r_{1s}; \lambda) = N_{1s}(r_{1s}; \lambda) + E_{1s}(r_{1s}; \lambda) \quad (\text{A.5a})$$

$$N_{1s}(r_{1s}; \lambda) = \sum_{i=0}^{\left(\frac{s-1}{2}\right)} \nu_i(r_{1s}) \lambda^i \quad (\text{A.5b})$$

$$E_{1s}(r_{1s}; \lambda) = \sum_{i=1}^{\left(\frac{s-1}{2}\right)} \epsilon_i(r_{1s}) \lambda^i \quad (\text{A.5c})$$

In the theory of fluids an integral relation exists between the nodal and elementary graphs given by the well-known Ornstein-Zernike equation. Similarly, for the single chain excluded volume problem a $(s-1)$ th-order integro-differential equation exists

$$\begin{aligned} N_{1s}(r_{1s}; \lambda) = & \sum_{l_{s-1}, m_{s-1}, n_{s-1}} E_{1s-1}(r_{1s-1}; \lambda) \delta(r_{s-1s} - 1) + \sum_{l_2, m_2, n_2} Z_{2s}(r_{2s}; \lambda) \delta(r_{12} - 1) \\ & + \sum_{i, m_i, n_i} \sum_{i=3}^{s-2} E_{1i}(r_{1i}; \lambda) Z_{is}(r_{is}; \lambda) \end{aligned} \quad (\text{A.6})$$

As in the integral equation theory of simple fluids, given another (approximate) relation between N_{1s} and E_{1s} , eq A.6 can be solved and the distribution function Z_{1s} can be obtained. An approximation analogous to the Percus-Yevick approximation is invoked

$$\begin{aligned} \epsilon_i(r_{1s}) &\simeq h_{1s} \xi_{i-1}(r_{1s}), & i &\geq 1, \\ \epsilon_0(r_{1s}) &= \xi_0(r_{1s}), & s &= 2, \\ \epsilon_0(r_{1s}) &= 0, & s &\geq 3. \end{aligned} \quad (\text{A.7})$$

Combining eqs A.4, A.5 and A.7 and putting $\lambda = -1$ the following equation results:

$$E_{1s}(r_{1s}; \lambda) = -\frac{h_{1s}}{H_{1s}} Z_{1s}(r_{1s}; \lambda) \quad (\text{A.8})$$

where $H_{1s} = 1 - h_{1s}$.

Substitution of eqs A.8 and A.5 into eq A.6 leads to

$$\begin{aligned}
Z_{1s}(r_{1s}) = & H_{1s} \left[\sum_{l_2, m_2, n_2} \delta(r_{12} - 1) Z_{2s}(r_{2s}) \right. \\
& - \sum_{l_{s-1}, m_{s-1}, n_{s-1}} \frac{h_{1s-1}}{H_{1s-1}} Z_{1s-1}(r_{1s-1}) \delta(r_{s-1s} - 1) - \sum_{i=3}^{s-2} \sum_{l_i, m_i, n_i} \frac{h_{1i}}{H_{1i}} Z_{1i}(r_{1i}) Z_{is}(r_{is}) \left. \right]
\end{aligned} \tag{A.9}$$

Eq A.9 can be rearranged to

$$\begin{aligned}
t_{1s}(r_{1s}) = & \sum_{l_2, m_2, n_2} \delta(r_{12} - 1) t_{2s}(r_{2s}) H_{2s}(r_{2s}) \\
& - \sum_{l_{s-1}, m_{s-1}, n_{s-1}} h_{1s-1}(r_{1s-1}) t_{1s-1}(r_{1s-1}) \delta(r_{s-1s} - 1) \\
& - \sum_{i=3}^{s-2} \sum_{l_i, m_i, n_i} h_{1i} t_{1i}(r_{1i}) H_{is} t_{is}(r_{is})
\end{aligned} \tag{A.10}$$

with

$$t_{ij}(r_{ij}) = \exp\left(\frac{u_{ij}}{kT}\right) Z_{ij}(r_{ij}) = \frac{Z_{ij}(r_{ij})}{H_{ij}} \tag{A.11}$$

Eq A.10 is conveniently solved in Fourier space. For a homogeneous system, the lattice Fourier transform and its inverse are defined as

$$\hat{f}(k_l, k_m, k_n) = \sum_{l, m, n} f(l, m, n) \cos(lu) \cos(mv) \cos(nw) \tag{A.12a}$$

$$f(l, m, n) = \left(\frac{1}{2\pi}\right)^3 \int_{-\pi}^{\pi} \int_{-\pi}^{\pi} \int_{-\pi}^{\pi} \hat{f}(k_l, k_m, k_n) \cos(lu) \cos(mv) \cos(nw) du dv dw \tag{A.12b}$$

Taking the Fourier transform of eq A.10, an algebraic recurrent equation is obtained.

$$\begin{aligned}
\hat{t}_{ij}(k_l, k_m, k_n) = & 2\psi [\hat{t}_{ij-1}(k_l, k_m, k_n) - t_{i+1j}(0, 0, 0) - t_{ij-1}(0, 0, 0)] \\
& - \sum_{k=3}^{s-2} t_{1k}(0, 0, 0) [\hat{t}_{ks}(k_l, k_m, k_n) - t_{ks}(0, 0, 0)]
\end{aligned} \tag{A.13}$$

where $\psi = \cos(u) + \cos(v) + \cos(w)$.

Successive applications of eqs A.13 and A.11 lead to the following results.

$$Z_{12}(r_{12}) = \exp(-\beta w_{12}(r_{12})) = \delta(r_{12} - 1) \tag{A.14}$$

Because the functions $t_{ij}(l, m, n)$ depend only on the difference in index of segments i and j , the $t_{ij}(l, m, n)$ can be written as $t_{l(l+i-j)}(l, m, n)$. For nearest neighbor segments l and $l + 1$, the function $t_{l+1}(r_{l+1})$ and the Fourier transform are given by

$$t_{l+1} = t_{12}(r_{12}) = Z_{12}/H_{12} = \delta(r_{12} - 1) \quad (\text{A.15})$$

$$\hat{t}_{l+1}(k_l, k_m, k_n) = 2[\cos(u) + \cos(v) + \cos(w)] = 2\psi \quad (\text{A.16})$$

$$\hat{t}_{l+1}(0) = 6 \quad (\text{A.17})$$

$$t_{l+1}(0) = \frac{1}{(2\pi)^3} \int_{-\pi}^{\pi} \int_{-\pi}^{\pi} \int_{-\pi}^{\pi} 2\psi du dv dw = 0 \quad (\text{A.18})$$

For next nearest neighbors l and $l + 2$ we find

$$\begin{aligned} \hat{t}_{l+2}(k_l, k_m, k_n) &= \hat{t}_{13}(k_l, k_m, k_n) = 2\psi[\hat{t}_{23} - t_{23}(0) - t_{12}(0)] \\ &= 2\psi[\hat{t}(k_l, k_m, k_n) - 2t_1(0)] = 2\psi[2\psi - 0 - 0] = (2\psi)^2 \end{aligned} \quad (\text{A.19})$$

$$\hat{t}_{l+2}(0) = \hat{t}_{13}(0) = 36 \quad (\text{A.20})$$

$$t_{l+2}(0) = t_{13}(0) = 6 \quad (\text{A.21})$$

For two segments l and $l + 3$ separated by 3 bonds the results are

$$\begin{aligned} \hat{t}_{l+3}(k_l, k_m, k_n) &= \hat{t}_{14}(k_l, k_m, k_n) \\ &= 2\psi[\hat{t}_{24}(k_l, k_m, k_n) - t_{24}(0) - t_{13}(0)] = (2\psi)^3 - 24\psi \end{aligned} \quad (\text{A.22})$$

$$\hat{t}_{l+3}(0) = \hat{t}_{14}(0) = 72 \quad (\text{A.23})$$

$$t_{l+3}(0) = t_{14}(0) = 0 \quad (\text{A.24})$$

For two segments separated by 4 bonds the t -function are

$$\begin{aligned} \hat{t}_{l+4}(k_l, k_m, k_n) &= \hat{t}_{15}(k_l, k_m, k_n) = 2\psi[\hat{t}_{25}(k_l, k_m, k_n) - t_{25}(0) - t_{14}(0)] \\ &\quad - t_{13}(0)[\hat{t}_{35}(k_l, k_m, k_n) - t_{35}] = (2\psi)^4 - 18(2\psi)^2 + 36 \end{aligned} \quad (\text{A.25})$$

$$\hat{t}_{l+4}(0) = \hat{t}_{15}(0) = 684 \quad (\text{A.26})$$

$$t_{l+4}(0) = t_{15}(0) = 18 \quad (\text{A.27})$$

For two segments separated by 5 bonds we obtain

$$\begin{aligned} \hat{t}_{l+5}(k_l, k_m, k_n) &= \hat{t}_{16}(k_l, k_m, k_n) = 2\psi[\hat{t}_4(k_l, k_m, k_n) - 2t_4(0)] \\ &- \sum_{i=3}^4 t_{1i}(0)[\hat{t}_{i6}(k_l, k_m, k_n) - t_{i6}(0)] = (2\psi)^5 - 24(2\psi)^3 + 72(2\psi) \end{aligned} \quad (\text{A.28})$$

$$\hat{t}_{l+5}(0) = \hat{t}_{16}(0) = 3024 \quad (\text{A.29})$$

$$t_{l+5}(0) = t_{16}(0) = 0 \quad (\text{A.30})$$

Appendix B

The parameters for the Freed theory

The Helmholtz free energy in the LC theory of Bawendi and Freed is given by

$$\begin{aligned} \beta A/Ns = & \frac{1-y}{y} \ln(1-y) + \frac{\phi_A}{s_A} \ln(\phi_A y) + \frac{\phi_B}{s_B} \ln(\phi_B y) \\ & + g_{01}(1-y)\phi_A + g_{02}(1-y)\phi_B + g_{12}\phi_A\phi_B y \end{aligned} \quad (\text{B.1})$$

The g_{01} , g_{02} and g_{12} are known functions of ϵ_{ij} and $1/z$ and defined as

$$g_{ij} = f_{ij}^0 + f_{ij}^1 - s_{ij} \quad (\text{B.2})$$

Where f_{ij}^0 is a mean field energetic contributions, f_{ij}^1 is an energetic contribution due to corrections to the mean field approximation and s_{ij} is an entropic contribution also arising from corrections to the mean field approximation. The expression for f_{ij}^0 , f_{ij}^1 and s_{ij} are given in the Table below

$$f_{01}^0(y) = z[\frac{e_{AA}}{2} - \frac{e_{AA}^2}{4}y(1-y) + o(e_{AA}^3)]$$

$$f_{02}^0(y) = z[\frac{e_{BB}}{2} - \frac{e_{BB}^2}{4}y(1-y) + o(e_{BB}^3)]$$

$$f_{12}^0(y_A, y_B) = z[\frac{e}{2} + \frac{e_{AA}^2}{4} + \frac{e_{BB}^2}{4} - \frac{e_{AB}^2}{2} + (-e_{AA}^2 - \frac{e_{BB}^2}{2} + e_{AA}e_{AB} + \frac{e_{AB}^2}{2})y_A$$

$$+ (-e_{BB}^2 - \frac{e_{AA}^2}{2} + e_{BB}e_{AB} + \frac{e_{AB}^2}{2})y_B + (\frac{3e_{AA}^2}{4} + \frac{e_{BB}^2}{4} - e_{AA}e_{AB})y_A^2$$

$$(\frac{3e_{BB}^2}{4} + \frac{e_{AA}^2}{4} - e_{BB}e_{AB})y_B^2 + (\frac{3e_{AA}^2}{4} + \frac{3e_{BB}^2}{4} - \frac{e_{AA}e_{BB}}{2} - e_{AB}^2)y_Ay_B + o(e_{ij}^3)]$$

$$f_{01}^1(y) = -e_{AA}(\frac{s-1}{s})(1-y) + o(e_{AA}^2, e_{AA}/z)$$

$$f_{02}^1(y) = -e_{BB}(\frac{s-1}{s})(1-y) + o(e_{BB}^2, e_{BB}/z)$$

$$f_{12}^1(y_A, y_B) = -2e_{AA}(\frac{s_A-1}{s_A}) - 2e_{BB}(\frac{s_B-1}{s_B}) + 2e_{AB}(\frac{s_A-1}{s} + \frac{s_B-1}{s_B})$$

$$+ y_A[2e_{AA}(\frac{s_A-1}{s_A}) - e_{AA}(\frac{s_B-1}{s_B}) + e_{BB}(\frac{s_B-1}{s_B}) - 2e_{AB}(\frac{s_A-1}{s_A})]$$

$$+ y_B[2e_{BB}(\frac{s_B-1}{s_B}) - e_{BB}(\frac{s_A-1}{s_A}) + e_{AA}(\frac{s_A-1}{s_A}) - 2e_{AB}(\frac{s_B-1}{s_B})] + o(z^{-1}e_{ij}, e_{ij}^2)$$

$$s_{01} = s_{02} = \frac{-1}{z}(\frac{s-1}{s})^2 - \frac{1}{3z^2} \frac{5(s-1)^4 + 2(s-1)^3 - 12(s-1)^2 - 12(s-1) + 3}{s^4}$$

$$- \frac{y}{3z^2} \frac{-4(s-1)^4 + 2(s-1)^3 + 12(s-1)^2}{s^4} - \frac{2y^2}{z^2}(\frac{s-1}{s})^4 + o(z^{-3})$$

$$s_{12}(y_A, y_B) = \frac{[(s_A-1)-(s_B-1)]^2}{s_A^2 s_B^2} \left\{ -\frac{1}{z} + \frac{1}{z^2}[-10 + \frac{1}{s_A s_B}[(18(s_A-1)(s_B-1) \right.$$

$$+ \frac{32}{3}(s_A-1) + \frac{10}{3}(s_B-1))]y_A + (18(s_A-1)(s_B-1) + \frac{32}{3}(s_A-1)$$

$$+ \frac{10}{3}(s_B-1))y_B] - \frac{1}{s_A^2 s_B^2} [(12(s_A-1)^2(s_B-1)^2 + 16(s_A-1)^2(s_B-1)$$

$$+ 8(s_A-1)(s_B-1)^2 + 6(s_A-1)^2 + 4(s_A-1)(s_B-1) + 2(s_B-1)^2)y_A^2$$

$$+ (12(s_A-1)^2(s_B-1)^2 + 16(s_A-1)(s_B-1)^2 + 8(s_A-1)^2(s_B-1)$$

$$+ 6(s_B-1)^2 + 4(s_A-1)(s_B-1) + 2(s_A-1)^2)y_B^2 + 6(2(s_A-1)(s_B-1)$$

$$+ (s_A-1) + (s_B-1))^2 y_A y_B \left. \right\}$$

$e_{ij} = \epsilon_{ij}/kT, y_j = \phi_j y$ in this table.

Table B.1: The energy and entropy correcting parameters of Freed theory for a polymer-polymer-void system.

Summary

The influence of chain connectivity on the thermodynamic and structural properties of compressible lattice polymers has been studied using the lattice polymer reference interaction site model (lattice-PRISM) and partition function theories. The theoretical results for pure components and mixtures have been compared with Monte Carlo simulation data for the same lattice model and with existing theories.

Intra-molecular correlations and PRISM theory

Ideal intra-molecular correlations

The application of the lattice-PRISM theory requires the definition of an intra-molecular correlation function for polymer chains. A frequently adopted intra-molecular correlation function is based on the ideal freely jointed chain model. The established theoretical results are in rather poor agreement with the Monte Carlo simulation data. In particular, the intra-molecular correlations at short distances are overestimated. But, the problems associated with the freely jointed chain model become most noticeable in the predicted thermodynamic properties. For instance, the compressibility factor of the lattice fluid is severely underestimated and qualitatively incorrect and unphysical results are obtained. Furthermore, the calculated liquid-vapor spinodal curve is located at too low temperatures and extends to unphysical packing fractions larger than unity.

Excluded volume and intra-molecular correlations

All these discrepancies can be related to the inadequate representation of the excluded volume by the freely jointed intra-molecular correlation function. Therefore, an intra-molecular correlation function ω_{excl}^{intr} for an athermal chain, that accounts for the excluded volume, has been derived, built upon an Ornstein-Zernike type of finite difference integral equation. The results of the intra-molecular excluded volume theory compare favorably to the MC data for the single chain.

Upon increasing the density, the MC intra-molecular correlations tend towards those of the freely jointed chain but, even at the highest investigated densities the latter are never reached. Notably, at short distances the correlations remain at all densities closer to the ω_{excl}^{intr} results.

The inter-molecular correlations for athermal and interacting chains at several densities have been calculated from the combination ω_{excl}^{intr} /lattice-PRISM. For athermal chains the new results are similar to the predictions based on the freely jointed chain model. For interacting chains the excluded volume theory produces better predictions at all investigated densities. The benefits of the new intra-molecular correlation function ω_{excl}^{intr} are most discernible in the thermodynamic behavior. For instance, a semi-quantitative prediction, void of unphysical artifacts, of the MC equation of state data is found. Furthermore, a qualitatively correct spinodal curve is obtained. The estimated critical density compares favorably to the critical density estimated from the MC simulation results. However, the estimated critical temperature is shifted upwards.

Intra-molecular correlations and the partition function theories

The Flory-Huggins theory, derived from the canonical partition function, is the earliest and probably most widely used theory. In this mean field theory the excluded volume effect due to the chain connectivity is completely ignored. In the present study a new theory, coined ω -theory, was developed starting from the definition of the insertion probabilities, i.e. the probability to insert a segment of the s -mer. The approximate nature of theoretical insertion probabilities makes the partition function and the thermodynamic state functions dependent on the particular order of insertion. We therefore define a practically useful insertion order which assures that the intensive thermodynamic state functions are functions of the appropriate thermodynamic variables, i.e. density, temperature and composition. Subsequently, theoretical insertion probabilities were derived that depend on the presence of intra-molecular or self-contacts related to the long range excluded volume of the chain molecules. These theoretical developments automatically resulted in a dependence on density and composition of the number of self-contacts.

Employing the new theory, predictions for compressible pure components (equation of state and liquid-vapor coexistence) and compressible binary mixtures (equation of state and liquid-liquid miscibility behavior) were provided. These results were compared to MC simulation results and a number of recently

published lattice theories (conformational theories of Szleifer, of Weinhold, Kumar and Szleifer and the Lattice Cluster (LC) theory of Freed and collaborators and the Non Random Mixing (NRM) theory).

Pure components

Equation of state The ω -theory accurately predicts the equation of state for all investigated interactions, temperatures and pressures. Also the variation in the number of intra-molecular contacts with chain length, density, temperature and/or pressure are successfully predicted. This demonstrates the effective incorporation of the chain connectivity in the ω -theory. Although the NRM and LC theories give fair predictions of the equation of state behavior of interacting polymers, deviations from the MC simulation data are noticeable at lower densities. These deviations can be attributed to the restricted account of the chain connectivity in both the NRM theory and the LC theory. The results of the conformational theory of Szleifer, that considers the influence of the chain conformations on the internal energy, yields rather poor predictions of the equation of state. It was made plausible that this is mainly due to an improper balance between entropy and energy. The theory of Weinhold, Kumar and Szleifer, which incorporates the influence of the conformational properties also in the entropy, gives an accurate prediction of the equation of state properties of athermal chains, virtually indistinguishable from the ω -theory. However, the precise dependence of the intra-molecular contacts on density and chain length are more accurately predicted by the ω -theory.

Liquid-vapor coexistence For all investigated chain lengths the Szleifer theory produces too narrow binodal curves with critical densities and temperatures not in agreement with MC data. Again the main reason is an imbalance between entropy and energy. Better but far from quantitative agreement with MC data is provided by the NRM theory. The predicted critical temperatures and densities are systematically too high and too small, the more so with increasing chain length. The LC theory gives a good prediction for the critical temperature, although for large chain lengths a peculiar shape of the coexistence curves and an incorrect course of the critical densities versus chain length are calculated. Also the ω -theory yields good critical temperatures. Combining information regarding the shape of the coexistence curve and the chain length dependence of both critical temperature and density, the ω -theory provides the best agreement of all theories discussed.

Binary mixtures

Equation of state The equation of state behavior of homogeneous mixtures A/B show deviations from the principle that a mixture may be modeled by an effective, single component with effective interaction parameter $\langle e \rangle = \phi_A e_{AA} + \phi_B e_{BB} - \phi_A \phi_B \Delta W / k_B T$ with $\Delta W = \epsilon_{AA} + \epsilon_{BB} - 2\epsilon_{AB}$. This principle established in the Flory-Huggins theory, is not quantitatively confirmed by MC simulations or other investigated theories.

The LC theory systematically predicts too high densities for all investigated mixtures, the more so at smaller values of the interactional parameter $\langle e \rangle$. The changes in density with variations in composition and in the values of the interaction constants ϵ_{AA} , ϵ_{BB} and ϵ_{AB} are in qualitative agreement with the MC simulation results.

Overall, the NRM theory provides the best agreement with the MC simulation data. Both the changes in density with variations in composition and interactional constants as well as the absolute values of the densities are in gratifying agreement with the MC data. The ω -theory yields excellent predictions for mixtures with zero exchange energy ΔW . In the situation that the interactions favor the formation of cross contacts, the ω -theory fails to correctly capture the variations in density. Likely, this is caused by an incorrect balance between the variations in the intra-molecular contacts due to the mixture environment, embodied in ω , and the non-random formation of self- and hetero-contacts utilized in the quasi-chemical approximation.

Liquid-liquid coexistence The liquid-liquid phase behavior is accurately predicted by the ω -theory. The predicted critical temperatures and compositions and the influence of pressure on the liquid-liquid coexistence curve are in excellent agreement with MC results. The NRM predictions are qualitatively similar to those of the ω -theory but the critical temperatures are located approximately 60K too high, also yielding a slightly too large pressure dependence. The LC critical temperatures are ca. 100K too high and are very sensitive to pressure. Furthermore, the predicted qualitative changes in binodal shape with pressure are not in agreement with the MC simulation results.

Samenvatting

De invloed van de ketenconnectiviteit op de thermodynamische eigenschappen en de microscopische structuur van compressiebele polymeren zijn bestudeerd met het rooster-'reference interaction site' model en met partitiefunctie theorieën. De theoretische resultaten voor pure componenten en binaire mengsels zijn vergeleken met Monte Carlo simulatie data voor hetzelfde roostermodel.

Intramoleculaire correlaties en de PRISM theorie

Ideale intramoleculaire correlaties

De rooster-PRISM theorie vereist de definitie van een intramoleculaire correlatie functie voor de geïsoleerde polymeermolecule. Een zeer gebruikelijke intramoleculaire correlatie functie is gebaseerd op het ideale model van de vrij-draaibare keten. De theoretische resultaten, verkregen met dit ideale model, zijn niet in overeenstemming met de Monte Carlo simulaties. In het bijzonder de korte afstand intramoleculaire correlaties worden overschat. De problemen met de vrij-draaibare keten komen echter vooral tot uiting in de voorspelde thermodynamische eigenschappen. Zo wordt de compressiebiliteitsfactor van de rooster-vloeistof sterk onderschat en worden zelfs fysisch zinloze dichtheden verkregen.

Uitgesloten volume en intramoleculaire correlaties

Alle voorgaande verschillen tussen theorie en simulaties komen voort uit de onvolledige representatie van het uitgesloten volume bij het ideale vrij-draaibare keten model. Een intramoleculaire correlatie functie ω_{excl}^{intr} , gebaseerd op een Ornstein-Zernike integraal vergelijking, is afgeleid. De resultaten van deze intramoleculaire uitgesloten volume theorie zijn in goede overeenstemming met de Monte Carlo resultaten voor de geïsoleerde keten. In de gecondenseerde toestand evolueren de MC intramoleculaire correlaties met toenemende dichtheid naar die

van de ideale keten. De ideale correlaties worden echter nooit bereikt en zeker voor korte afstanden zijn de MC-correlaties steeds dichterbij de ω_{excl}^{intr} -resultaten. De intermoleculaire correlaties zijn als een functie van de dichtheid en de temperatuur berekend door middel van de theoretische combinatie ω_{excl}^{intr} /rooster-PRISM. Voor athermische ketens zijn de nieuwe resultaten gelijk aan de voorspellingen gebaseerd op het vrij-draaibare ketenmodel. Voor ketens die interacties ondervinden is de uitgesloten volume theorie beter voor alle onderzochte dichtheden. De voordelen van de nieuwe intramoleculaire correlatie functie zijn het best waarneembaar bij het thermodynamische gedrag. Zo wordt bijvoorbeeld een semi-kwantitatieve voorspelling van de Monte Carlo simulatie resultaten gerealiseerd.

Intra-moleculaire correlaties en partitiefunctie theorieën

In de veel gebruikte Flory-Huggins theorie wordt het uitgesloten volume, veroorzaakt door de keten-connectiviteit, volledig verwaarloosd. In dit onderzoek is, vertrekkende van de definitie van de insertiewaarschijnlijkheid, de zogenoemde ω -theorie ontwikkeld. Het benaderend karakter van de theoretische uitdrukkingen voor de insertiewaarschijnlijkheid heeft tot gevolg dat de partitiefunctie en de thermodynamische toestandfuncties afhankelijk zijn van de gedetailleerde insertievolgorde. Daarom is een praktische insertievolgorde gedefinieerd die er voor zorgt dat de thermodynamische toestandfuncties uitsluitend afhankelijk zijn van de geschikte thermodynamische variabelen zoals dichtheid, temperatuur en concentratie. Vervolgens werd een nieuwe theoretische uitdrukking voor de insertiewaarschijnlijkheid afgeleid die afhankelijk is van het uitgesloten volume via de intramoleculaire of 'eigen'-contacten. Deze theoretische ontwikkelingen resulteren in een dichtheid en samenstellingsafhankelijkheid van het aantal 'eigen'-contacten. Met de ω -theorie zijn voorspellingen gedaan voor zuivere componenten (toestandsvergelijking en gas-vloeistof evenwicht) en compressiebele binaire mengsels (toestandsvergelijking en vloeistof-vloeistof ontmenggedrag). De resultaten zijn vergeleken met Monte Carlo simulaties en verschillende recente roostertheorieën (de theorie van Szleifer, de theorie van Weinhold, Kumar en Szleifer, de 'Lattic Cluster' (LC) theorie van Freed en medewerkers en de 'Non Random Mixing' (NRM) theorie).

Zuivere componenten

Toestandsvergelijking De ω -theorie geeft een nauwkeurige voorspelling van de toestandsvergelijking voor alle onderzochte waarden van interacties, temperatuur en druk. Ook de variatie in het aantal intramoleculaire contacten met de ketenlengte, dichtheid, temperatuur en/of druk worden goed voorspeld. Hoewel de NRM en LC theorie redelijke voorspellingen geven van de toestandsvergelijking van polymeren zijn er bij lagere dichtheden systematische afwijkingen van de MC simulatie data. Deze afwijkingen kunnen worden toegeschreven aan de beperkte bijdrage van het uitgesloten volume in deze theorieën. De theorie van Szleifer, die de invloed van ketenconnectiviteit meeneemt op de inwendige energie, geeft slechte voorspellingen van de toestandsvergelijking. Dit is toe te schrijven aan een overcorrectie van de inwendige energie ten opzichte van de entropie. De theorie van Weinhold, Kumar en Szleifer, die ook de invloed van de ketenconformaties op de entropie in rekening brengt, geeft een nauwkeurige voorspelling van athermische ketens die niet te onderscheiden is van de ω -theorie. De afhankelijkheid van de intramoleculaire contacten van de dichtheid en ketenlengte wordt echter beter voorspeld door de ω -theorie.

Gas-vloeistof evenwicht Voor alle onderzochte ketenlengtes geeft de Szleifer theorie te smalle binodale curven en kritische temperaturen en dichtheden die niet in overeenstemming zijn met de Monte Carlo data. Dit wordt wederom veroorzaakt door de onvoldoende uitgebalanceerde verhouding tussen entropie- en energiebijdragen. Een betere maar ver van kwantitatieve overeenstemming wordt gegeven door de NRM theorie. De voorspelde kritische temperaturen en dichtheden zijn systematisch te hoog en dit wordt slechter naarmate de ketenlengte groter wordt. De LC theorie geeft goede voorspellingen voor de kritische temperatuur hoewel voor grotere ketenlengtes een onverwachte vorm van de co-existentie curve en een incorrecte kritische dichtheid wordt berekend. Ook de ω -theorie geeft goede kritische temperaturen. Indien de resultaten betreffende de vorm van de co-existentie curve en de ketenlengte-afhankelijkheid van de kritische dichtheid en temperatuur worden vergeleken, is de ω -theorie de beste keus van alle onderzochte theorieën.

Binaire mengsels

Toestandsvergelijking De toestandsvergelijking van homogene mengsels vertonen afwijkingen van het principe dat een mengsel gemodelleerd kan worden als

een effectieve zuivere component met een effectieve interactie parameter $\langle e \rangle = \phi_A e_{AA} + \phi_B e_{BB} - \phi_A \phi_B \Delta W / k_B T$ met $\Delta W = \epsilon_{AA} + \epsilon_{BB} - 2\epsilon_{AB}$. Dit principe, afgeleid uit de Flory-Huggins theorie, wordt noch door de MC simulatie data, noch door de andere theorieën kwantitatief bevestigd. De LC theorie voorspelt systematisch te hoge dichtheden voor alle onderzochte mengsels. De resultaten worden slechter naarmate de effectieve interactie parameter $\langle e \rangle$ kleiner wordt. De veranderingen in dichtheid met variaties in samenstelling en variaties in de waarden van de interactieconstanten e_{AA} , e_{BB} en e_{AB} zijn in kwalitatieve overeenstemming met MC simulatie resultaten. In het algemeen komt de NRM theorie het beste overeen met de MC simulaties. De absolute waarden van de dichtheid alsook de verandering in dichtheid met samenstelling en interactieconstanten zijn in goede overeenstemming met de MC data. De ω -theorie geeft uitstekende voorspellingen voor mengsels waarvoor geldt $\Delta W = 0$. In de gevallen dat de interacties de vorming van AB contacten stimuleren is de ω -theorie niet in staat de variaties in dichtheid correct weer te geven. Waarschijnlijk wordt dit veroorzaakt door de incorrecte balans tussen de variaties in intramoleculaire contacten en de preferentiële vorming van AA, BB en AB contacten.

Vloeistof-Vloeistof coexistentie De vloeistof-vloeistof fase-evenwichten worden nauwkeurig voorspeld door de ω -theorie. De voorspelde kritische temperaturen en samenstellingen en de invloed van druk op de vloeistof-vloeistof coexistentiecurve zijn in uitstekende overeenstemming met de MC resultaten. De NRM voorspellingen gelijken kwalitatief op de ω -resultaten maar de kritische temperaturen zijn ongeveer 60K te hoog en vertonen een iets te grote drukafhankelijkheid. De LC kritische temperaturen zijn circa 100K te hoog en zeer gevoelig voor druk. Verder zijn de gevonden kwalitatieve verandering in de vorm van de binodale curve met druk niet in overeenstemming met de simulatieresultaten.

Notation

Symbols

\mathbf{a}_σ	vectors from a given lattice site to the z nearest neighbor lattice sites
A	Helmholtz free energy
$c(r_{12})$	direct correlation function
$c_{ij}(\mathbf{r}_1, \mathbf{r}_2)$	direct correlation function between segments i and j
$\mathbf{C}(\mathbf{r}_1, \mathbf{r}_2)$	$s \times s$ matrix with elements $c_{ij}(\mathbf{r}_1, \mathbf{r}_2)$
$\hat{\mathbf{C}}(k_l, k_m, k_n)$	Fourier transform of $\mathbf{C}(\mathbf{r}_1, \mathbf{r}_2)$ with elements $\hat{c}(k_l, k_m, k_n)$
C_{ij}	numbers of contact of a segment
$C(N_A, N_B, N_L, T, x_{AB}, x_{Ah}, x_{Bh})$	configurational factor
$C_{ins}(N_A, N_B, N_L, T)$	configurational contribution which arises from the insertion of the chain molecules on the lattice
D_N	configurational probability density function
e_{ij}	$\epsilon_{ij}/k_B T$, reduced interaction energy
$\langle e \rangle$	effective interaction parameter
E_s	internal energy of pure s -mer
E_h	internal energy of pure holes
f^{ij}	Mayer function
$g^s(\mathbf{r}^s)$	s -particle correlation functions
$g(\mathbf{r}_1, \mathbf{r}_2)$	pair distribution function
$G(l, m, n)$	total 2-segment distribution function
G	Gibbs free energy
h	Planck constant
h_N	normalization factor in ω -theory
h_{sc}	normalization factor in WKS theory

$h(N_A, N_B)$	normalizing factor in the Guggenheim expression
$h(r_{12})$	total correlation function
$h_{ij}(\mathbf{r}_1, \mathbf{r}_2)$	total correlation function between segments i and j
$\mathbf{H}(\mathbf{r}_1, \mathbf{r}_2)$	$s \times s$ matrix with elements $h_{ij}(\mathbf{r}_1, \mathbf{r}_2)$
$\hat{\mathbf{H}}(k_l, k_m, k_n)$	Fourier transform of $\mathbf{H}(\mathbf{r}_1, \mathbf{r}_2)$ with elements $\hat{h}(k_l, k_m, k_n)$
\mathcal{H}_N	Hamiltonian
k_B	Boltzmann constant
l_b	length of a bond
(l, m, n)	lattice indices
(k_l, k_m, k_n)	Fourier variables conjugate to (l, m, n)
m	mass of a particle
$n_{ij}(\Psi)$	number of contact pairs of species i and j in the lattice configuration Ψ
$n_{hp}(\nu)$	number of contacts of an s -mer with solvent molecules in conformation ν
$n_e(\nu)$	total number of neighbors that a chain has with other chains or with solvent molecules.
n_{ij}^*	value of n_{ij} in the case of athermal mixtures
N	number of particles or number of chains
N_i	number of particles i or the number of s -mers of component i
N_h	number of solvent molecules or holes
N_L	number of lattice sites
\mathcal{N}	number of configurations
\mathbf{p}_i	momentum of particle i
p	pressure
\bar{p}	reduced pressure
p_i	chain insertion probability depending on the intensive variables of the system
p_e	insertion probability of an effective component
P_i	chain insertion probability depending on the extensive variables of the system
$P_0(\nu)$	probability of a single athermal chain in conformation ν
$P(\nu)$	probability of chains in conformation ν
$P_{\omega_j}(\Omega_j, \text{con}, y)$	probability distribution of ω_j
q	inter-segmental contact fraction

q_i	external contact fraction of component i obtained from NRM theory
$q_f(\phi, T)$	internal partition function
q_t	total number of segmental contact pairs
\mathbf{q}	wave vector
Q_N	configurational partition function
\mathbf{r}^N	positions of the centers of mass of the N particles
\mathbf{r}_i	position of the i th lattice site or position of the i th particle
$\langle r^2 \rangle$	average squared end-to-end distance
s	chain length
s_j	chain length of component j
S	entropy
S_h	entropy of pure solvent (or pure holes)
S_p	entropy of pure s -mer
S_{pack}	configurational entropy
S_{conf}	conformational entropy
S_k	denoting the set of lattice sites occupied by segments
$\hat{S}(k)$	Fourier transform of static structure factor
$t_{ij}(l, m, n)$	auxiliary function in the excluded volume theory
T	absolute temperature
\mathcal{T}	total number of inter-molecular contact pairs
$u(\mathbf{r}_i, \mathbf{r}_j)$	pair interaction potential between particles i and j
$u(l, m, n)$	pair interaction potential on the lattice
$U_N(\mathbf{r}^N)$	total interaction potential energy
$U_{N,ext}$	external field
v^*	lattice site volume
$w_{ii+1}(l, m, n)$	pair potential between covalently bonded consecutive segments i and $i + 1$
ΔW	the Flory-Huggins exchange energy parameter
$W(l)$	probability of choosing a configuration l
$dW_N(\mathbf{r}^N, \mathbf{p}^N)$	probability to find N particles in phase space volume $d\Gamma_N$
x_{ij}^*	value of x_{ij} in the case of athermal mixtures
\bar{x}	value of x that minimizes the Helmholtz free energy
$X(\mathbf{r}^N)$	any function of the coordinates
$\langle X \rangle$	average of the configurational function X
$X_{\nu, m}$	function accounting for the corrections arising from the correlations in monomer positions

y	packing fraction
y_c	packing fraction at critical state
z	lattice coordination number
$z\alpha_j$	average number of covalent contacts of a segment in an s -mer
$z\omega_j$	average number of intra-molecular contacts of a segment in an s -mer
$z\omega'$	average number of intra-molecular contacts of a segment in an s -mer defined by Weinhold et al.
$z\Omega_{con}$	intra-molecular contact positions of a segment of an s_j -mer
zq_c	number of non-bonded contacts of an s -mer
zx	numbers of contact of AB pairs or the number of contacts of segment-vacancy pairs for pure polymers
Z_N	canonical partition function
$Z_A(Z_B)$	intra-molecular contribution to the partition function of a single chain
β	$\beta = 1/k_B T$
γ	$\gamma = 2/z$
$d\Gamma_N$	an element of the phase space volume
$\delta(\mathbf{r}_i, \mathbf{r}_j + \mathbf{a}_\sigma)$	Kronecker delta function
ϵ_{ij}	nearest neighbor interaction energy between segments i and j
θ_i	intermolecular contact fraction of component i obtained from ω theory
κ_T	compressibility
Λ	de Broglie thermal wavelength
μ_i	chemical potential of component i
ξ	a coupling parameter
ρ	number density
ρ_s	segmental density
$\rho^s(\mathbf{r}^s)$	s -particle distribution function
$\sigma = 1, \dots, z$	index for z nearest neighbors
τ	1-bond-jump probability
ϕ_i	chemical composition of component i
χ_{pack}	'interaction parameter' originating exclusively from entropic packing considerations in WKS theory
ψ	$\psi = \cos(u) + \cos(v) + \cos(w)$
Ψ	a lattice configuration of the chain molecules

$\hat{\omega}^{intr}(k_l, k_m, k_n)$	Fourier transform of the average intra-molecular 2-segment correlation function
ω^{intr}	average intra-molecular correlation function
$\hat{\omega}_{id}^{intr}$	intra-molecular correlation function in Fourier space obtained from ideal chain model
$\hat{\omega}_{excl}^{intr}$	intra-molecular correlation function in Fourier space obtained from excluded volume theory
ω_{MC}^{intr}	intra-molecular correlation function obtained from MC simulation
$\omega_{ij}^{intr}(\mathbf{r}_1, \mathbf{r}_2)$	intra-molecular correlation function between segments i and j
$\Omega^{intr}(\mathbf{r}_1, \mathbf{r}_2)$	matrix with elements $\omega_{ij}^{intr}(\mathbf{r}_1, \mathbf{r}_2)$
$\hat{\Omega}^{intr}(k_l, k_m, k_n)$	$s \times s$ matrices in Fourier transform of $\Omega^{intr}(\mathbf{r}_1, \mathbf{r}_2)$ with elements $\hat{\omega}_{ij}^{intr}(k_l, k_m, k_n)$
Ω	total number of allowed lattice configurations

Abbreviations

CBP	Curro, Blatz and Pings
EoS	equation of state
FH	Flory-Huggins
LC	lattice cluster
LCST	lower critical solution temperature
MC	Monte Carlo
MSA	mean-spherical approximation
NRM	nonrandom mixing
OZ	Ornstein-Zernike
PRISM	polymer reference interaction site model
PY	Percus Yevick
RISM	reference interaction site model
UCST	upper critical solution temperature
WKS	Weinhold, Kumar and Szleifer

Acknowledgments

First of all, I would like to express my sincere gratitude to dr. Erik Nies, my supervisor, who brought me into the world of polymer physics. For more than four years' cooperation with him, I have learned enormously from his creative ideas, critical mind and original approaches in scientific research. His sense of humor always led me to a pleasant study environment. Without his encouragement and continuous help, the completion of this thesis would have been impossible. I couldn't find words in my vocabulary to show my appreciation of his support during my stay in Eindhoven.

I am indebted to prof.dr. P.J. Lemstra for his hospitality and support in many ways. It was always helpful and encouraging to talk with him. I wish to express my most sincere gratitude to prof.dr. M.A.J. Michels, my second promoter, for his nice comments and wise advices; dr. Vitaly Kalikmanov for his critically reading of this thesis. Most of their comments have been incorporated in the final version of the thesis. I would also like to thank Peter Cifra for his pleasant cooperation and providing valuable simulation data. For the nice cooperation, I would like to mention my former colleague, Rob Janssen. I enjoyed the discussions with him very much.

I am grateful to Sabine Fisher, Peter Koets, Yongqing Xue, Hans Wilderbeek and all the member of TPK research group, too many to name them all, for their help not only in scientific field but also in many aspects of life.

Last but not least, thanks are due to my husband, Yingjun Du, for his encouragement during the years and also to my daughter, Weiwei Du, for her impatient waiting to the completion of the thesis. This thesis is dedicated to my husband and my daughter and also to the memory of my mother.

Curriculum Vitae

The author was born on 13 October 1963 in Jin County, Hebei Province, China. After receiving her B. Sc. degree in Polymer Chemistry in 1982, she worked at Shijiazhuang Oil Refinery for 3 years. From Sept. 1985 to July 1988, she studied at East China Normal University and got her M. Sc. degree in Organic and Polymer Chemistry. From July 1988 to May 1992, she worked in Beijing University of Aeronautics and Astronautics. In November 1992 she began her Ph.D. study in P. J. Lemstra's research group of Eindhoven University of Technology under the guidance of dr. E. Nies.

Stellingen

behorende bij het proefschrift

The Influence of Chain Connectivity on Thermodynamic and Structural Properties of Lattice Polymers

van

Suxin Wang

1. The polymer reference interaction site model (PRISM) has been applied in predicting the intermolecular correlations starting from the intra-molecular correlations. In most applications of PRISM theory, the oversimplified ideal chain model is used and the excluded volume effect is completely ignored. However, it can be shown that the intermolecular correlations obtained from the PRISM theory are substantially influenced by the excluded volume effect.

- K. S. Schweizer and J. G. Curro *J. Chem. Phys.*, **89**, 3350 (1988).
- J. Melenkevitz, J. G. Curro, K. S. Schweizer *J. Chem. Phys.*, **99**, 5571, 1993.
- Chapter 3, this thesis.

2. In principle, the lattice cluster (LC) theory provides an exact solution of the lattice model. However, in present applications of the LC theory, the theoretical expression for the Helmholtz free energy is truncated at a certain (relatively low) order in $1/z$, with z the coordination number. As a result of this the long range intra-molecular correlations are insufficiently taken into account.

- K. F. Freed, *J. Phys. A* **18**, 871, 1985.
- J. Dudowicz, K. F. Freed, W. G. Madden, *Macromolecules*, **23**, 4830, 1990.
- Chapter 5, this thesis.

3. In the conformational theory of Szleifer, the correction to Helmholtz free energy describing the chain conformational properties involves only the energy contribution while the Flory expression for the combinatorial entropy remains unchanged. Due to the improper balance between entropy and energy contributions, the Szleifer theory yields poor predictions, e.g. for the equation of state.

- I. Szleifer, *J. Chem. Phys.* **92**, 6940, 1990.

- Chapter 5, this thesis.

4. The interfacial tension in a demixed system of colloid and polymer can be computed from a theory developed by Kalikmanov and Hofmans for one component liquid-vapour system, in which the (effective) pair potential is modeled as a depletion potential.

- A. Vrij *Physica A* **235**, 120, 1997.

- V. I. Kalikmanov, G. C. J. Hofmans *J. Phys.: Condens. Matter*, **6**, 2207, 1994.

5. According to Kurja, the forward Debye scattered intensity of a polymer solution depends on the *number* average molar mass of the polymer and hence is a colligative property. It is well known that this Debye scattering of a polymer solution depends on the *mass* average molar mass.

- J. Kurja, eq 2.9A, p 24, PhD-thesis, (Eindhoven University of Technology, The Netherlands - 1997).

- W. H. Stockmayer *J. Chem. Phys.*, **18**, 58, 1950.

6. Behind the success of a woman, there must be a great man who supports her by all means. This man might be her father, her husband, her mentor, etc.

- Anonymous Chinese novelist Pi Lem Stra.

7. Reading 10,000 books and traveling 10,000 miles make one smart.

8. A good political system must be a boring one.

9. Man proposes, God disposes.

谋事在人，成事在天。

10. A long journey is started by taking the first step.

千里之行始于足下。